

Artificial Intelligence and Biomechanical Modeling  
Towards Patient-Specific Oral Surgical Procedures



*Pierre Lahoud*

2024

# **Artificial Intelligence and Biomechanical Modeling Towards Patient-Specific Oral Surgical Procedures**

Pierre Lahoud

**Promotor:**

Prof. Dr. Reinhilde Jacobs (KU Leuven, Belgium)

**Co-Promotors:**

Prof. Dr. Marc Quirynen (KU Leuven, Belgium)

Prof. Dr. Michael M. Bornstein (Universität Basel, Switzerland)

Dr. Mostafa EzEldeen (KU Leuven, Belgium)

**Chair:**

Prof. Dr. Koen Van Laere (KU Leuven, Belgium)

**Jury Members:**

Prof. Dr. Peter Claes (KU Leuven, Belgium)

Prof. Dr. Andy Temmerman (KU Leuven, Belgium)

Prof. Dr. Selena Toma (UC Louvain, Belgium)

Prof. Dr. Georgios N. Belibasakis (Karolinska Institutet, Sweden)

December 2024

Dissertation presented in partial fulfilment of the requirements for the degree of Doctor in Biomedical Sciences.

Copyright © Pierre Lahoud, 2024

All rights reserved. No part of this thesis may be reproduced or transmitted in any form or by any means, without prior written permission of the authors, or when appropriate, from the publishers of the publications.



## Table of Contents

Preface.....	7
List of abbreviations.....	9
General Introduction.....	11
PART I – LITTERATURE REVIEW	
<b>Chapter 1:</b> <i>Precision medicine using patient-specific modeling: state of the art and perspectives in dental practice.....</i>	21
<b>Chapter 2:</b> <i>Finite element models: a road to in-silico modeling in the age of personalized dentistry.....</i>	51
PART II – DEVELOPMENT AND VALIDATION STUDIES	
<b>Chapter 3:</b> <i>Artificial intelligence for fast and accurate 3-dimensional tooth segmentation on cone-beam computed tomography.....</i>	85
<b>Chapter 4:</b> <i>Development and validation of a novel artificial intelligence driven tool for accurate mandibular canal segmentation on CBCT.. ..</i>	111
<b>Chapter 5:</b> <i>Developing advanced patient-specific in silico models: a new era in biomechanical analysis of tooth autotransplantation.....</i>	137
PART III – APPLICATION OF PATIENT-SPECIFIC MODELING IN PLANNING ORAL SURGICAL PROCEDURES	
<b>Chapter 6:</b> <i>Real-time simulation of the transplanted tooth using model order reduction.....</i>	159
<b>Chapter 7:</b> <i>Individual "alveolar phenotype" limits dimensions of lateral bone augmentation.....</i>	175
General Discussion.....	203
Summary.....	211
Samenvatting.....	214
Scientific Acknowledgments .....	217
Personal Acknowledgments .....	218
Conflict Of Interest .....	224
Curriculum Vitae .....	229
Scientific Output .....	233



## **PREFACE**

This doctoral thesis consists of three parts, which in turn are made of seven chapters.

Additionally, this manuscript is framed by an introductory and a general discussion, conclusions, and future perspectives sections.

Each chapter was based on one peer-reviewed international publication which follows the standard IMRD structure (introduction, material and methods, results, and discussion). Parts and chapters were arranged as follows:

### **Part I - Literature Review**

**Chapter 1:** *Lahoud P, Jacobs R, Boisse P, EzEldeen M, Ducret M, Richert R. Precision medicine using patient-specific modelling: State of the art and perspectives in dental practice. Clinical Oral Investigations. 2022 Aug;26(8):5117-28.*

**Chapter 2:** *Lahoud P, Faghihian H, Richert R, Jacobs R, EzEldeen M. Finite element models: A road to in-silico modeling in the age of personalized dentistry. Journal of Dentistry. 2024 Sep 5:105348.*

### **Part II - Development and Validation of AI-Driven Tools Aiding Automation of Oral Surgical Planning**

**Chapter 3:** *Lahoud P, EzEldeen M, Beznik T, Willems H, Leite A, Van Gerven A, Jacobs R. Artificial intelligence for fast and accurate 3-dimensional tooth segmentation on cone-beam computed tomography. Journal of Endodontics. 2021 May 1;47(5):827-35.*

**Chapter 4:** Lahoud P, Diels S, Niclaes L, Van Aelst S, Willems H, Van Gerven A, Quirynen M, Jacobs R. Development and validation of a novel artificial intelligence driven tool for accurate mandibular canal segmentation on CBCT. *Journal of dentistry*. 2022 Jan 1;116:103891.

**Chapter 5:** Lahoud P, Jacobs R, Elahi SA, Ducret M, Lauwers W, van Lenthe GH, Richert R, EzEldeen M. Developing advanced patient-specific in silico models: a new era in biomechanical analysis of tooth autotransplantation. *Journal of Endodontics*. 2024 Jun 1;50(6):820-6.

### **Part III - Application of Patient-specific Modeling In Planning Oral Surgical Procedures**

**Chapter 6:** Lahoud P, Badrou A, Ducret M, Farges JC, Jacobs R, Bel-Brunon A, EzEldeen M, Blal N, Richert R. Real-time simulation of the transplanted tooth using model order reduction. *Frontiers in Bioengineering and Biotechnology*. 2023 Jun 29;11:1201177.

**Chapter 7:** Quirynen M, Lahoud P, Teughels W, Cortellini S, Dhondt R, Jacobs R, Temmerman A. Individual “alveolar phenotype” limits dimensions of lateral bone augmentation. *Journal of Clinical Periodontology*. 2023 Apr;50(4):500-10.

## LIST OF ABBREVIATIONS

2D	Two-Dimensional
3D	Three-Dimensional
AI	Artificial Intelligence
CAD	Computer-Aided Design
CAM	Computer-Aided Manufacturing
CBCT	Cone Beam Computed Tomography
CGAL	Computational Geometry Algorithms Library
CNN	Convolutional Neural Network
CPU	Central Processing Unit
CSO	Contour Segmentation Object
CT	Computed Tomography
DD	Digital Dentistry
DICOM	Digital Imaging and Communications in Medicine
DL	Deep Learning
DSC	Dice Similarity Coefficient
$E_{res}$	Early Graft Resorption
EBD	Evidence-Based Dentistry
E-FEA	Extended Finite Element Analysis
F-AI	Fully Automated AI-driven Segmentation
FDBA	Freeze-Dried Bone Allograft
FE	Finite Element
FEA	Finite Element Analysis
FEM	Finite Element Models
FOV	Field of View
GBR	Guided Bone Regeneration
Hd	Hausdorff distance
HOPGD	Higher-Order Proper Generalized Decomposition
HR	High Resolution
IoU	Intersection over Union
IPD	Individual Phenotypical Dimension
$L_{res}$	Late Graft Resorption
L-PRF	Leukocyte - Platelet Rich Fibrin
MC	Mandibular Canal
MIC	Minimally Invasive Endodontics
ML	Machine Learning
mm	Millimeter
MOR	Model Order Reduction
MPa	Megapascal
MPR	Multi-Planar Reconstruction
MRI	Magnetic Resonance Imaging

MTA	Mineral Trioxide Aggregate
N	Newton
OT	Occlusal Trauma
OTM	Orthodontic Tooth Movement
PDL	Periodontal Ligament
PGD	Proper Generalized Decomposition
POD	Proper Orthogonal Decomposition
PSM	Patient-Specific Modeling
R-AI	Refined AI-driven Segmentation
RCT	Randomized Controlled Trial
REM	Regenerative Endodontic Procedures
SA	Semi-Automated Segmentation
SD	Standard Deviation
SPCA	Surface Part Comparison Analysis
STL	Standard Tessellation Language
TAT	Tooth Autotransplantation
VMS	von Mises root stress
VTM	Virtual Treatment Planning
WTA	Wall Thickness Analysis



## INTRODUCTION



## GENERAL INTRODUCTION

**Artificial intelligence (AI)** has witnessed extraordinary advancements over the last decade, predominantly fueled by breakthroughs in training **deep neural networks** with **large datasets**. These developments have transformed various domains, initially proving their efficacy in processing and interpreting natural images, speech, and text. The profound impact of AI is now extending into the field of **medical imaging**, where it is poised to revolutionize **diagnostic** and **treatment** paradigms. While AI's applications in broader medical disciplines are rapidly expanding, the exploration of AI within the realm of **oral and maxillofacial surgery** remains surprisingly sparse. This gap in the literature presents a compelling opportunity to investigate the potential of AI to enhance and transform **surgical practices** within this specialized field.

The integration of AI into medicine has garnered colossal **investments**, with **research** and **development** efforts intensifying across the globe. The primary focus of these initiatives has been on leveraging AI to improve the **efficiency** and **accuracy** of **medical diagnoses**. By analyzing vast amounts of data, AI systems can detect patterns and anomalies with remarkable **precision**, often surpassing **human capabilities**. This has led to the development of AI-driven diagnostic tools that are increasingly being adopted in **clinical settings**. However, while significant progress has been made in the diagnostic domain, there remains an untapped potential for AI to contribute to the **planning** and **execution** of **medical treatments**, particularly in oral and maxillofacial surgery.

Simultaneously, the field of **digital dentistry** has been evolving, albeit at a slower pace than initially anticipated. Over the past two decades, digital technologies have gradually been integrated into dental practices, enabling more **precise** and **personalized care**. Notably, **software solutions** for the

**virtual planning** of **oral and maxillofacial surgeries** have emerged, offering dentists and surgeons the ability to create detailed **virtual simulations** of patients. These digital tools have the potential to significantly improve surgical planning and outcomes by allowing practitioners to **simulate** various scenarios and **optimize** treatment strategies accordingly. However, the adoption of these technologies has been limited, with less than 10% of all **3D images** taken for **implant placement** procedures being further processed for the creation of **surgical guides**, as evidenced by internal data from UZ Leuven.

The slow uptake of **digital planning technologies** can be attributed to several factors, including the **complexity** of the **workflow** required to prepare for **surgery**, as well as the associated **time** and **cost** burdens. The current digital planning process often involves multiple steps, each of which demands a high level of **expertise** and **resources**. As a result, many practitioners are hesitant to fully embrace these technologies, despite their potential **benefits**. This hesitancy underscores the need for more streamlined and **accessible digital solutions** that can be seamlessly **integrated** into clinical practice.

AI has the potential to address these challenges by **automating** and **optimizing** various aspects of **surgical planning**. By harnessing the power of AI-driven tools, it may be possible to reduce the **time** and **effort** required to prepare for surgery, thereby **lowering costs** and making these technologies more accessible to a broader range of practitioners. Moreover, AI can enhance the **precision** and **predictability** of surgical outcomes by generating **patient-specific treatment proposals** based on a comprehensive **analysis** of **individual anatomical** and **biomechanical characteristics**.

This doctoral project aims to **develop** and **validate** AI-driven planning tools specifically tailored for oral surgical procedures, such as **tooth replacement** through **tooth autotransplantation (TAT)** and **implant placement**. The

project will build upon existing knowledge in TAT surgical planning, tooth and jawbone **biomechanics**, and **artificial intelligence**, integrating these elements with a deep understanding of oral and maxillofacial structures. The ultimate goal is to create a **patient-specific** AI-driven **simulations** that can help **optimize** surgical outcomes, offering a more **reliable** and **efficient** approach to treatment planning.

By advancing AI-driven technologies in this field, this research has the potential to reshape the way oral surgeries are **planned** and **executed**. The anticipated outcomes include more **predictable** surgical results, **enhanced** patient care, and a deeper understanding of tissue remodeling processes following **dento-alveolar surgical procedures**. As AI continues to evolve, its **integration** into oral and maxillofacial surgery could mark a significant leap forward, paving the way for a new era of **precision medicine in dentistry**.

## **AIMS**

The general aim of this PhD project will be to:

- Analyze existing knowledge on personalized dentistry and finite element modeling in dentistry
- Develop and validate AI-driven modules for enhancing automation in oral surgical planning
- Evaluate the clinical applications and potential of AI-driven tools in oral surgery, with a focus on biomechanics and patient-specific modeling

## **HYPOTHESES AND OBJECTIVES**

Artificial Intelligence could help clinicians and researchers improve their digital workflow through:

- Rendering the use of complex planning tools user-friendly and accessible to a wider audience
- Being as accurate as expert users
- Providing a solid foundation for promoting in-silico studies and patient-specific modeling

## **METHODOLOGY**

### **Part I - Literature Study**

I.A. Scoping Review: Personalized Dentistry (Objective 1)

I.B. Literature Review: Finite Element Modeling in Dentistry (Objective 2)

### **Part II - Development of AI-Driven Tools for Aiding Automation of Oral Surgical Planning**

II.A. Development and Validation of an AI-driven Module for Automated Fast and Accurate Tooth Segmentation on CBCT (Objective 3)

II.B. Development and Validation of an AI-Driven Module for Automated Fast and Accurate Mandibular Canal Segmentation on CBCT (Objective 4)

II.C. Development of Patient-Specific In-Silico Models for Biomechanical Analysis of Tooth Auto-Transplantation (Objective 5)

**Part III - Applications of AI-Driven Tools for Planning Oral Surgical Procedures**

III.A. Real-time Simulation of Tooth Autotransplantation Using Model Order Reduction (Objective 6)

III.B. The Use of CBCT-Based Patient-Specific Models to Study the Individual “Alveolar Phenotype” in Guided Bone Regeneration (Objective 7)



The background is a complex marbled paper pattern. It features swirling, organic shapes in shades of cream, beige, and light brown, interspersed with deep blue and navy blue tones. The overall effect is reminiscent of traditional marbling techniques. In the lower-middle section, there is a dark silhouette of a tree with a thick, gnarled trunk and several smaller, branching limbs, set against the lighter, more intricate marbled background.

LITERATURE REVIEW



# CHAPTER I | Precision medicine using patient-specific modeling: state of the art and perspectives in dental practice

*This chapter is based on the following publication: **Lahoud P, Jacobs R, Boisse P, EzEldeen M, Ducret M, Richert R. (2022). Precision medicine using patient-specific modelling: State of the art and perspectives in dental practice. Clinical Oral Investigations, 26(8), 5117-5128.***

## Affiliations

1. OMFS-IMPACT Research Group, Department of Imaging and Pathology, Faculty of Medicine, KU, Leuven, Belgium
2. Department of Oral and Maxillofacial Surgery, University Hospitals Leuven, Leuven, Belgium
3. Division of Periodontology and Oral Microbiology, Department of Oral Health Sciences, KU Leuven, Leuven, Belgium
4. Department of Dental Medicine, Karolinska Institute, Stockholm, Sweden
5. Laboratoire de Mécanique Des Contacts Et Structures, UMR 5259, CNRS/INSA, Villeurbanne, France
6. Department of Oral Health Sciences, KU Leuven and Paediatric Dentistry and Special Dental Care, University Hospitals Leuven, Leuven, Belgium
7. Hospices Civils de Lyon, PAM d'Odontologie, Lyon, France
8. Faculty of Odontology, Lyon 1 University, Lyon, France
9. Laboratoire de Biologie Tissulaire Et Ingénierie Thérapeutique, UMR5305 CNRS/UCBL, Lyon, France

# Precision medicine using patient-specific modeling: state of the art and perspectives in dental practice

*Lahoud P, Jacobs R, Boisse P, EzEldeen M, Ducret M, Richert R.*

## **ABSTRACT**

**Aim(s):** The present narrative review aimed to present and discuss the current literature investigating patient-specific modeling in dentistry, its state-of-the-art applications, and research perspectives.

**Materials and Methods:** The review was conducted by systematically analyzing and synthesizing current literature on patient-specific modeling (PSM) in dentistry. Key sources were selected from databases such as PubMed, Scopus, and Google Scholar, focusing on recent advancements, applications, and research perspectives in PSM, with particular attention to AI-driven developments, clinical implementation challenges, and ethical considerations.

**Results:** PSM may allow optimized surgical treatment planning, increase predictability, and potentially lower risks of pre- and post- operative complications. Recent advancements in the fields of AI may allow for the automation of several parts of these laborious modeling technologies, bringing user-assisted decision-support tools closer than ever to both clinicians and researchers.

**Conclusion(s):** Recent advancements in artificial intelligence make it now possible to automate several parts of the laborious modeling task, bringing such user-assisted decision-support tools closer to both clinicians and researchers. Yet, more research is still needed to develop in-vivo protocols to enable implementation and clinical validation of PSM in dental practice. At the same time, ethical and legal constraints should be carefully considered when applying data-driven models in current clinical practice.

## INTRODUCTION

Medical knowledge and innovation in healthcare have continuously grown in the past decades, but this has added greater complexity to the decision-making process in clinical practice. As a response to the diversity of practices, evidence-based dentistry (EBD) was proposed to guide decision-making in accordance with the overall conclusions of clinical trials with a high level of evidence (Kishore et al. 2014). EBD makes it possible to provide the most recommended treatment option to an entire population. Yet, the conclusions are based on comparisons of populations and not on the characteristics of individuals. However, numerous patients still encounter treatment failures despite biomedical and digital advancements. This is particularly true in dental biomechanics, for which several recommendations were proposed to prevent cracks (Hilton et al. 2020); research methods such as finite element (FE) models have been developed to investigate reasons for failure (Versiani et al. 2021; Ordinola-Zapata et al. 2022). Still, many clinicians face difficulties assessing patient- and tooth-specific risks (Santos et al. 2009; Yoshino et al. 2015; von Arx et al. 2020). Indeed, most published results were produced using standard FE models without considering patient- specific parameters, but many of these, such as the root canal anatomy or occlusions, can modify the biomechanical behavior of the tooth (Chatvanitkul & Lertchirakarn, 2010; Benazzi et al. 2014).

Recent imaging technologies such as CBCT enable researchers and clinicians to gather patient-specific characteristics with sufficient accuracy for patient-specific modeling (PSM) (Baumgaertel et al. 2009; Neal & Kerckhoffs, 2009). These digital twins are proposed to individually simulate the biomechanics of different treatments for a given patient and adapt the treatment accordingly (Zadpoor & Weinans, 2015). This customized approach is well developed in several fields, such as maxillofacial surgery, in which medical devices are being developed to model surgical procedures (Resnick et al. 2016) or orthopedics where FE models based on patient femurs

were reported to better predict potential bone fractures than assumptions of experimented clinicians (Eggermont et al. 2018). However, its use in dentistry is still rare as PSM requires powerful computer hardware, dedicated software, time, and operator experience; these aspects have delayed the practical application of the first proofs of concept using standard FE published more than three decades ago (Trivedi, 2014). More recently, advances in the fields of artificial intelligence (AI) have allowed the automation of several steps of the PSM, such as automated anatomical segmentations and CAD (Lahoud et al. 2021), reducing the time needed as well as operator experience and therefore making this digital tool more than ever available to both clinicians and researchers.

Therefore, the present narrative review aimed to present and discuss the literature investigating PSM in dentistry, its current state-of-the-art applications, and to identify future research required before its integration into routine clinical practice.

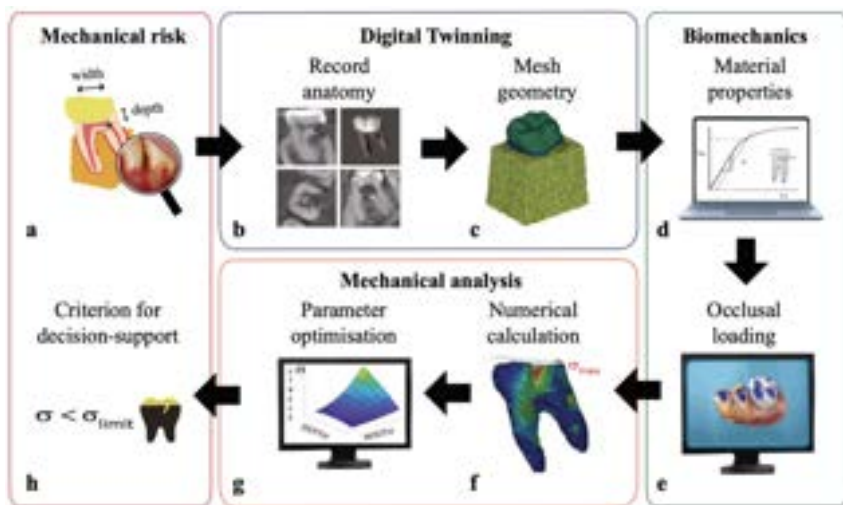


**Figure 1.** Patient-specific modeling: (a) detection of a mechanical risk in a specific clinical situation: example for a damaged tooth indicated for a crown, (b) anatomical record using computed tomography illustrated by grayscale image and segmented tooth, (c) volume and surface meshing, (d) integration of material properties, illustrated by a stress/strain curve representing the capacity of the material to deform under load,

(e) simulation of occlusal loading and boundaries representative of the masticatory forces of the patient, (f) numerical calculation of stress  $\sigma$ , (g) parameter optimisation to define the most conservative therapeutical choices (for example, width and depth for a post space preparation), and (h) decision-making supported by a mechanical criterion: herein a limit on the stress value.

## **Principles of Patient-Specific Modeling**

Creating a patient-specific model can be divided into different steps, ranging from recording patient data to customized therapy. This requires first to create a digital twin representative of the given clinical situation (Figure 1a–c). These digital twins of anatomical structures such as teeth and bone are frequently built using data from a CBCT scan that is then imported into dedicated platforms such as Amira (Mercury Computer Systems, Chelmsford, MA, USA) and Mimics 10.01 (Materialise, Leuven, Belgium) (Trivedi, 2014; Richert et al. 2020). Segmentation of anatomical structures on CBCT enables partitioning the initial image into multiple virtual segments of the structure of interest and its environment; for these, several strategies are reported, including grey-level threshold, region-based growing techniques, and the level-set method (Lahoud et al. 2021). The segmented object is then meshed for subsequent biomechanical calculations (Trivedi, 2014; Richert et al. 2020).

It should be noted that smaller voxel size enables for more a precise mesh, yet requires more computational power (Richert et al. 2020). To define the biomechanical behavior of a tooth requires the solving of complex partial differential equations, and FE analysis was reported to be the reference method due to its widespread use in multiple fields of application and implementation in many commercially available software. The principle of FE analysis is based on the division of the structure into a finite number of smaller parts called elements. In these elements, a system of algebraic equations is defined, and solutions can then be approximated and recombined into a larger system to model the entire problem (Trivedi, 2014). Biomechanical parameters such as material laws and occlusal loading should

then be considered in the model (Figure 1d–e). Material laws have been traditionally classified according to the nature and composition of the material, ranging from soft tissues, such as the periodontal ligament (PDL), to hard tissues, such as the dentine, enamel, and bone (Kinney et al. 2003). Young's modulus value describes virtually the capacity to deform under masticatory forces. This constant was reported to vary, according to the location on the tooth, from 7 to 25 GPa for dentine and from 48 to 84 GPa for enamel (Kinney et al. 2003; Richert et al.2020). Then, occlusal loading is commonly simulated with a unique force in PSM, ranging from 100 to 300 N, according to the type of tooth and patient profile (Kinney et al. 2003; Richert et al.2020).

Mechanical analysis is the final step, and this enables the investigation of the stress distribution related to a specific clinical situation and the comparison between different therapeutical strategies. Numerical calculi can be conducted using software such as Abaqus (Dassault Systèmes, Vélizy-Villacoublay, France), Ansys (Work- bench, Swanson Analysis Inc., Houston, TX, USA), or Nastran (MSC Software, Newport Beach, CA, USA) (Kinney et al. 2003; Erdemir et al. 2012; Richert et al.2020). PSM promises to offer clinicians and researchers the possibility to digitally assess the influence of several biomechanical parameters such as depth of post space preparation ( de Rodrigues et al. 2017; Knoops et al. 2019; de Rodrigues et al. 2020). This approach aims to find the optimal mathematical solution and help decide the most conservative treatment options, with minimal stress constraints and increased durability for each patient (Merema et al. 2021) (Figure 1f–h).

More recently, democratization of AI and machine learning have enabled the development of new models based directly on meshes or results of FE models. The principle of AI is based on classification of data primarily by learning their key features and then making predictions using the resulting models. Different AI approaches have been applied in medicine, such as principal component analysis, to automatically generate FE models representing the

anatomy of a femur (Grassi et al. 2014) or model order reduction to minimize computing time (Marquat et al. 2020). Another important aspect of AI is its capacity to deal with missing data due to artefacts in the acquisition for example (Lahoud et al. 2021).

## **CURRENT APPLICATIONS OF PSM IN DENTISTRY**

### **Restorative dentistry**

For the last 50 years, the development of adhesive materials and techniques has dramatically changed the mechanical concepts of modern restorative dentistry by progressively aiming for minimally invasive restorations and therefore the preservation of more dental tissue (Tvas & Burrow, 2004). This paradigm shift has led to colossal research on the bio-mechanical properties of teeth, and numerous materials have been developed to minimize the stress concentration induced by restorations. This was achieved by adapting the modulus of elasticity of new restorations to that of the natural dental tissue, but no ideal direct restoration has emerged from published clinical studies (de Kuijper et al. 2021; Souza et al. 2021). Similarly monolithic zirconia crowns have recently conquered the market and were presented as a promising alternative to conventional metal-ceramic crowns considering 3 years (Mikeli et al. 2021); however, a weaker clinical performance was also found at 5 years (Sailer et al. 2015). These contradictory results highlight the difficulty of adequately understanding the bio-mechanical factors involved in the restorative procedure owing to numerous hurdles such as adequate follow-up or sufficient recall rate. In comparison, fine mechanisms have been discovered through FE studies, and new studies based on PSM appear to be of utmost importance to link material development to clinical use. For instance, Ausiello and coworkers (2004) developed a FE model to investigate the biomechanical behavior of the inlay restoration and found that composite inlay transmits less stress to the other tooth structures (Ausiello et

al. 2004); however, the morphology of the dentine and enamel was defined from the literature which limits the clinical significance of these findings. Later, Barak et al. validated by interferometry a new FE model of a premolar based on CBCT and found that enamel mostly dictates the mechanical behavior of the whole tooth (Barak et al. 2009). Similar models were used by Magne and Oganessian to evaluate the influence of material for inlays and smaller cuspal deformations were reported for ceramic compared to composite resins (Magne & Oganessian, 2009). These biomechanical studies could be used to understand fine mechanisms explaining the most frequently reported clinical failures such as chipping or loss of retention; this does not seem to be the case for the many randomized clinical trials (and the systematic reviews of these) that have been conducted to explain these failures owing to differences in the baseline characteristics of the included patients such as amount of tissue (Morimoto et al. 2016; de Kuijper et al. 2021; Dioguardi et al. 2021). These obstacles could be overcome by systematically simulating the biomechanics using patient-specific models and predicting the true impact of each factor such as the amount of tissue or occlusion. There is a real opportunity to connect FE studies to clinical data and reach a higher level of understanding of adequate material properties for each patient.

Stress analysis was also widely used to investigate potential factors influencing biomechanics, and more than 20 possible parameters have been reported to explain the fracture of restorations. In this regard, FE models are proving to have great potential due to their ability to numerically assess each parameter separately and in combination. This digital tool could help clinicians and researchers identify factors having the greatest influence on biomechanics. For example, general guidelines were proposed to avoid failure of adhesive restorations mostly by evaluating residual tooth structure and wall thickness. However, more recent studies suggest that occlusion contributes to 49% of stresses, whereas the cavity's interaxial thickness 1%, and isthmus width 5% (Lin et al. 2009). Measuring the occlusion for individual patients in clinical

practice is technically complex; this is unlikely to be done in routine. Therefore, PSM constitutes an interesting tool to simulate this patient-specific parameter. A protocol based on force sensors was thus recently developed and proposed to adapt restorations according to the results of a FE analysis (de Rodrigues et al. 2020). Such accurate assessments based on PSM could open new ways to conceive biomimetic and personalized rehabilitations, potentially widening the indication of direct restorations instead of systematically crowning teeth.

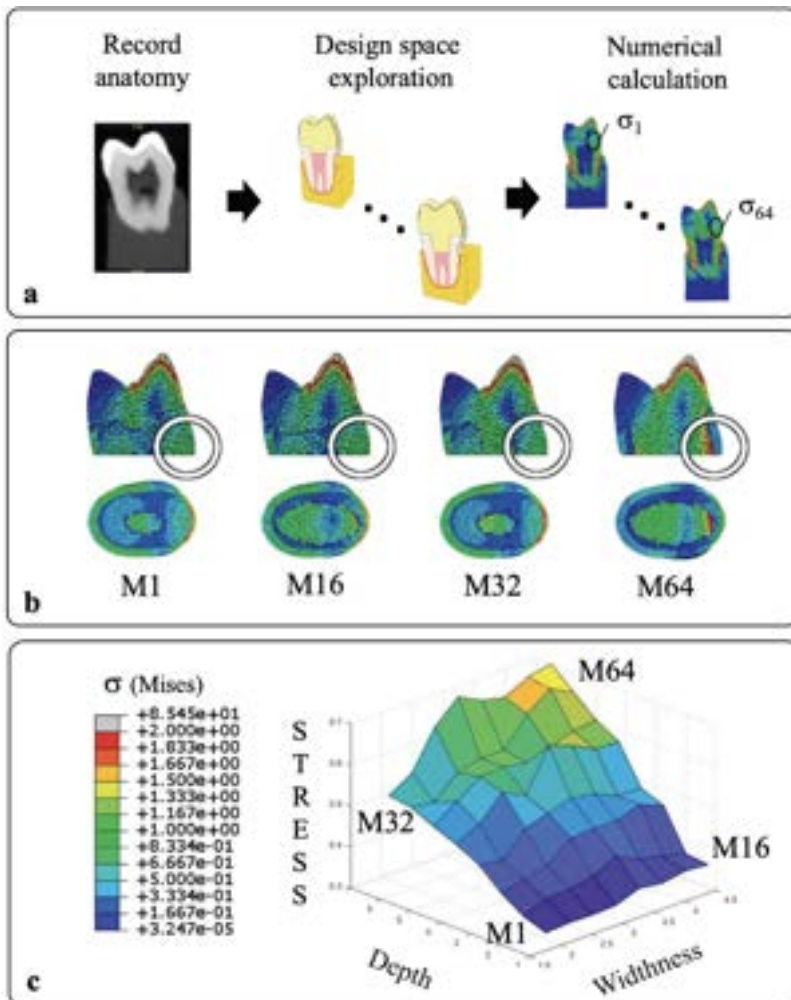


**Figure 2.** Parameter optimisation for an endocrown rehabilitation with (a) process of

constitution of models to evaluate the impact of width and depth of pulp chamber cavity on a specific damaged premolar: 64 models were generated by design space exploration to calculate stress values  $\sigma$ ; (b) sagittal and occlusal views of 4 representative models; M1: small width and depth of pulp chamber, M16: large width and small depth of pulp chamber, M32: small width and high depth of pulp chamber, M64: large width and depth of pulp chamber; the model M64 presented an unfavourable stress distribution with high stresses on the resin luting (white circle); and (c) surface of response generated by each mean stress value  $\sigma$  of the resin luting for the 64 finite element models; width alone has a small impact on stresses but depth of pulp chamber had a great impact increasing stresses by 115%.

## **Endodontics**

In the past decades, guided endodontics and conservative access cavity designs have gained interest in the dental community (Moreno-Rabié et al. 2020; Shabbir et al. 2021). As for restorative dentistry, this reflects a will to conduct minimally invasive endodontics as the success of endodontically treated teeth greatly depends on mechanical conditions such as vertical root fracture (Fuss et al. 1999). Many studies have tried to investigate this fracture resistance using extracted teeth or standard FE models, but the biomechanical behavior of the root in clinical practice is mostly influenced by patient-specific parameters such as bone level, root canal curvature, or root length (Kishen, 2006). These parameters are now considered in PSM using patient CBCT and this appears particularly adapted to predict the ideal fiber-post rehabilitation in clinical practice (de Rodrigues et al. 2017; de Rodrigues et al. 2020). More recently, extended FE models were developed to define the ideal access cavity by identifying the model with the lowest risk of crack propagation (Zhang et al. 2019). A perspective would then be to combine these approaches with guided endodontics to reproduce the mechanically optimal strategy in the patient, which could reduce the risk of iatrogenic damage to the root but also treatment time.

FE analysis has also been widely used to investigate the mechanisms behind the separation of endodontic instruments. In 2008, Necchi et al. developed models to compare the stress distributions in different rotary instruments and found that the radius and position of the canal curvature as the most critical

parameters in determining the stress (Necchi et al. 2008). This work led to the restriction of stainless files and favored Ni–Ti ones in the apical portions of highly curved root canals. Similar models were used by Lee et al. to understand cyclic fatigue fracture (Lee et al. 2011); it was found that stiffer instruments presented the greatest stress and stiffness which was related to a smaller number of rotations in the cyclic fatigue test compared to less rigid instruments. More recently, FE models based on patient CBCT were used to compare instrument removal strategies and help practitioners decide the most conservative strategy (Richert et al. 2021). This approach could also be used to understand the biomechanical stresses of endodontic instruments to choose an instrument that is the most adapted to each root anatomy, but also to design new instruments for a more personalized treatment to avoid breakage.

### **Prosthodontics**

Recently, digital smile design and augmented reality concepts have profoundly changed how prosthetic rehabilitations are conceived by delivering real-time smile projections (Touati et al., 2019; Touati et al., 2021). Consequently, patient's expectations for a customized 'ideal' smile are getting increasingly greater (Touati et al., 2021). However, these new aesthetic expectations of prosthetic treatments require rigorous biomechanical analyses to avoid early failures and prosthetic breakage. Such treatment failures can be caused by various reasons, most frequently crown loosening, prosthetic fracture, or root fracture. Historically, the mechanisms leading to crown loosening were studied using FE analysis based on CBCT scans of extracted teeth (Ordinola-Zapata et al., 2022). These studies suggested notably a higher fracture rate of teeth reconstructed using a metal post due to the high Young's modulus of metal and helped understand the essential role of the ferrule effect (Pegoretti et al., 2002; Richert et al., 2018). Recently, advances in CAD and CAM technologies have allowed us to conceive and produce prostheses with a high degree of precision and

reproducibility, unachievable before. These possibilities open a new field of investigation to identify the dimensions of prostheses that have the optimal mechanical properties, and FE models prove to be the ideal tool capable of studying and optimizing clasp and crown design with regard to supported stresses (Figure 2) (Alshegri et al., 2018; Richert et al., 2021). Considering overdentures, a perspective could be a more individualized design and lighter prosthesis for better comfort without increasing the risk of failure, similarly to that done in other medical fields using topology optimization to calculate the ideal design of, for instance, craniofacial implants (Merema et al., 2021). This could be of potential value as the time and cost related to digital denture protocols are reported to be smaller than conventional complete denture protocols (Srinivasan et al., 2019), but the literature remains scarce on the mechanical indicators required to guarantee the clinical performance promised by digital dentistry.

### **Orthodontics**

The practice has greatly evolved in orthodontics following the high demand of adult patients for aesthetic treatments such as lingual brackets and clear aligners (Rossini et al., 2015). This has been made possible following the development of CBCT- based models and has led to a shift towards virtual treatment planning (VTP), relying on integrated soft tissues, hard tissues, and dentition. One major advantage of such modeling lies in the possibility of assessing and comparing different treatment options, such as extraction versus non- extraction strategies. The promise of VTP is to reproduce the perfect alignment predicted before treatment on the virtual setup (Camardella et al., 2016). Despite great hopes brought by initial proof-of- concept studies, our understanding as to the effectiveness and stability of ideal orthodontic treatments remains relatively low. However, interactions between teeth, bone, PDL, and the orthodontic appliances are currently being widely assessed using standard FE analysis to better understand these interactions and their repercussions on the treatment and its long-term stability (Ammar et al., 2011;

Feng et al., 2019). PSM could simulate with greater precision the mechanical response of each patient, leading to customized treatments and possible personalized designs of orthodontic appliances (Barone et al., 2017). This approach could also be combined with AI algorithms to train meta-models based on clinical data to better predict outcomes, reduce treatment time, and increase long-term treatment stability.

### **Implant dentistry**

Prosthetic failures in dental implant therapy are strongly related to mechanical complications such as prosthetic failure or bone loss (Ueda et al., 2011; Sailer et al., 2022). Numerous FE models have been developed to investigate the reasons of failure, leading to reinforce implant-retained overdentures (Amaral et al., 2018), or the effects of implant length, leading to prefer longer implants in a jaw with bone of low density (Eraslan & Inan, 2010). Other patient-specific parameters, including bone anatomy, greatly influence mechanical failure in dental implants or bone analogues (Kuroshima et al., 2017). These parameters are now simulated in the PSM based on CBCT scans, which led to the development and evaluation of personalized prosthetic rehabilitations using FE analysis (Roy et al., 2018; Tamura et al., 2018; Cheng et al., 2020). Personalized prosthetic rehabilitations present more favorable stress distributions than traditional prosthetics, and customized bone analogues have lower bone stresses and higher success rate after 1 year compared to conventional methods (Tamura et al., 2018). These positive results led to the development of software to mathematically optimize the design of plates and bone analogues to minimize bone stresses and thus favor osseointegration. In addition, since its development, guided implantology has been increasingly used and PSM offers new possibilities to adjust the position planned for guided implant surgery or dynamic navigation following mechanical expectations delivered by FE analysis.

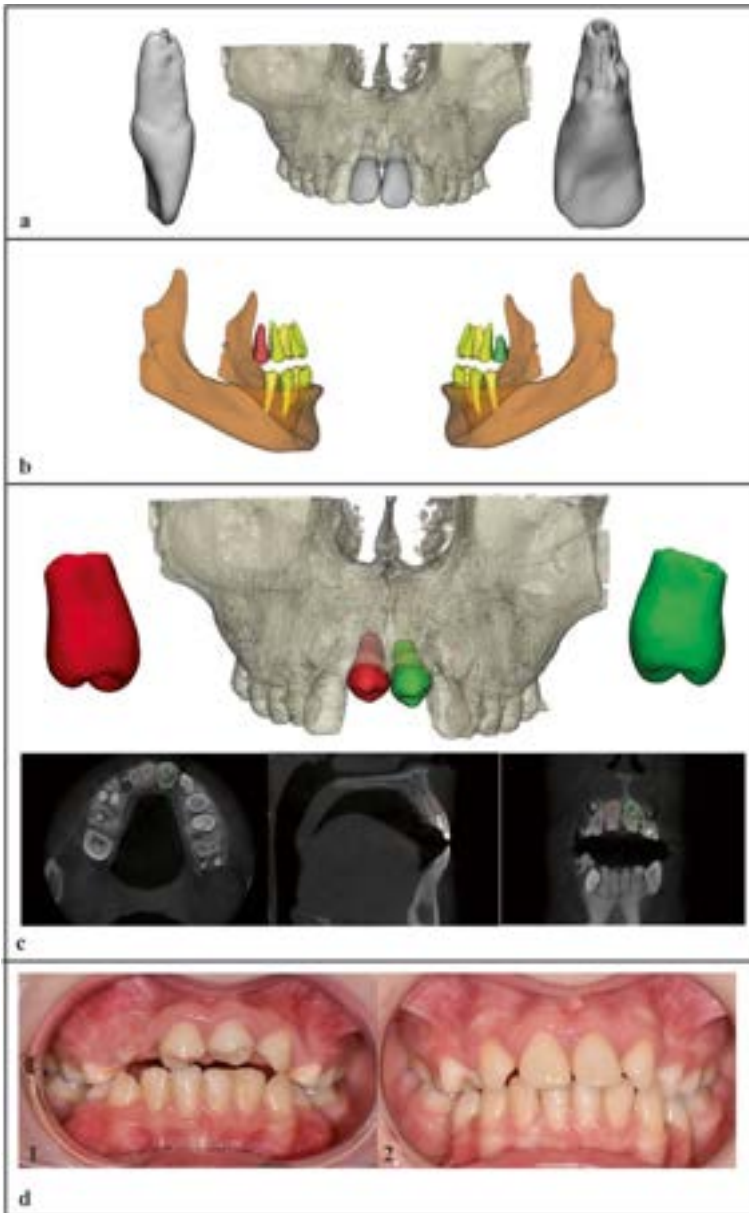


**Figure 3.** Case simulation to illustrate the virtual treatment planning for tooth autotransplantation. Following detection of post-traumatic external root resorption at the level of the maxillary central incisors (a), potential donor teeth, consisting of maxillary and mandibular premolars, are assessed regarding their dimensions and developmental conditions to find the optimal donor element and its ideal position

with regard to the recipient site (b). The chosen donor elements (in this case right upper premolar in red and left upper premolar in green) are then modelled and a simulation of the final position of the transplantation is performed regarding the 3D virtual model and of the CBCT slices (c). Subfigure d(1) shows a vestibular view of the outcome of the autotransplantation 3 months after surgery and sub-figure d(2) a vestibular view 1 year after autotransplantation and aesthetic rehabilitation of the two maxillary central incisors.

### **Traumatology and tooth auto-transplantation**

Oral and maxillofacial trauma represents a major public dental health problem, particularly due to its high prevalence in children (Andersson, 2013). More recently, strategies preserving or regenerating the pulp are now recognized approaches to maintain the biological functions of traumatized teeth (Torabinejad et al., 2017). Similarly, tooth auto-transplantation (TAT) also became a reference strategy in cases of complete tooth loss or agenesis due to the limited treatment options available for children and its potential for preserving the alveolar ridge and consequently future growth (Mendoza-Mendoza et al., 2012). Despite great hopes, these strategies are difficult to plan and execute adequately due to the complexity of the workflow involved in precisely planning TAT surgery. However, recent advances in PSM have led to increased surgical predictability of CBCT-guided TAT compared to conventional approaches, thanks to the use of digital twins to shape the recipient site and match the virtually planned position of the transplant without damaging the PDL and dental components of the donor element (Figure 3) (EzEldeen et al., 2019). These approaches also raise questions as to the mechanical resistance of the damaged or transplanted tooth. These questions were widely investigated using laboratory studies, but these approaches could appear limited to understanding certain mechanical mechanisms as tested mature teeth were cut to mimic immature one (EzEldeen et al., 2019; Mello et al., 2020). FE models offer the possibility to simulate the true anatomy of immature teeth based on CBCT and appear effective in improving our understanding of these complex phenomena (Belli

et al. 2018; Anthrayose et al., 2021; Demirel et al., 2021); these approaches were used on extracted teeth to understand the mechanical behavior of apical plug or even compare strategies of revascularization and apexification (Belli et al., 2018; Anthrayose et al., 2021) and, more recently, simulated patient-specific bone to evaluate the mechanical value of root maturation and type of restorative material (Demirel et al., 2021). More generally, young patients present high variability of tooth anatomy, position and/or occlusion, which is extremely difficult to reproduce *in vitro* and PSM appears therefore to be the most effective method to consider the many patient-specific parameters (Shen et al., 2018).

### **Periodontics**

Digital dentistry has also considerably altered the way to diagnose and treat periodontitis. In first, recent developments in intraoral scanners have allowed the visualization of gingival margin changes in patients who had undergone root coverage procedures and treatment of periodontal disease in a non-invasive and precise manner (Kuralt & Fidler, 2021). Secondly, patient-specific surgical guides were proposed in guided bone augmentation procedures to help improve the accuracy of the resulting graft shape and reduce the amount of graft material placed outside the planned volume (Tarce et al., 2022). Considering biomechanics, influence of periodontal ligament or bone level was widely evaluated using FE analysis in several fields, including apicoectomy, orthodontics, and implantology (Eraslan & Inan, 2010; Ammar et al., 2011; Schmidt & Lapatki, 2019). Different biomechanical laws were also developed and experimentally validated to simulate these tissues and considerations of periodontium appear decisive in constructing a PSM (Ren et al., 2010; Nikolaus et al., 2017). While clinical studies show that several biomechanical factors such as excessive occlusal forces or bone loss play a decisive role in the patient-specific response to periodontal infection (Genco, 2000), there is, to the best of our knowledge, no published FE study that has explored this.

## **Current limitations and futures challenges of PSM**

In dental research, FE analysis has already proven its great potential for the study of biomechanisms owing to its capacity to obtain the stress distribution of the tooth without destroying it (Ordinola-Zapata et al., 2022). PSM could now bring dental practitioners into a new more predictive era of medicine, but such evolutions raise technical, ethical, and economic questions among the different stakeholders.

## **CBCT artefacts and perspective with an intraoral scan**

Since the advent of CBCT, distortions and segmentation errors have been noted and labelled as artefacts. Such artefacts are mainly related to the beam hardening phenomenon and can be correlated to the presence of high-density materials such as amalgam and alloys (Celikten et al., 2017; Celikten et al., 2019). These artefacts greatly reduce image quality and consequently the clinical potential of PSM. However, several strategies have been recently developed to treat these; for example, intraoral scanners (IOS) register the dental surfaces without radio- graphic artefact and could be combined with CBCT for a more precise PSM (Rangel et al., 2013; Buchgreitz et al., 2016), and AI methods have recently been developed to automate CBCT segmentation and could be trained to reduce the effects of artefacts during the volume reconstruction (Figure 4) (Ezhov et al., 2021; Lahoud et al., 2021).

## **Technical and scientific challenges**

Numerous technical and scientific challenges currently limit the clinical scope of FE analyses. For instance, the mechanical behavior of the tooth has been reported to be greatly modified by patient-specific characteristics surrounding the tooth, including the PDL, bone, and occlusion (Murakamiet al., 2014; Lee et al., 2021). However, most of our knowledge is currently

based on experimental studies and FE models from extracted teeth, which, by definition, does not consider the tooth environment (Kinney et al., 2003; Richert et al., 2020). An open-source PSM was recently proposed to consider the complete mandible, but this approach involved large meshes and multiple dental contacts, therefore resulting in long calculation times that are unrealistic to implement in the everyday clinical practice (Vukicevic et al., 2021). A solution to this may lie in new strategies such as model order reductions (MOR) that have been proposed for real-time simulations of complex biomechanical behavior such as for tongue or guidewires for endovascular surgery (Badrou et al., 2020; Calka et al., 2021). These approaches are based on different mathematical techniques, mainly proper orthogonal decomposition methods, but further developments remain crucial before its full implementation in the dental field (Grassi et al., 2014; Badrou et al., 2020; Maquart et al., 2020; Calka et al., 2021). Simulation of the dental and periodontal environments appears therefore of great importance, yet still extremely challenging. Furthermore, these complex simulations will require user-friendly software to encourage dental practitioners to use PSM approaches. Such software are yet to be developed in dentistry but do exist for maxillofacial surgery where they have recently been reported to lead to more streamlined and predictive orthognathic surgery (Resnick et al., 2016).

Several limitations are also raised by imaging of soft tissues surrounding the tooth using CBCT, in particular the PDL, which has been reported to possess Hounsfield unit values similar to those of the surrounding bone and dental cement, further complicating the segmentation of these structures (Nikolaus et al., 2017). Consequently, the PDL is often not segmented and artificially simulated with a continuous thickness of 0.2 mm around the tooth (Nikolaus et al. 2017; Richert et al., 2020). Moreover, the PDL was reported to present *in vitro* a complex mechanical behavior associating non-linearity, viscosity, and time dependency (Ren et al., 2010; Nikolaus et al., 2017; Schmidt et al., 2019). While these complex material laws still require to be experimentally validated, experimental tests are reported to be extremely difficult due to rapid

tissue damage caused by dehydration (Bergomi et al., 2010).

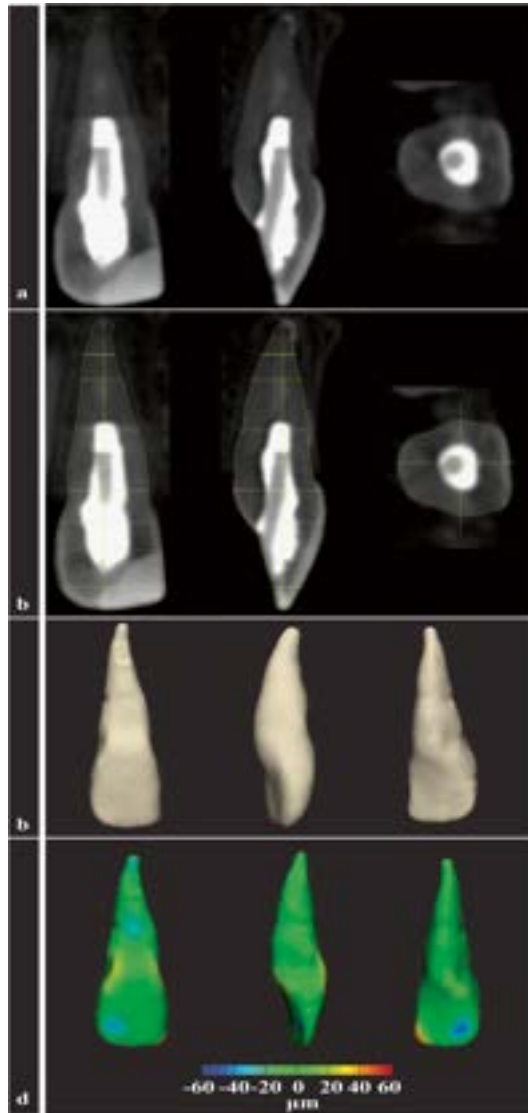


**Figure 4.** Interest of AI-driven tooth segmentation with: a) sagittal, frontal, and horizontal views of the cone-beam computed tomography (CBCT) of (a) maxillary central incisor presenting artefacts due to the root canal treatment and coronal rehabilitation; (b) automatic detection of the borders of the tooth (yellow lines) using the AI-algorithm; (c) automatic 3D segmentation based on the interpolation of the segmented slices (yellow lines); and (d) vestibular, lateral, and palatal views of a part comparison analysis deriving from the superimposition of expert manual segmentation (taking on average 12 min for completion) and fully automated AI segmentation (< 30 s for completion). The colour map depicts a mean deviation of 7.85 µm between the 2 segmentation methods (manual versus AI).

## **Model validation and economic considerations before clinical implementation**

The premise of PSM is to propose to practitioners optimal treatment options based on anatomical, aesthetic, and bio-mechanical considerations. However, inappropriate models could result in unfavorable therapeutic decisions and potentially dramatic clinical consequences (Viceconti et al., 2005). Model verification and validation were largely described *in vitro*, but no error estimator is currently available for a clinical use (Erdemir et al., 2012). Moreover, recent reviews have highlighted the increasing number of published papers reporting FE models, although most of these have not yet been experimentally validated (Viceconti et al., 2005; Chang et al., 2018). This observation raises the question of the appropriate choice of model parameters and emphasizes the need to develop protocols to reduce uncertainty of future PSM software. PSM is already partly used in numerous medical fields such as orthopedics (Boudissa et al., 2021), and FE studies are currently recognized as necessary for the design of personalized osteosynthesis to reconstruct the human mandible (Merema et al., 2021). Furthermore, several software now exist to help practitioners decide the most appropriate treatment, such as PrediSurge (PrediSurge, Saint-Etienne, France) to optimise stent deployment in cardiac surgery (Derycke et al., 2020). However, such dedicated software is still not commercially available in the dental field although this seems technically possible as teeth are more easily obtainable than cardiac tissue for experimental studies and their behavior as hard tissue has been analysed and validated many years ago (Kinney et al., 2003). This is likely to be related to the proven economic value of PSM in many medical fields, but which has yet to be explored in dentistry. For instance, the use of computer-aided surgical simulation divides by two the time needed for complex cranio-maxillofacial surgery, and it was reported that the cost of the software is amortized for 6 patients per year (Xia et al., 2006). These reductions in time and cost were also found for

shoulder arthroplasty and orthognathic surgery in different countries and what is now to be determined is when virtual model surgery will completely eliminate the need for traditional surgery (Sheth et al. 2022). Furthermore, all these evolutions will require a training effort from the health professionals, dentists, assistants, and prosthetists. It was reported that 2 weeks of training would be necessary to use the software for orthognathic surgery (Xia et al., 2006). However, it is unclear if dental practitioners are ready to such evolutions in their daily practice, as it could reduce clinical time for simulation and virtual planning. Consequently, a growing number of companies is emerging to plan and send surgical guides to dental practitioners, but it raises questions as to the responsibility in cases of failure.

### **Ethical issues in precision medicine**

Following the rise of computing power, an increasing amount of data are being generated, which led to a new trend for data-driven models, not only based on physical properties but also factors related to the medical or dental history of the patient (Schwendicke & Krois, 2022). Nonetheless, this trend raises several legal and ethical questions as to the use and potential applications of such models, but these considerations are unfortunately rarely discussed in the development of PSM, mainly because the medical and dental communities remain “ill-informed” about the ethical complexities that budding AI or PSM technologies can introduce (Mörch et al., 2021). PSM software are likely to require an additional cost for the patient, whereas the development of PSM may use a patient data and medical information to be calibrate and then commercialize the software without having directly paid these patients. This additional cost for treatment could aggravate the inequalities in access to healthcare (Schwendicke et al., 2020), but the economic discrimination could be even worse if these models begin to be used by insurance companies to justify higher premiums in cases where there

is a greater risk of treatment failure. Numerous laws such as the Artificial Intelligence Act in Europe are currently under development to protect patients and regulate research, but the exact definition of AI is difficult to establish and is a rapidly evolving technology that makes it hard for governments to remain well informed. States, digital dentistry companies, and the field of dental research must therefore collaborate to provide full transparency for both patients and practitioners through detailed and exhaustive informed consent and ethical approval (Mörch et al., 2021). This collective effort might help reduce ethical concerns and misconception, which could thus strengthen confidence between industry, clinicians, and patients.

## **CONCLUSION**

The growing use of CBCT in clinical practice has opened doors to gathering the data required to develop patient-specific models based on anatomical, biomechanical, aesthetic, and other derived patient-specific parameters. PSM may allow optimized surgical treatment planning, increase predictability, and potentially lower risks of pre- and post-operative complications. Recent advancements in the fields of AI may allow for the automation of several parts of these laborious modeling technologies, bringing user-assisted decision-support tools closer than ever to both clinicians and researchers. More research is still needed to develop *in vivo* protocols to enable implementation and clinical validation of PSM in dental practice. At the same time, ethical and legal constraints should be carefully considered when applying data-driven models in current clinical practice.

## REFERENCES

1. Kishore M, Panat SR, Aggarwal A et al (2014) Evidence based dental care: integrating clinical expertise with systematic research. *J Clin Diagn Res* 8:259–262.
2. Hilton TJ, Funkhouser E, Ferracane JL et al (2020) Recommended treatment of cracked teeth: results from the national dental practice-based research network. *J Prosthet Dent* 123:71–78.
3. Versiani MA, Cavalcante DM, Belladonna FG et al (2021) A critical analysis of research methods and experimental models to study dentinal microcracks. *Int J Endod* 55:178–226.
4. Ordinola-Zapata R, Lin F, Nagarkar S et al (2022) A critical analysis of research methods and experimental models to study the load capacity and clinical behaviour of the root filled teeth. *Int Endod J* 55:471–494.
5. von Arx T, Maldonado P, Bornstein MM (2020) Occurrence of vertical root fractures after apical surgery: a retrospective analysis. *J Endod* 47:239–246.
6. Yoshino K, Ito K, Kuroda M, Sugihara N (2015) Prevalence of vertical root fracture as the reason for tooth extraction in dental clinics. *Clin Oral Investig* 19:1405–1409.
7. Santos AFV, Tanaka CB, Lima RG et al (2009) Vertical root fracture in upper premolars with endodontic posts: finite element analysis. *J Endod* 35:117–120.
8. Benazzi S, Grosse IR, Gruppioni G et al (2014) Comparison of occlusal loading conditions in a lower second premolar using three-dimensional finite element analysis. *Clin Oral Investig* 18:369–375.
9. Chatvanitkul C, Lertchirakarn V (2010) Stress distribution with different restorations in teeth with curved roots: a finite element analysis study. *J Endod* 36:115–118.
10. Neal ML, Kerckhoffs R (2009) Current progress in patient-specific modeling. *Brief Bioinform* 11:111–126.
11. Baumgaertel S, Palomo JM, Palomo L, Hans MG (2009) Reliability and accuracy of cone-beam computed tomography dental measurements. *Am J Orthod Dentofacial Orthop* 136:18–19.
12. Zadpoor AA, Weinans H (2015) Patient-specific bone modeling and analysis: the role of integration and automation in clinical adoption. *J Biomech* 48:750–760.
13. Resnick CM, Inverso G, Wrzosek M, Padwa BL, Kaban LB, Peacock ZS

- (2016) Is there a difference in cost between standard and virtual surgical planning for orthognathic surgery? *J Oral Maxillofac Surg* 74:1827–1833.
14. Eggermont F, Derikx LC, Verdonschot N et al (2018) Can patient-specific finite element models better predict fractures in metastatic bone disease than experienced clinicians? *Bone Jt Res* 7:430–439.
  15. Trivedi S (2014) Finite element analysis: a boon to dentistry. *J Oral Biol Craniofacial Res* 4:200–203.
  16. Lahoud P, EzEldeen M, Beznik T et al (2021) Artificial intelligence for fast and accurate 3D tooth segmentation on CBCT. *J Endod* 47:825–827.
  17. Richert R, Farges JC, Tamimi F et al (2020) Validated finite element models of premolars: a scoping review. *Materials* 13:3280.
  18. Kinney JH, Marshall SJ, Marshall GW (2003) The mechanical properties of human dentin: a critical review and re-evaluation of the dental literature. *Crit Rev Oral Biol Med* 14:13–29.
  19. Erdemir A, Guess TM, Halloran J, Tadepalli SC, Morrison TM (2012) Considerations for reporting finite element analysis studies in biomechanics. *J Biomech* 45:625–633.
  20. de Rodrigues M, P, Soares PBF, Valdivia ADCM, et al (2017) Patient-specific finite element analysis of fiber post and ferrule design. *J Endod* 43:1539–1544.
  21. Knoops PGM, Papaioannou A, Borghi A et al (2019) A machine learning framework for automated diagnosis and computer-assisted planning in plastic and reconstructive surgery. *Sci Rep* 9:1–12.
  22. de Rodrigues M, P, Soares PBF, Gomes MAB, et al (2020) Direct resin composite restoration of endodontically-treated permanent molars in adolescents: bite force and patient-specific finite element analysis. *J Appl Oral Sci* 28:1–11.
  23. Merema BBJ, Kraeima J, Glas HH et al (2021) Patient-specific finite element models of the human mandible: lack of consensus on current setups. *Oral Dis* 27:42–51.
  24. Grassi L, Schileo E, Boichon C et al (2014) Comprehensive evaluation of PCA-based finite element modelling of the human femur. *Med Eng Phys* 36:1246–1252.
  25. Maquart T, Wenfeng Y, Elguedj T et al (2020) 3D volumetric isotopological meshing for finite element and isogeometric based reduced order modeling. *Comput Methods Appl Mech Eng* 362:112809.
  26. Tyas MJ, Burrow MF (2004) Adhesive restorative materials: a review. *Aust Dent J* 49:112–121.
  27. de Kuijper MCFM, Cune MS, Özcan M, Gresnigt MMM (2021) Clinical performance of direct composite resin versus indirect restorations on

- endodontically treated posterior teeth: a systematic review and meta-analysis. *J Prosthet Dent* 21:1–12.
28. Souza J, Fuentes MV, Baena E, Ceballos L (2021) One-year clinical performance of lithium disilicate versus resin composite CAD/CAM onlays. *Odontology* 109:259–270.
  29. Mikeli A, Walter MH, Rau A et al (2021) Three-year clinical performance of posterior monolithic zirconia single crowns. *J Prosthet Dent* 21:1–6.
  30. Sailer I, Makarov NA, Thoma DS et al (2015) All-ceramic or metal-ceramic tooth-supported fixed dental prostheses (FDPs)? A systematic review of the survival and complication rates. Part I: Single crowns (SCs). *Dent Mater* 31:603–623.
  31. Ausiello P, Rengo S, Davidson CL, Watts DC (2004) Stress distributions in adhesively cemented ceramic and resin-composite class II inlay restorations: a 3D-FEA study. *Dent Mater* 20:862–872.
  32. Barak MM, Geiger S, Chattah NLT et al (2009) Enamel dictates whole tooth deformation: a finite element model study validated by a metrology method. *J Struct Biol* 168:511–520.
  33. Magne P, Oganessian T (2009) Premolar cuspal flexure as a function of restorative material and occlusal contact location. *Quintessence Int* 40:363–370.
  34. Dioguardi M, Alovisi M, Troiano G et al (2021) Clinical outcome of bonded partial indirect posterior restorations on vital and non-vital teeth: a systematic review and meta-analysis. *Clin Oral Investig* 25:6597–6621.
  35. Morimoto S, Rebello De Sampaio FBW et al (2016) Survival rate of resin and ceramic inlays, onlays, and overlays: a systematic review and meta-analysis. *J Dent Res* 95:985–994.
  36. Lin CL, Chang WJ, Lin YS et al (2009) Evaluation of the relative contributions of multi-factors in an adhesive MOD restoration using FEA and the Taguchi method. *Dent Mater* 25:1073–1081.
  37. Shabbir J, Zehra T, Najmi N et al (2021) Access cavity preparations: classification and literature review of traditional and minimally invasive endodontic access cavity designs. *J Endod* 14:1229–1244.
  38. Moreno-Rabié C, Torres A, Lambrechts P, Jacobs R (2020) Clinical applications, accuracy and limitations of guided endodontics: a systematic review. *Int Endod J* 53:214–231.
  39. Fuss Z, Lustig J, Tamse A (1999) Prevalence of vertical root fractures in extracted endodontically treated teeth. *Int Endod J* 32:283–286.
  40. Kishen A (2006) Mechanisms and risk factors for fracture predilection in endodontically treated teeth. *Endod Top* 13:57–83.

41. Zhang Y, Liu Y, She Y et al (2019) The effect of endodontic access cavities on fracture resistance of first maxillary molar using the extended finite element method. *J Endod* 45:316–321.  
Necchi S, Taschieri S, Petrini L et al (2008) Mechanical behaviour of nickel-titanium rotary endodontic instruments in simulated clinical conditions: a computational study. *Int Endod J* 41:939–949.
42. Lee M, Versluis A, Kim B et al (2011) Correlation between experimental cyclic fatigue resistance and numerical stress analysis for nickel-titanium rotary files. *J Endod* 37:1152–1157.
43. Richert R, Farges JC, Villat C, Valette S, Boisse P, Ducret M (2021) Decision support for removing fractured endodontic instruments: a patient-specific approach. *Appl Sci* 11:2602.
44. Touati R, Fehmer V, Ducret M, Sailer I, Marchand L (2021) Augmented reality in esthetic dentistry: a case report. *Curr Oral Heal Reports* 8:23–28.
45. Touati R, Richert R, Millet C, Farges JC, Sailer I, Ducret M (2019) Comparison of two innovative strategies using augmented reality for communication in aesthetic dentistry: a pilot study. *J Healthc Eng* 7019046.
46. Richert R, Robinson P, Viguie G, Farges JC, Ducret M (2018) Multi-fiber-reinforced composites for the coronaradicular reconstruction of premolar teeth: a finite element analysis. *Biomed Res Int* 4302607.
47. Pegoretti A, Fambri L, Zappini G, Bianchetti M (2002) Finite element analysis of a glass fibre reinforced composite endodontic post. *Biomaterials* 23:2667–2682.
48. Richert R, Alshegri AA, Alageel O et al (2021) Analytical model of I-bar clasps for removable partial dentures. *Dent Mater* 37:1066–1072.
49. Alshegri AA, Alageel O, Caron E, Ciobanu O, Tamimi F, Song J (2018) An analytical model to design circumferential clasps for laser-sintered removable partial dentures. *Dent Mater* 34:1474–1482.
50. Srinivasan M, Schimmel M, Naharro M et al (2019) CAD/CAM milled removable complete dentures : time and cost estimation study. *J Dent* 80:75–79.
51. Rossini G, Parrini S, Castroflorio T, Deregibus A, Debernardi CL (2015) Efficacy of clear aligners in controlling orthodontic tooth movement: a systematic review. *Angle Orthod* 85:881–889.
52. Camardella LT, Rothier EKC, Vilella OV, Ongkosuwito EM, Breuning KH (2016) Virtual setup: application in orthodontic practice. *J Orofac Orthop* 77:409–419.
53. Ammar HH, Ngan P, Crout RJ, Mucino VH, Mukdadi OM (2011) Three-dimensional modeling and finite element analysis in treatment planning for

- orthodontic tooth movement. *Am J Orthod Dentofac Orthop* 139:59–71.
54. Feng Y, Kong WD, Cen WJ et al (2019) Finite element analysis of the effect of power arm locations on tooth movement in extraction space closure with miniscrew anchorage in customized lingual orthodontic treatment. *Am J Orthod Dentofac Orthop* 156:210–219.
  55. Barone S, Paoli A, Razionale AV, Savignano R (2017) Computational design and engineering of polymeric orthodontic aligners. *Int J Numer Method Biomed Eng* 33:1–15.
  56. Sailer I, Karasan D, Todorovic A et al (2022) Prosthetic failures in dental implant therapy *Periodontol* 2000(1):130–144.
  57. Ueda T, Kremer U, Katsoulis J et al (2011) Long-term results of mandibular implants supporting an overdenture: implant survival, failures, and crestal bone level changes. *Int J Oral Maxillofac Implants* 26:365–372.
  58. Amaral CF, Gomes RS, Rodrigues Garcia RCM, Del Bel Cury AA (2018) Stress distribution of single-implant retained overdenture reinforced with a framework: a finite element analysis study. *J Prosthet Dent* 119:791–796.
  59. Eraslan O, Inan Ö (2010) The effect of thread design on stress distribution in a solid screw implant: a 3D finite element analysis. *Clin Oral Investig* 14:411–416.
  60. Kuroshima S, Kaku M, Ishimoto T et al (2017) A paradigm shift for bone quality in dentistry: a literature review. *J Prosthodont Res* 61:353–362.
  61. Roy S, Dey S, Khutia N, Roy A, Datta S (2018) Design of patient specific dental implant using FE analysis and computational intelligence techniques. *Appl Soft Comput J* 65:272–279.
  62. Cheng K, Liu Y, Wang R, Zhang J, Jiang X (2020) Topological optimization of 3D printed bone analog with PEKK for surgical mandibular reconstruction. *J Mech Behav Biomed Mater* 107:103758.
  63. Tamura N, Takaki T, Takano N, Shibahara T (2018) Three-dimensional finite element analysis of bone fixation in bilateral sagittal split ramus osteotomy using individual models. *Bull Tokyo Dent Coll* 59:67–78.
  64. Andersson L (2013) Epidemiology of traumatic dental injuries. *J Endod* 39:S2-5.
  65. Torabinejad M, Nosrat A, Verma P, Udochukwu O (2017) Regenerative endodontic treatment or mineral trioxide aggregate apical plug in teeth with necrotic pulps and open apices: a systematic review and meta-analysis. *J Endod* 43:1806–1820.
  66. Mendoza-Mendoza A, Solano-Reina E, Iglesias-Linares A, Garcia-Godoy F, Abalos C (2012) Retrospective long-term evaluation of autotransplantation of premolars to the central incisor region. *Int Endod J*

- 45:88–97.
67. EzEldeen M, Wyatt J, Al-Rimawi A et al (2019) Use of CBCT guidance for tooth autotransplantation in children. *J Dent Res* 98:406–413.
  68. Jamshidi D, Homayouni H, Majd NM (2018) Impact and fracture strength of simulated immature teeth treated with mineral trioxide aggregate apical plug and fiber post versus. *J Endod* 44:1878–1882.
  69. Mello I, Michaud P, Butt Z (2020) Fracture resistance of immature teeth submitted to different endodontic procedures and restorative protocols. *J Endod* 46:1465–1469.
  70. Demirel A, Bezgin T, Sari Ş (2021) Effects of root maturation and thickness variation in coronal mineral trioxide aggregate plugs under traumatic load on stress distribution in regenerative endodontic procedures: A 3-dimensional finite element analysis study. *J Endod* 47:492–499.
  71. Belli S, Eraslan O, Eskitaşcıoğlu G (2018) Effect of different treatment options on biomechanics of immature teeth: a finite element stress analysis study. *J Endod* 44:475–479.
  72. Anthrayose P, Nawal RR, Yadav S, Talwar S, Yadav S (2021) Effect of revascularisation and apexification procedures on biomechanical behaviour of immature maxillary central incisor teeth: a three-dimensional finite element analysis study. *Clin Oral Investig* 26.
  73. Shen L, He F, Zhang C, Jiang H, Wang J (2018) Prevalence of malocclusion in primary dentition in mainland China, 1988– 2017: a systematic review and meta-analysis. *Sci Rep* 8:2–11.
  74. Kuralt M, Fidler A (2021) Assessment of reference areas for superimposition of serial 3D models of patients with advanced periodontitis for volumetric soft tissue evaluation. *J Clin Periodontol* 48:765–773.
  75. Tarce M, Merheb J, Meeus M et al (2022) Surgical guides for guided bone augmentation: an *in vitro* study. *Clin Oral Implants Res* 5:558–567.
  76. Schmidt F, Lapatki BG (2019) Effect of variable periodontal ligament thickness and its non-linear material properties on the location of a tooth's centre of resistance. *J Biomech* 94:211–218.
  77. Ren LM, Wang WX, Takao Y, Chen ZX (2010) Effects of cementum-dentine junction and cementum on the mechanical response of tooth supporting structure. *J Dent* 38:882–891.
  78. Nikolaus A, Currey JD, Lindtner T, Fleck C, Zaslansky P (2017) Importance of the variable periodontal ligament geometry for whole tooth mechanical function: a validated numerical study. *J Mech Behav Biomed Mater* 67:61–73.

79. Genco R (2000) Borgnakke W (2014) Risk factors for periodontal disease. *Periodontol* 2014(4):59–94.
80. Celikten B, Jacobs R, deFaria VK, Huang Y, Nicolielo LFP, Orhan K (2017) Assessment of volumetric distortion artifact in filled root canals using different cone-beam computed tomographic devices. *J Endod* 43:1517–1521.
81. Celikten B, Jacobs R, de Faria VK et al (2019) Comparative evaluation of cone beam CT and micro-CT on blooming artifacts in human teeth filled with bioceramic sealers. *Clin Oral Investig* 23:3267–3273.
82. Rangel FA, Maal TJJ, Bronkhorst EM et al (2013) Accuracy and reliability of a novel method for fusion of digital dental casts and cone beam computed tomography scans. *PLoS ONE* 8:1–7.
83. Buchgreitz J, Buchgreitz M, Mortensen D, Bjørndal L (2016) Guided access cavity preparation using cone-beam computed tomography and optical surface scans – an ex vivo study. *Int Endod J* 49:790–795.
84. Ezhov M, Gusarev M, Golitsyna M et al (2021) Clinically applicable artificial intelligence system for dental diagnosis with CBCT. *Sci Rep* 11:1–16.
85. Lee SKY, Salinas TJ, Wiens JP (2021) The effect of patient specific factors on occlusal forces generated: best evidence consensus statement. *J Prosthodont* 30:52–60.
86. Murakami N, Wakabayashi N (2014) Finite element contact analysis as a critical technique in dental biomechanics: a review. *J Prosthodont Res* 58:92–101.
87. Vukicevic AM, Zelic K, Milasinovic D et al (2021) OpenMandible: an open-source framework for highly realistic numerical modelling of lower mandible physiology. *Dent Mater* 37:612–624.
88. Calka M, Perrier P, Ohayon J, Grivot-Boichon C, Rochette M, Payan Y (2021) Machine-learning based model order reduction of a biomechanical model of the human tongue. *Comput Methods Programs Biomed* 105786.
89. Badrou A, Bel-Brunon A, Hamila N, Tardif N, Gravouil A (2020) Reduced order modeling of an active multi-curve guidewire for endovascular surgery. *Comput Methods Biomech Biomed Engin* 23:S23–24.
90. Bergomi M, Cugnoni J, Botsis J, Belser UC, Anselm Wiskott HW (2010) The role of the fluid phase in the viscous response of bovine periodontal ligament. *J Biomech* 43:1146–1152.
91. Viceconti M, Olsen S, Nolte LP, Burton K (2005) Extracting clinically relevant data from finite element simulations. *Clin Biomech* 20:451–454.
92. Chang Y, Tambe AA, Maeda Y, Wada M, Gonda T (2018) Finite element analysis of dental implants with validation: to what extent can we expect

- the model to predict biological phenomena? A literature review and proposal for classification of a validation process. *Int J Implant Dent* 4:1–7.
93. Boudissa M, Bahl G, Oliveri H et al (2021) Virtual preoperative planning of acetabular fractures using patient-specific biomechanical simulation : a case-control study. *Orthop Traumatol Surg Res* 107:1–6.
  94. Derycke L, Sénémaud J, Perrin D et al (2020) Patient specific computer modelling for automated sizing of fenestrated stent grafts. *Eur J Vasc Endovasc Surg* 59:237–246.
  95. Xia JJ, Phillips CV, Gateno J et al (2006) Cost-effectiveness analysis for computer-aided surgical simulation in complex cranio- maxillofacial surgery. *J Oral Maxillofac Surg* 64:1780–1784.
  96. Park SY, Hwang DS, Song JM, Kim UK (2019) Comparison of time and cost between conventional surgical planning and virtual surgical planning in orthognathic surgery in Korea. *Maxillofac Plast Reconstr Surg* 41:1–7.
  97. Sheth B, Lavin AC, Martinez C, Sabesan VJ (2022) The use of preoperative planning to decrease costs and increase efficiency in the OR. *JSES Int* 6:454–458.
  98. Schwendicke F, Krois J (2022) Precision dentistry—what it is, where it fails (yet), and how to get there. *Clin Oral Investig* 26:3395–3403.
  99. Mörch CM, Atsu S, Cai W et al (2021) Artificial intelligence and ethics in dentistry: a scoping review. *J Dent Res* 100:1452–1460.

## CHAPTER II | Finite Element Models: A Road to In-Silico Modeling in The Age of Personalized Dentistry

*This chapter is based on the following publication: **Lahoud P, Faghihian H, Richert R, Jacobs R, EzEldeen M. Finite element models: A road to in-silico modeling in the age of personalized dentistry. Journal of Dentistry. 2024 Sep 5:105348.***

### Affiliations

1. OMFS-IMPACT Research Group, Department of Imaging and Pathology, Faculty of Medicine, KU, Leuven, Belgium
2. Department of Oral and Maxillofacial Surgery, University Hospitals Leuven, Leuven, Belgium
3. Division of Periodontology and Oral Microbiology, Department of Oral Health Sciences, KU Leuven, Leuven, Belgium
4. Department of Dental Medicine, Karolinska Institute, Stockholm, Sweden
5. Laboratoire de Mécanique Des Contacts Et Structures, UMR 5259, CNRS/INSA, Villeurbanne, France
6. Hospices Civils de Lyon, PAM d'Odontologie, Lyon, France
7. Faculty of Odontology, Lyon 1 University, Lyon, France
8. Department of Oral Health Sciences, KU Leuven and Paediatric Dentistry and Special Dental Care, University Hospitals Leuven, Leuven, Belgium

# Finite Element Models: A Road to In-Silico Modeling in The Age of Personalized Dentistry

*Lahoud P, Faghihian H, Richert R, Jacobs R, EzEldeen M.*

## **ABSTRACT**

**Aim(s):** This article reviews the applications of Finite Element Models (FEMs) in personalized dentistry, focusing on treatment planning, material selection, and CAD-CAM processes. It also discusses the challenges and future directions of using Finite Element Analysis (FEA) in dental care.

**Materials and Methods:** This study synthesizes current literature and case studies on FEMs in personalized dentistry, analyzing research articles, clinical reports, and technical papers on the application of FEA in dental biomechanics. Sources for this review include peer-reviewed journals, academic publications, clinical case studies, and technical papers on dental biomechanics and Finite Element Analysis. Studies were selected based on their relevance to the application of FEMs in personalized dentistry. Inclusion criteria were studies that discussed the use of FEA in treatment planning, material selection, and CAD-CAM processes in dentistry. Exclusion criteria included studies that did not focus on personalized dental treatments or did not utilize FEMs as a primary tool.

**Results:** FEMs are essential for personalized dentistry, offering a versatile platform for in-silico dental biomechanics modeling. They can help predict biomechanical behavior, optimize treatment outcomes, and minimize clinical complications. Despite needing further advancements, FEMs could help significantly enhance treatment precision and efficacy in personalized dental care.

**Conclusion(s):** FEMs in personalized dentistry hold the potential to significantly improve treatment precision and efficacy, optimizing outcomes and reducing complications. Their integration underscores the need for interdisciplinary collaboration and advancements in computational techniques to enhance personalized dental care.

## INTRODUCTION

Finite Element Analysis (FEA) is a numerical computational method widely used in engineering to map stress distributions, displacements, and deformations in response to different mechanical loads (Keshavarzian et al., 2019; Mengoni, 2020). In recent years, FEA has gained prominence in biomedical engineering for gaining insight into tissue stress distribution patterns, optimizing medical and dental procedures, and improving the design of biomaterials used inside the human body (Szabó & Babuška, 2021).

In the context of healthcare, in-silico modeling uses computational methods to predict physiological outcomes (Geris et al., 2018; Lahoud et al., 2024). This approach ranges from physical modeling, which incorporates fundamental scientific laws, to data-driven modeling, which relies on experimental input/output data from the real world (Solle et al., 2017). As a physics-based modeling approach that numerically solves differential equations, FEA aligns with the principles of Industry 4.0 (Schwab, 2017) and Digital Twin technology (Maddahi & Chen, 2022; Mora-Macías et al., 2020), which involve creating virtual representations of physical objects to simulate and predict their behavior in various applications. These advancements have made FEA a valuable translational research tool to bridge fundamental sciences with clinical applications, particularly in dentistry (Figure 1).

FEA subdivides a complex system into smaller units, called finite elements, to simplify and speed up analysis. This process is achieved by discretization, which involves converting a continuous model with an infinite degree of freedom into discrete elements by building a mesh around the object. Meshing is a fundamental step in FEA that allows equations to be applied to each element. By calculating each element, the results are systematically recombined and extrapolated into a global system to determine the final equation according to the model (Szabó & Babuška, 2021).

Three distinct ways can be used to obtain models for FEA in dental applications (Yang, 2019):

- Geometrical models: The studied objects or tissues are simplified into rudimentary mathematical shapes, like cubes, paraboloids, and spheres. This approach allows for faster model generation but may not provide accurate results for complex objects.
- Anatomical simplified models: Based on the mean average dimension of specific tissues. This modeling system can help obtain results faster; however, in case of abnormalities or variabilities in tissue morphology, the accuracy of the modeling and the obtained results will be significantly reduced.
- Anatomically corrected models: A factual 3D representation of the tissue(s) of interest. Although FEA operation takes more time with this approach, it gives the most accurate results compared to the previously described methods.

Advancements in imaging modalities, such as computed tomography (CT) and magnetic resonance imaging (MRI), coupled with accurate segmentation software and powerful workstations, have made it feasible to generate anatomically corrected models for FEA (Zysset et al., 2015). In dental research, FEA has provided new insights into oral and maxillofacial biomechanical properties, such as understanding the impact of dental implants on bone stress distribution. The workflow needed to conduct FEA in dental research is illustrated in Figure 2.

Despite the increasing availability of advanced medical imaging tools and computational resources, a limited number of studies have evaluated FEA as a tool for personalized dentistry. This review aims to cover FEA studies for customized applications in various fields of dentistry. We will discuss the current state of FEA research in dental biomechanics, endodontics, orthodontics, and other relevant areas, highlighting the potential of FEA in offering more personalized dental and maxillofacial treatments.

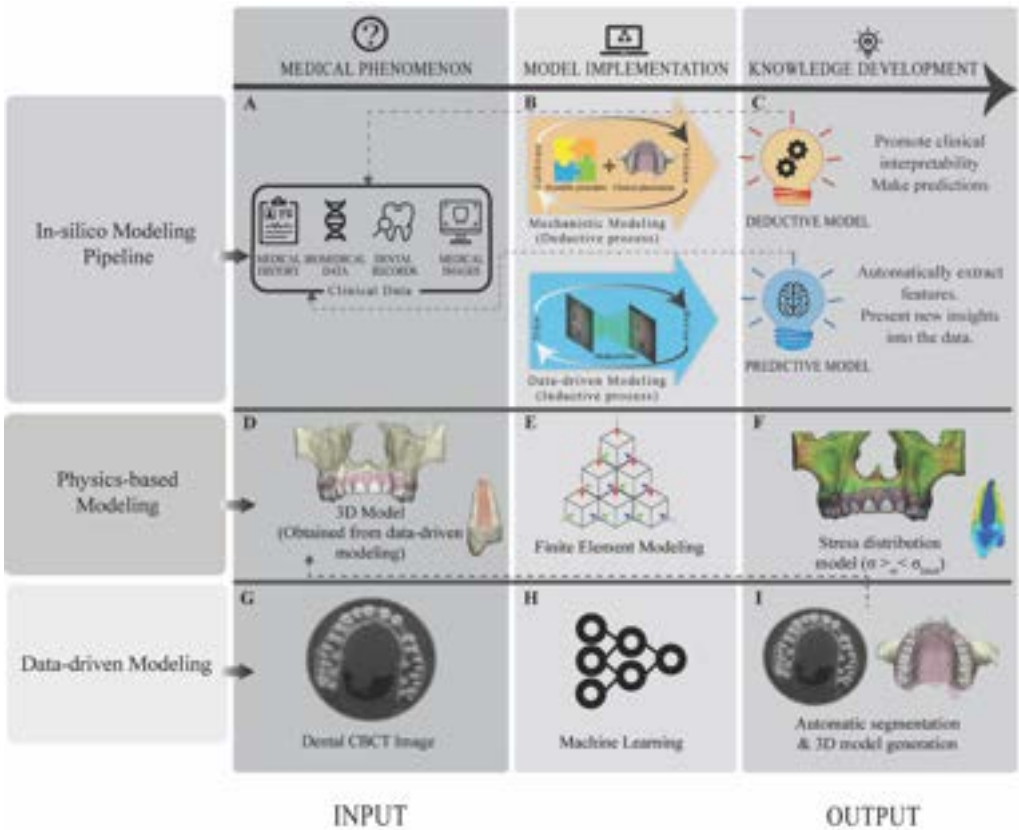


**Figure 1.** The overall architecture of in-silico modeling with examples of its two pillars, physics-based and data-driven modeling, in dentistry. Quantified or digital medical data, such as patient medical records, medical images, or genetic data, can be deployed in in-silico modeling (A). Physics-based modeling exerts proven scientific concepts on the input data, while data-driven modeling looks for hidden patterns in the data to create rational, empirical results that may be used (B). Its modeling results in a deductive model that promotes clinical interpretation and predictability (C). As an illustration of physics-based modeling, a digital 3D model consisting of digital values in mathematical space (D) can be investigated via finite element modeling (E) to explore the impact of oral biomechanical loads. Based on principles derived from materials science, this modeling system computes strain-displacement relations in response to any given external load. The outcome of this modeling is a stress distribution map that assists the dentist in interpreting the component's long-term prognosis according to the stress levels and location (F). For data-driven modeling, dental CBCTs (G) can be imported in validated machine- and deep neural network systems (H) that can (I) automatically segment anatomical structures and produce 3D models. Interestingly, the results of one modeling technique may be used as input for another approach.

## **MATERIALS AND METHODS**

### **Search Strategy**

An extensive literature search was conducted across several academic databases, including PubMed, Scopus, and Web of Science, to ensure comprehensive coverage of the topic. The search employed specific keywords and phrases such as “finite element”, “finite element modeling”, “in-silico modeling”, “personalized dentistry”, “biomechanics in dentistry”, “dental biomechanics” and “patient-specific dental models”. Boolean operators (AND, OR, NOT) were used to refine the search results, capturing relevant literature while excluding irrelevant studies. The search strategy was initially broad, with no publication date limitations, to include seminal works and identify trends over time. Emphasis was later placed on studies published in the last two decades to focus on the latest advancements in the field.

### **Inclusion Criteria**

The review included only peer-reviewed articles, conference proceedings, and high-quality reviews. Studies were selected based on their relevance to the topics of FEA, in-silico modeling, and personalized dentistry. Emphasis was placed on works that contributed to the understanding of these areas, particularly those published within the last two decades to reflect recent advancements.

### **Exclusion Criteria**

Studies that did not meet the relevance criteria, such as those outside the scope of FEA and personalized dentistry, were excluded. Non-peer-reviewed articles, editorials, opinion pieces, and studies lacking rigorous scientific methodology were also excluded from the review.

## Study Selection and Data Extraction

After conducting the initial search, the titles and abstracts of the retrieved studies were screened for relevance. Full texts of potentially relevant articles were then reviewed in detail to confirm their inclusion. Data extraction focused on capturing key findings, methodologies, and conclusions related to FEA, in-silico modeling, and personalized dentistry. References of the selected articles were manually reviewed to identify additional studies that might have been missed during the initial search.

## Data Synthesis

The data from the included studies were synthesized to provide a comprehensive overview of the current state of research in FEA, in-silico modeling, and personalized dentistry in the different sub-fields of dentistry. Trends, gaps, and advancements in these fields were identified, with an emphasis on how recent developments could impact clinical practice in personalized dentistry. The synthesized data were used to draw conclusions, discuss current limitations and suggest directions for future research.

### Workflow of Finite Element Analysis

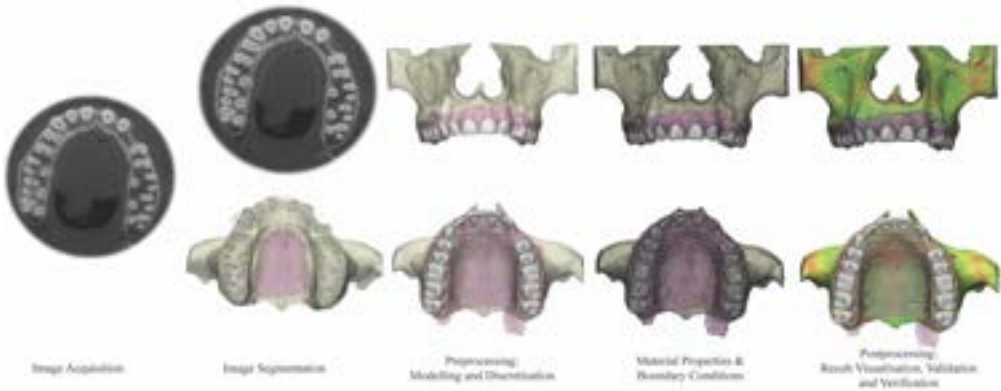


**Figure 2.** Workflow of using finite element analysis for analyzing biomechanical responses to given stimuli, in a patient-specific manner.

## RESULTS

### Applications of FEM in Dentistry

#### *Endodontics*

Mechanical preparation of the tooth's root canal system is essential to root canal therapy, in addition to chemical treatment. The process can be assessed in terms of access cavity preparation, root canal instrumentation, and canal obturation. Each step adds mechanical constraints and can jeopardize the tooth's long-term survival rate to a certain degree (Hiebert et al., 2017). Vertical root fractures, for instance, are a relatively common endodontic failure primarily caused by overloading regions with low fracture resistance, rendering the remaining dental tissues more susceptible to developing microcracks and craze lines (von Arx et al., 2012; von Arx et al., 2021).

Performing FEA before endodontic treatment could help dentists identify compromised regions of the tooth, potentially guiding them in deciding on the technique and materials to maximize the treatment's success rate for specific cases. Advancements in high-resolution CT and CBCT devices, along with accurate segmentation software (Lahoud, Diels, et al., 2022; Lahoud et al., 2021; Lahoud, Jacobs, et al., 2022; Leite et al., 2020), have made it possible to produce three-dimensional (3D) models of specific dental structures, such as enamel, dentin, pulp tissues (root canal system), bone, and biomaterials used for accurate finite element modeling (Duan et al., 2021; Preda et al., 2022; Xu et al., 2018).

Minimally Invasive Endodontics (MIE) has also been recently proposed as a novel approach to preserve dental tissue integrity more effectively (Gluskin et al., 2014). However, MIE introduces challenges for dentists in locating foramen(s), achieving straight-line access, and ensuring adequate root canal preparation (Anjum et al., 2019; Gluskin et al., 2014). The high variability in

tooth morphology and canal anatomy (Peters, 2004) makes decision-making on the potential use of MIE for specific teeth challenging when there aren't significant biomechanical differences between traditional and MIE approaches.

Qian Wang and co-workers (Qian Wang et al., 2020) evaluated the effect of access cavity shapes and different canal tapering using an in-silico modeling approach. They first acquired micro-CT images of extracted maxillary first molars and used biomedical modeling software to simulate various access cavity modifications (conservative vs. conventional) and different canal enlargements on the three-dimensional (3D) STL file. The reconstructed treated models underwent FEA in response to an 800N vertical force on four occlusal points for biomechanical analysis. While this ex-vivo approach was used for one specific extracted tooth (maxillary first molar), the concept appears translatable in clinical practice, aiding dentists in choosing the best treatment approach.

FEA combined with in-silico modeling can also be helpful for endodontists in selecting the appropriate rotary file system. NiTi alloy is the most common material for rotary files (Patil et al., 2017); since each proprietary system has unique geometrical features, different stress and strain profiles are expected during canal preparation. FEA has been used to study the biomechanical behavior of rotary files, incorporating static bending, torsion, and/or bending-torsion forces on the file model to mimic clinical conditions (Celikten et al., 2022; Jiang et al., 2018; Richert et al., 2022; Q. Wang et al., 2020). However, these studies only investigated the files' biomechanical behavior under static testing properties. Current research aims to enhance the file models by incorporating them into a virtual model mimicking the root canal, measuring reaction torque, von Mises stress, and the principal strain on dental tissues (Kim et al., 2010). A file generating higher values on the dentinal wall suggests a higher susceptibility to causing more crack lines on the dentine and possibly leading to vertical root fractures. Technological advancements in

FEA and in-silico modeling enable accurate modeling of any tooth's root canal morphology, allowing practitioners to study which rotary file system in their office and under their specific workflow would cause the least stress on dental tissues while performing optimal root canal therapy.

### *Periodontology*

One of the primary functions of the periodontium is the absorption and distribution of masticatory forces (da Rocha et al., 2021). Biomechanical masticatory forces generated during mastication are transferred from the dental occlusal surfaces to the underlying periodontal ligament (PDL) and, ultimately, to the alveolar bone and surrounding structures (da Rocha et al., 2021).

In healthy physiological conditions, the periodontal complex plays a vital role in maintaining the stability of teeth and preserving homeostatic behavior in response to physiological loads (da Rocha et al., 2021). Damage to the PDL can result in periodontitis, dental/bony resorptions, tooth mobility/loss, malocclusion, and myalgia (Hatch et al., 2001; Organization, 2013). Occlusal trauma (OT) has been identified as a factor that may compromise periodontal health, potentially initiating or progressing periodontal diseases (Ericsson, 1986; Glickman, 1965; Glickman & Smulow, 1969; Nyman et al., 1978). Primary OT occurs when the occlusal forces exceed the threshold of tolerance, while secondary OT is observed when tissues cannot withstand physiological loads due to their weakened state (Polson, 1986). It has been shown that OT increases hydrostatic pressure, quickly inducing osteoclastic stimulation within the bone marrow toward the PDL (Latuta et al., 2022). Once resorption reaches the PDL, sudden and often significant tooth mobility may be observed (Crespo Vázquez et al., 2011). Despite advancements in periodontal therapy in general and regenerative periodontal techniques in particular, treatment of clinical attachment loss and bone regeneration around teeth remains challenging (Van Dyke et al., 2015). Although OT is a widely accepted

fundamental concept, it is often less tangible in clinical practice due to its primarily silent and chronic nature. Suenaga and colleagues (Suenaga et al., 2015) conducted biomechanical analyses on in vivo PET/CT scans of the mandible bone subjected to biomechanical stimuli, demonstrating that FEA could provide valuable information regarding tissue activity. Moreover, FEA based on 3D models has been extensively employed to study the potential effects of mechanical forces on the periodontium (Kondo & Wakabayashi, 2009; Ona & Wakabayashi, 2006; Papadopoulou et al., 2013; Poiate et al., 2008; Tajima et al., 2009).

While most FEA-based studies have only investigated biomechanical forces with a constant value and fixed loading direction (e.g., following the vertical axis of the tooth), the variability and complexity of dental movements can generate different intensities of occlusal loads and in various directions (e.g., parafunction or traumatic occlusion), potentially affecting the periodontal apparatus in multiple ways (Ortún-Terrazas et al., 2020). Additionally, the anatomy of the oral and maxillofacial tissues plays a significant role. For instance, Tribst and co-workers (da Rocha et al., 2021) showed that an increase in crestal bone loss leads to increased stress concentration on the surrounding bone. Oral biomechanics, therefore, is an essential factor that can affect periodontal health status, which plays a critical role alongside other determinants, including pH, temperature, microbiological profile, and antagonist tooth biomaterials (Wong et al., 2021).

### ***Implantology***

Osseointegration is a significant factor in determining the success of an implant, that is, the complete structural and functional attachment of an implant to the surrounding bone without connective tissue interference (Breinemark et al., 1969; Davies, 2003). Studies have shown that mechanical loads significantly influence osseointegration (Li et al., 2020), while stresses from neighboring oral and maxillofacial components (muscles, soft tissues,

etc) could influence bone remodeling following guided bone regeneration (GBR) procedures (Calciolari et al., 2023; Quirynen et al., 2023; Yu et al., 2023). It has been shown, for instance, that stress-shielding phenomena are more prominent when the bone-implant contact ratio value is low, which may disrupt osseointegration and lead to bone loss around implants (Lee et al., 2012; Misch et al., 2005). The influence of biomechanical load on implant lifetime and bone remodeling has been the focus of many FEA investigations. FEA research in implantology has revealed that the geometry and constitutive behavior of bone and implant, in addition to the loading situations, are primary determinants of biomechanical response (Marcian et al., 2021; Marcian et al., 2018; Ueda et al., 2017).

The thickness of the cortical and trabecular bone also plays an essential role in the stress and strain profile following mechanical loading scenarios (Lee et al., 2021; Ueda et al., 2017). Indeed, implant osteointegration mainly occurs at the level of the trabecular bone. It is, therefore, vital to emphasize the effect of the trabecular architectural network on the stress distribution profile. Lekholm & Zarb introduced a qualitative classification for the alveolar bone, classifying it into four groups (D1- D4) based on cortical bone thickness and trabecular bone density (Lekholm, 1985). Several studies include this classification on the implant finite element model, evaluating the biomechanical response for each bone quality (Gomez-Polo et al., 2016; Junior et al., 2016; Linetskiy et al., 2017). Furthermore, alveolar bone mechanobiology has been further investigated by performing FEA on models obtained from high-resolution micro-CT images obtained from cadaveric bone segments (Linetskiy et al., 2017; Marcian et al., 2021). Micro-CT imaging aids in developing finite element models consisting of cortical and trabecular bone with better dimensional accuracy compared to conventional CT imaging. Utilizing these models as input and combining them into intricate in-silico models can potentially elucidate the impact of trabecular bone microstructure networks on dental implants. However, due to the excessive

radiation exposure inherent to such imaging techniques, their use remains limited to cadaver studies and is therefore not applicable in clinical settings. Implant geometry and materials are also important in the stress/strain profile at the bone-implant interface (Fabris et al., 2022; GÜngör & Yılmaz, 2016; Marcian et al., 2021; Tekin et al., 2019). Dental implants demonstrate high variability in terms of diameter, length, thread length, thread pitch, number of components, type of connector, tapering, and the biomaterials/coatings used in the manufacture. Each of the aforementioned factors can directly and indirectly impact biomechanical stress and implant stability in the long term. CAD dental implant geometry and prosthetic components files could be used to simulate accurate patient-specific FE models and critically evaluate the possibilities before implant surgery.

We refer the reader to a recent review on FEA application in implant dentistry written by Falcinelli and co-workers to address several aspects of FE modeling in implant dentistry, such as bone and implant geometry, their constitutive behavior, boundaries, and loading condition (Falcinelli et al., 2023).

However, and despite being a powerful modeling tool, FEA has notable limitations in implantology, particularly in simulating dynamic loading effects (Falcinelli et al., 2023; Galbusera et al., 2014). One major challenge is the accurate representation of complex biomechanical behaviors under varying load conditions, such as those experienced during mastication and/or bruxism. Also, FEA models often assume static or simplified loading scenarios, which do not fully capture the time-dependent and cyclic nature of real-world forces on dental implants (Li et al., 2019). Additionally, accurately modeling the interface between the implant and bone, considering factors like osseointegration and bone remodeling, remains difficult (Galbusera et al., 2014). The material properties of biological tissues, which are heterogeneous and anisotropic, further complicate the simulations (Marcian et al., 2021). These limitations can lead to discrepancies between FEA predictions and clinical outcomes, underscoring the need for more advanced modeling

techniques and validation through experimental data (Li et al., 2019; Marcian et al., 2021; Marcian et al., 2018).

### ***Restorative Dentistry and Prosthodontics***

The advent of computer-aided design/computer-aided manufacturing (CAD/CAM) marked a turning point in the use of digital systems in dentistry, particularly for restorative and prosthetic works. CAD/CAM has been fully embraced as a chairside tool for preparing veneers, crowns, and bridges, aiming to achieve high-quality restorations while reducing delivery time and the number of consultations (Fasbinder, 2010; Van Noort, 2012).

CAD/CAM is based on three pillars: (I) Data acquisition, which involves obtaining 3D digital models of teeth and surrounding periodontal tissues, primarily using intraoral scanners. (II) Data processing is during which the dentist and/or dental technician designs the restoration with the desired features, and finally, (III) the manufacturing phase, where the predesigned restoration is manufactured accordingly.

The manufacturing process can involve Subtractive Manufacturing, where a material block is shaped to achieve the final morphology, or Additive Manufacturing, where thin layers of a specific material are deposited upon each other to create the final restoration in 3D. A wide range of materials, including ceramics, resin-infiltrated ceramics, composite resins, and metals, are used depending on each manufacturing system, each encompassing different biomechanical properties (Sulaiman, 2020).

Clinically, endodontically treated teeth have shown more susceptibility to biomechanical failures than their vital counterparts, primarily due to reduced water content and compromised structural integrity. Different tooth preparation modifications have been found to affect stress distribution patterns, leading to variability in the longevity of the tooth and its restoration (ElAyouti et al., 2011; Eraslan et al., 2011; Lin et al., 2009; Lin et al., 2010). Such preparation changes include cervical finish lines, cusp reduction level and angle, and endodontic cavity preparation (shape, depth). These

modifications influence the long-term success rate of CAD/CAM restorations (Ichim et al., 2006; Oyar et al., 2014; Zarone et al., 2005).

Therefore, biomechanical considerations are essential when preparing and designing dental restorations. FEA can be integrated into the data processing stages of CAD/CAM restorations to optimize their biomechanical performance. In a recent study, Karaer and co-workers created an input model for FEA by merging the implant, abutment, abutment screw, and crown, which had been designed in a CAD software with the 3D human teeth model obtained from a CT scan; followed by which the authors measured the stress levels and distributions in the bone, fixture, and abutment for each of the resin composite blocks (Karaer et al., 2023). In a similar approach, Zupancic and co-workers studied the biomechanical performance of short implant-supported, 3-unit, fixed CAD/CAM prostheses in the posterior mandible in response to vertical and oblique biomechanical loads. According to their results, the biomechanical response can vary based on individual patient-specific parameters (Zupancic Cepic et al., 2022).

The biomechanical properties of materials are thus paramount for the durability, functionality, and aesthetics of dental restorations and prostheses. A substantial body of literature explores the mechanical properties of materials such as dental ceramics, composites, metals, and polymers (Karaer et al., 2023; Li et al., 2005; Lin et al., 2010; Zarone et al., 2005). Publications examining dental ceramics, for instance, often highlight their high compressive strength and fracture resistance, which make them suitable for dental crowns and bridges (Lin et al., 2010; Oyar et al., 2014). Studies on composite resins emphasize their versatility and improved wear resistance, which are crucial for fillings and veneers (Zarone et al., 2005). Metals, particularly gold alloys and cobalt-chromium, are noted for their exceptional strength and toughness, suitable for frameworks in removable and fixed prostheses. Polymers, including PMMA, are frequently investigated for their application in denture bases due to their favorable aesthetics and ease of manipulation (Ichim et al., 2006; Tekin et al., 2019; Zarone et al., 2005).

Understanding these biomechanical properties through rigorous research aids clinicians and dental technicians in selecting appropriate materials based on specific clinical requirements, ensuring optimal patient outcomes. The continual advancement in material science, guided by empirical data therefore drives innovation in material selection and prosthetic design, enhancing the overall effectiveness and longevity of dental restorations.

### ***Orthodontics***

The principles of biomechanics form the core of orthodontics. All orthodontic appliances, from fixed to removable, whether intra- or extra-oral, use forces to influence dental movements. When forces are applied to a tooth, they initially cause elastic deformation of the PDL, which is responsible for the initial tooth movement. If this mechanical load persists, it results in bone remodeling (apposition/resorption) that can potentially lead to the long-term displacement of the specific tooth. This phenomenon is known as orthodontic tooth movement (OTM).

Wang and co-workers (Wang et al., 2014) examined four types of orthodontic loadings (buccal tipping, rotation around the long axis, intrusion, and extrusion) on a virtual model of a central incisor using FE modeling. They demonstrated that FEA could be used in a clinical setting to predict the magnitude of initial tooth movement and the changes affecting the surrounding bone morphology resulting from orthodontic treatment. FEA has also been used to study the long-term effects of orthodontic tooth movements and subsequent bone remodeling, both for individual teeth (Bourauel et al., 2000; Schneider et al., 2002) as well as in more complex models (Kojima & Fukui, 2014; Kojima et al., 2012). FEA has been extensively used to study biomechanics in orthodontics. Its strength lies in its potential to examine the impacts of mechanical loadings and their results in a non-destructive way and predict tooth displacement with acceptable accuracy (Farah et al., 1973).

## *Pediatric Dentistry*

Root development of a permanent tooth typically takes 1-4 years following its initial eruption into the oral cavity. During this period, the tooth is susceptible to various injuries that can affect the pulp's integrity at the early stages of development, causing developmental anomalies, resorptions, calcification, and/or ankylosis (Camp, 2002; Fuks & Nuni, 2019).

Preserving pulp vitality and utilizing the affected pulp's regenerative capacity to continue root maturation is a challenge in pediatric dentistry. Regenerative endodontic procedures (REP) have recently been introduced as a biological approach to help achieve root maturation in immature teeth with potentially necrotic pulpal tissue. The aim is to obtain root lengthening and thickening, closure of the root apex, and preservation of pulp vitality (Hargreaves et al., 2008).

In this context, Demirel and co-workers (Demirel et al., 2021) demonstrated that increasing root maturation by 15% leads to decreased stress on the cervical root surfaces of maxillary incisors. They also found that increasing the length of the cervical MTA barrier from 3 mm to 5 mm resulted in reduced stress values, while the thickness of MTA did not affect stress levels. Additionally, Bucchi and co-workers (Bucchi et al., 2019) assessed the biomechanical performance of a central maxillary incisor after revitalization, comparing the stress distribution when either dentin or cementum was applied at the apex to close the root. They observed that dentine-reinforced teeth exhibited significant biomechanical improvement compared to cementum application, particularly in response to biting forces, trauma, and orthodontic movements.

Also, Lahoud and co-workers (Lahoud et al., 2024) demonstrated through the use of patient-specific in-silico models of tooth autotransplantation that biomechanical variations occur on similar teeth due to individual anatomical

and tissue differences, further emphasizing the importance of personalized plannings. Therefore, such studies offer valuable insights into the biomechanical dynamics of immature teeth, aiding in the prediction of their prognosis when exposed to daily masticatory forces.

Furthermore, patient-specific treatment planning of tooth autotransplantation using the CBCT-guided approach have been shown to significantly enhance treatment predictability and outcomes by allowing precise preoperative planning and execution (EzEldeen et al., 2019): by creating a patient-specific replica of the donor tooth, clinicians can accurately shape the recipient site, ensuring a close fit that minimizes trauma to the periodontal ligament cells during transplantation, while ensuring a biomechanically sound position based on FEMs (Lahoud et al., 2024). This precise matching reduces the risk of damage to these crucial cells, which are vital for successful reattachment and healing (EzEldeen et al., 2019; Shahbazian et al., 2010). Consequently, the likelihood of transplant success is improved, as the approach allows for a more favorable environment for periodontal regeneration and tooth stability.



**Figure 3.** Flowchart showing the summary of the applications of finite elements in each dental specialty.

## DISCUSSION

This review explores the role of FEM in advancing in-silico modeling for personalized dentistry, considering the challenges and opportunities that arise in this multidisciplinary field.

**Knowledge and Skills among Dentists** is a key concern, as many practicing dentists lack the expertise required to effectively utilize FEM and in-silico modeling. Despite the growing prevalence of these technologies in dental biomaterials, oral implantology, and orthodontics (Figure 3), the complexity of creating accurate FEMs demands multidisciplinary knowledge. This includes image analysis, segmentation, modeling, meshing, biomechanics, and material science, which are essential for producing biofidelic models that offer accurate and reproducible predictions for treatment planning. Developing such expertise requires significant time and effort but is crucial for the successful application of these technologies in clinical practice (Lahoud, Jacobs, et al., 2022).

**Working Time** is another significant consideration. The time required to perform FEA can vary widely based on model complexity, size, and computational resources. Small models often demand highly accurate analyses, requiring fine meshing and a high number of nodes, which increases computational time and power requirements (Jin et al., 2015). Simply put, the more complex and the larger a model is, the more elements and nodes it will have, and the more calculations will need to be performed. However, in practice, this is often not the case: small models frequently require highly accurate analyses and involve an array of different materials, requiring very fine meshing and a high number of nodes and elements to be incorporated in the model for precise predictive analysis. This increases the need for computational time and power to run small, accurate FE models. In addition, different types of analysis require different computational demands: linear

analyses are generally faster than their non-linear counterpart. Furthermore, running such intricate models requires robust computational hardware, significantly affecting the computational time needed to run FE analyses. The last few years have seen a surge in the use of machine learning techniques to improve FEA efficiency. One such approach is the creation of "reduced finite element models" or "machine learning-assisted FEA". Reduced models rely on machine learning techniques to learn the relationship between a given FE model's input and output parameters. This machine-learning technique can predict the output data for a new set of input parameters without running a full FEA simulation, resulting in faster data processing. However, reduced models should be used to complement traditional FEA, and care should be taken to ensure accuracy (Lahoud et al., 2023; Liang et al., 2018; Pellicer-Valero et al., 2020; Roewer-Despres et al., 2018).

**Validation and Bio-Fidelity** of FEMs are critical for ensuring the reliability of in-silico models. Validating FEMs typically involves comparing simulation results with experimental and analytical data (Szabó & Babuška, 2021). Although comparison with experimental data is often considered the most accurate validation method, achieving bio-fidelity—accurately replicating the behavior of biological structures—remains challenging due to the complexity of biological systems (Pavan et al., 2022). Accurate modeling requires detailed patient-specific data and appropriate boundary conditions, which can be time-consuming and costly to obtain (Migueis et al., 2019). The inherent limitations of FEM, such as the difficulty in modeling complex, heterogeneous dental tissues and the reliance on simplifications, highlight the need for ongoing refinement of these techniques. Integrating FEM with other modeling approaches and machine learning can enhance their accuracy, user-friendliness, and clinical relevance in personalized dentistry.

**Interdisciplinary Collaborations** are essential for advancing FEM research in dentistry. Successful FEM application requires collaboration across

dentistry, engineering, and computer science. Dentists provide patient-specific data, engineers apply their expertise in material properties and biomechanics, and computer scientists develop algorithms to improve simulation accuracy. Strategies such as integrated research teams, joint workshops, interdisciplinary training programs, collaborative platforms, and co-authored projects and grants can facilitate this collaboration. By fostering synergy between these disciplines, we can achieve more accurate, efficient, and clinically relevant FEM research in dentistry, ultimately leading to better patient outcomes.

## **CONCLUSION**

The Finite Element Method (FEM) is growing in importance within both the broader medical field and specifically in dental research. Its utilization is on the rise in personalized dentistry and in-silico modeling, assisting in the analysis and development of optimal treatment plans for patients.

## REFERENCES

1. Anjum, S. A., Hegde, S., & Mathew, S. (2019). Minimally invasive endodontics-A review. *Journal of Dental and Orofacial Research*, 15(2), 77-88.
2. Bourauel, C., Vollmer, D., & Jäger, A. (2000). Application of bone remodeling theories in the simulation of orthodontic tooth movements. *Journal of Orofacial Orthopedics/Fortschritte der Kieferorthopädie*, 61(4), 266-279.
3. Breinemark, P., Adell, R., Breine, U., Hansson, B., Lindstrom, I., & Ohlsson, A. (1969). Intraosseous anchorage of dental prostheses. part 1: experimental studies. *Scand J Plast Reconstr Surg*, 3(2), 81-100.
4. Bucchi, C., Marcé-Nogué, J., Galler, K., & Widbiller, M. (2019). Biomechanical performance of an immature maxillary central incisor after revitalization: a finite element analysis. *International Endodontic Journal*, 52(10), 1508-1518.
5. Calciolari, E., Corbella, S., Gkrantias, N., Vigano, M., Sculean, A., & Donos, N. (2023). Efficacy of biomaterials for lateral bone augmentation performed with guided bone regeneration. A network meta-analysis. *Periodontol 2000*, 93(1), 77-106.
6. Camp, J. (2002). Pediatric endodontics, endodontic treatment for the primary and young permanent dentition. *Pathways of the Pulp*, 833-839.
7. Celikten, B., Koohnavard, M., Oncu, A., Sevimay, F. S., Orhan, A. I., & Orhan, K. (2022). A new perspective on minimally invasive endodontics: a systematic review. *Biotechnology & Biotechnological Equipment*, 35(1), 1758-1767.
8. Crespo Vázquez, E., Crespo Abelleira, A., Suárez Quintanilla, J., & Rodríguez Cobos, M. (2011). Correlation between occlusal contact and root resorption in teeth with periodontal disease. *Journal of periodontal research*, 46(1), 82-88.
9. da Rocha, M. C., da Rocha, D. M., Tribst, J. P. M., Borges, A. L. S., & Alvim-Pereira, F. (2021). Reduced periodontal support for lower central incisor-A 3D finite element analysis of compressive stress in the periodontium. *J. Int. Acad. Periodontol*, 23, 65-71.
10. Davies, J. E. (2003). Understanding peri-implant endosseous healing. *Journal of dental education*, 67(8), 932-949.
11. Demirel, A., Bezgin, T., & Sarı, Ş. (2021). Effects of root maturation and thickness variation in coronal mineral trioxide aggregate plugs under traumatic load on stress distribution in regenerative endodontic

- procedures: A 3-dimensional finite element analysis study. *Journal of endodontics*, 47(3), 492-499. e494.
12. Duan, W., Chen, Y., Zhang, Q., Lin, X., & Yang, X. (2021). Refined tooth and pulp segmentation using U-Net in CBCT image. *Dentomaxillofacial Radiology*, 50(6), 20200251.
  13. ElAyouti, A., Serry, M., Geis-Gerstorfer, J., & Löst, C. (2011). Influence of cusp coverage on the fracture resistance of premolars with endodontic access cavities. *International Endodontic Journal*, 44(6), 543-549.
  14. Eraslan, Ö., Eraslan, O., Eskitaşcıoğlu, G., & Belli, S. (2011). Conservative restoration of severely damaged endodontically treated premolar teeth: a FEM study. *Clinical Oral Investigations*, 15(3), 403-408.
  15. Ericsson, I. (1986). The combined effects of plaque and physical stress on periodontal tissues. *Journal of Clinical Periodontology*, 13(10), 918-922.
  16. EzEldeen, M., Wyatt, J., Al-Rimawi, A., Coucke, W., Shaheen, E., Lambrechts, I., Willems, G., Politis, C., & Jacobs, R. (2019). Use of CBCT Guidance for Tooth Autotransplantation in Children. *J Dent Res*, 98(4), 406-413.
  17. Fabris, D., Moura, J. P., Fredel, M. C., Souza, J. C., Silva, F. S., & Henriques, B. (2022). Biomechanical analyses of one-piece dental implants composed of titanium, zirconia, PEEK, CFR-PEEK, or GFR-PEEK: Stresses, strains, and bone remodeling prediction by the finite element method. *Journal of Biomedical Materials Research Part B: Applied Biomaterials*, 110(1), 79-88.
  18. Falcinelli, C., Valente, F., Vasta, M., & Traini, T. (2023). Finite element analysis in implant dentistry: State of the art and future directions. *Dental Materials*.
  19. Farah, J., Craig, R. G., & Sikarskie, D. L. (1973). Photoelastic and finite element stress analysis of a restored axisymmetric first molar. *Journal of biomechanics*, 6(5), 511-520.
  20. Fasbinder, D. J. (2010). Digital dentistry: innovation for restorative treatment. *Compendium of continuing education in dentistry (Jamesburg, NJ: 1995)*, 31, 2-11; quiz 12.
  21. Fuks, A. B., & Nuni, E. (2019). Pulp therapy for the young permanent dentition. In *Pediatric dentistry* (pp. 482-496). Elsevier.
  22. Galbusera, F., Taschieri, S., Tsesis, I., Francetti, L., & Del Fabbro, M. (2014). Finite element simulation of implant placement following extraction of a single tooth. *J Appl Biomater Funct Mater*, 12(2), 84-89.

23. Geris, L., Lambrechts, T., Carlier, A., & Papanтониου, I. (2018). The future is digital: In silico tissue engineering. *Current Opinion in Biomedical Engineering*, 6, 92-98.
24. Glickman, I. (1965). Clinical significance of trauma from occlusion. *The Journal of the American Dental Association*, 70(3), 607-618.
25. Glickman, I., & Smulow, J. (1969). The combined effects of inflammation and trauma from occlusion in periodontitis. *International dental journal*, 19(3), 393-407.
26. Gluskin, A. H., Peters, C. I., & Peters, O. A. (2014). Minimally invasive endodontics: challenging prevailing paradigms. *British dental journal*, 216(6), 347-353.
27. Gomez-Polo, M., Ortega, R., Gomez-Polo, C., Martin, C., Celemin, A., & Del Río, J. (2016). Does length, diameter, or bone quality affect primary and secondary stability in self-tapping dental implants? *Journal of Oral and Maxillofacial Surgery*, 74(7), 1344-1353.
28. Güngör, M. B., & Yılmaz, H. (2016). Evaluation of stress distributions occurring on zirconia and titanium implant-supported prostheses: A three-dimensional finite element analysis. *The Journal of prosthetic dentistry*, 116(3), 346-355.
29. Hargreaves, K. M., Giesler, T., Henry, M., & Wang, Y. (2008). Regeneration potential of the young permanent tooth: what does the future hold? *Pediatric dentistry*, 30(3), 253-260.
30. Hatch, J., Shinkai, R., Sakai, S., Rugh, J., & Paunovich, E. (2001). Determinants of masticatory performance in dentate adults. *Archives of oral biology*, 46(7), 641-648.
31. Hiebert, B. M., Abramovitch, K., Rice, D., & Torabinejad, M. (2017). Prevalence of second mesiobuccal canals in maxillary first molars detected using cone-beam computed tomography, direct occlusal access, and coronal plane grinding. *Journal of endodontics*, 43(10), 1711-1715.
32. Ichim, I., Kuzmanovic, D., & Love, R. (2006). A finite element analysis of ferrule design on restoration resistance and distribution of stress within a root. *International Endodontic Journal*, 39(6), 443-452.
33. Jiang, Q., Huang, Y., Tu, X., Li, Z., He, Y., & Yang, X. (2018). Biomechanical Properties of First Maxillary Molars with Different Endodontic Cavities: A Finite Element Analysis. *J Endod*, 44(8), 1283-1288.
34. Jin, B., Lazarov, R., Liu, Y., & Zhou, Z. (2015). The Galerkin finite element method for a multi-term time-fractional diffusion equation. *Journal of Computational Physics*, 281, 825-843.

35. Junior, J. F. S., Verri, F. R., de Faria Almeida, D. A., de Souza Batista, V. E., Lemos, C. A. A., & Pellizzer, E. P. (2016). Finite element analysis on influence of implant surface treatments, connection and bone types. *Materials Science and Engineering: C*, 63, 292-300.
36. Karaer, O., Yamaguchi, S., Imazato, S., & Terzioglu, H. (2023). In Silico Finite Element Analysis of Implant-Supported CAD-CAM Resin Composite Crowns. *Journal of Prosthodontics*, 32(3), 259-266.
37. Keshavarzian, M., Meyer, C. A., & Hayenga, H. N. (2019). In Silico Tissue Engineering: A Coupled Agent-Based Finite Element Approach. *Tissue Eng Part C Methods*, 25(11), 641-654.
38. Kim, H. C., Lee, M. H., Yum, J., Versluis, A., Lee, C. J., & Kim, B. M. (2010). Potential relationship between design of nickel-titanium rotary instruments and vertical root fracture. *J Endod*, 36(7), 1195-
39. Kojima, Y., & Fukui, H. (2014). A finite element simulation of initial movement, orthodontic movement, and the centre of resistance of the maxillary teeth connected with an archwire. *The European Journal of Orthodontics*, 36(3), 255-261.
40. Kojima, Y., Kawamura, J., & Fukui, H. (2012). Finite element analysis of the effect of force directions on tooth movement in extraction space closure with miniscrew sliding mechanics. *American journal of orthodontics and dentofacial orthopedics*, 142(4), 501-508.
41. Kondo, T., & Wakabayashi, N. (2009). Influence of molar support loss on stress and strain in premolar periodontium: a patient-specific FEM study. *Journal of Dentistry*, 37(7), 541-548.
42. Lahoud, P., Badrou, A., Ducret, M., Farges, J. C., Jacobs, R., Bel-Brunon, A., EzEldeen, M., Blal, N., & Richert, R. (2023). Real-time simulation of the transplanted tooth using model order reduction. *Front Bioeng Biotechnol*, 11, 1201177.
43. Lahoud, P., Diels, S., Niclaes, L., Van Aelst, S., Willems, H., Van Gerven, A., Quiryne, M., & Jacobs, R. (2022). Development and validation of a novel artificial intelligence driven tool for accurate mandibular canal segmentation on CBCT. *J Dent*, 116, 103891.
44. Lahoud, P., EzEldeen, M., Beznik, T., Willems, H., Leite, A., Van Gerven, A., & Jacobs, R. (2021). Artificial intelligence for fast and accurate 3D tooth segmentation on CBCT. *J Endod*.
45. Lahoud, P., Jacobs, R., Boisse, P., EzEldeen, M., Ducret, M., & Richert, R. (2022). Precision medicine using patient-specific modelling: state of the art and perspectives in dental practice. *Clin Oral Investig*, 26(8), 5117-5128.

46. Lahoud, P., Jacobs, R., Elahi, S. A., Ducret, M., Lauwers, W., van Lenthe, G. H., Richert, R., & EzEldeen, M. (2024). Developing Advanced Patient-Specific In Silico Models: A New Era in Biomechanical Analysis of Tooth Autotransplantation. *J Endod*.
47. Latuta, N., Corbella, S., Taschieri, S., Diachkova, E., Tarasenko, S., Oksentyuk, A., Trifonova, D., & Admakin, O. (2022). Use of an antiseptic rinse (N an A rgol) for the oral hygiene maintenance of subjects with fixed appliances: A randomized clinical trial. *International Journal of Dental Hygiene*.
48. Lee, H., Jo, M., & Noh, G. (2021). Biomechanical effects of dental implant diameter, connection type, and bone density on microgap formation and fatigue failure: A finite element analysis. *Comput Methods Programs Biomed*, 200, 105863.
49. Lee, W. T., Koak, J. Y., Lim, Y. J., Kim, S. K., Kwon, H. B., & Kim, M. J. (2012). Stress shielding and fatigue limits of poly-ether-ether-ketone dental implants. *Journal of Biomedical Materials Research Part B: Applied Biomaterials*, 100(4), 1044-1052.
50. Leite, A. F., Gerven, A. V., Willems, H., Beznik, T., Lahoud, P., Gaeta-Araujo, H., Vranckx, M., & Jacobs, R. (2020). Artificial intelligence-driven novel tool for tooth detection and segmentation on panoramic radiographs. *Clin Oral Investig*.
51. Lekholm, U. (1985). Patient selection and preparation. *Tissue integrated prosthesis*, 199-209.
52. Li, H., Shi, M., Liu, X., & Shi, Y. (2019). Uncertainty optimization of dental implant based on finite element method, global sensitivity analysis and support vector regression. *Proc Inst Mech Eng H*, 233(2), 232-243.
53. Li, J., Jansen, J. A., Walboomers, X. F., & van den Beucken, J. J. (2020). Mechanical aspects of dental implants and osseointegration: A narrative review. *Journal of the mechanical behavior of biomedical materials*, 103, 103574.
54. Li, W., Swain, M. V., Li, Q., & Steven, G. P. (2005). Towards automated 3D finite element modeling of direct fiber reinforced composite dental bridge. *J Biomed Mater Res B Appl Biomater*, 74(1), 520-528.
55. Liang, L., Liu, M., Martin, C., & Sun, W. (2018). A deep learning approach to estimate stress distribution: a fast and accurate surrogate of finite-element analysis. *Journal of The Royal Society Interface*, 15(138), 20170844.
56. Lin, C.-L., Chang, Y.-H., & Pa, C.-A. (2009). Estimation of the risk of failure for an endodontically treated maxillary premolar with MODP

- preparation and CAD/CAM ceramic restorations. *Journal of endodontics*, 35(10), 1391-1395.
57. Lin, C. L., Chang, Y. H., Chang, C. Y., Pai, C. A., & Huang, S. F. (2010). Finite element and Weibull analyses to estimate failure risks in the ceramic endocrown and classical crown for endodontically treated maxillary premolar. *European journal of oral sciences*, 118(1), 87-93.
  58. Linetskiy, I., Demenko, V., Linetska, L., & Yefremov, O. (2017). Impact of annual bone loss and different bone quality on dental implant success—A finite element study. *Computers in biology and medicine*, 91, 318-325.
  59. Maddahi, Y., & Chen, S. (2022). Applications of Digital Twins in the Healthcare Industry: Case Review of an IoT-Enabled Remote Technology in Dentistry. *Virtual Worlds*, 1(1), 20-41.
  60. Marcian, P., Borák, L., Zikmund, T., Horáčková, L., Kaiser, J., Joukal, M., & Wolff, J. (2021). On the limits of finite element models created from (micro) CT datasets and used in studies of bone-implant-related biomechanical problems. *Journal of the mechanical behavior of biomedical materials*, 117, 104393.
  61. Marcian, P., Wolff, J., Horackova, L., Kaiser, J., Zikmund, T., & Borak, L. (2018). Micro finite element analysis of dental implants under different loading conditions. *Comput Biol Med*, 96, 157-165.
  62. Mengoni, M. (2020). Biomechanical modelling of the facet joints: a review of methods and validation processes in finite element analysis. *Biomechanics and Modeling in Mechanobiology*, 20(2), 389-401
  63. Migueis, G., Fernandes, F., Ptak, M., Ratajczak, M., & de Sousa, R. A. (2019). Detection of bridging veins rupture and subdural haematoma onset using a finite element head model. *Clinical Biomechanics*, 63, 104-111.
  64. Misch, C. E., Suzuki, J. B., Misch-Dietsh, F. M., & Bidez, M. W. (2005). A positive correlation between occlusal trauma and peri-implant bone loss: literature support. *Implant dentistry*, 14(2), 108-116.
  65. Mora-Macías, J., Ayensa-Jiménez, J., Reina-Romo, E., Doweidar, M. H., Domínguez, J., Doblaré, M., & Sanz-Herrera, J. A. (2020). A multiscale data-driven approach for bone tissue biomechanics. *Computer Methods in Applied Mechanics and Engineering*, 368.
  66. Nyman, S., Lindhe, J., & Ericsson, I. (1978). The effect of progressive tooth mobility on destructive periodontitis in the dog. *Journal of Clinical Periodontology*, 5(3), 213-225.
  67. Ona, M., & Wakabayashi, N. (2006). Influence of alveolar support on stress in periodontal structures. *Journal of dental research*, 85(12), 1087-1091.

68. Organization, W. H. (2013). *Oral health surveys: basic methods*. World Health Organization.
69. Ortún-Terrazas, J., Cegoñino, J., & Del Palomar, A. P. (2020). In silico study of cuspid'periodontal ligament damage under parafunctional and traumatic conditions of whole-mouth occlusions. A patient-specific evaluation. *Computer Methods and Programs in Biomedicine*, 184, 105107.
70. Oyar, P., Ulusoy, M., & Eskitaşçıoğlu, G. (2014). Finite element analysis of stress distribution in ceramic crowns fabricated with different tooth preparation designs. *The Journal of prosthetic dentistry*, 112(4), 871-877.
71. Papadopoulou, K., Hasan, I., Keilig, L., Reimann, S., Eliades, T., Jäger, A., Deschner, J., & Bourauel, C. (2013). Biomechanical time dependency of the periodontal ligament: a combined experimental and numerical approach. *European journal of orthodontics*, 35(6), 811-818.
72. Patil, T. N., Saraf, P. A., Penukonda, R., Vanaki, S. S., & Kamatagi, L. (2017). A Survey on Nickel Titanium Rotary Instruments and their Usage Techniques by Endodontists in India. *J Clin Diagn Res*, 11(5), ZC29-ZC35.
73. Pavan, P. G., Nasim, M., Brasco, V., Spadoni, S., Paoloni, F., d'Avella, D., Khosroshahi, S. F., de Cesare, N., Gupta, K., & Galvanetto, U. (2022). Development of detailed finite element models for in silico analyses of brain impact dynamics. *Computer Methods and Programs in Biomedicine*, 227, 107225.
74. Pellicer-Valero, O. J., Rupérez, M. J., Martínez-Sanchis, S., & Martín-Guerrero, J. D. (2020). Real-time biomechanical modeling of the liver using machine learning models trained on finite element method simulations. *Expert Systems with Applications*, 143, 113083.
75. Peters, O. A. (2004). Current challenges and concepts in the preparation of root canal systems: a review. *Journal of endodontics*, 30(8), 559-567.
76. Poiate, I. A., Vasconcellos, A. B., Andueza, A., Pola, I. R., & Poiate Jr, E. (2008). Three dimensional finite element analyses of oral structures by computerized tomography. *Journal of bioscience and bioengineering*, 106(6), 606-609.
77. Polson, A. M. (1986). The relative importance of plaque and occlusion in periodontal disease. *Journal of Clinical Periodontology*, 13(10), 923-927.
78. Preda, F., Morgan, N., Van Gerven, A., Nogueira-Reis, F., Smolders, A., Wang, X., Nomidis, S., Shaheen, E., Willems, H., & Jacobs, R. (2022). Deep convolutional neural network-based automated segmentation of the maxillofacial complex from cone-beam computed tomography: A validation study. *Journal of Dentistry*, 124, 104238.

79. Quiryneen, M., Lahoud, P., Teughels, W., Cortellini, S., Dhondt, R., Jacobs, R., & Temmerman, A. (2023). Individual "alveolar phenotype" limits dimensions of lateral bone augmentation. *J Clin Periodontol*, *50*(4), 500-510.
80. Richert, R., Farges, J. C., Maurin, J. C., Molimard, J., Boisse, P., & Ducret, M. (2022). Multifactorial Analysis of Endodontic Microsurgery Using Finite Element Models. *J Pers Med*, *12*(6).
81. Richert, R., Farges, J. C., Tamimi, F., Naouar, N., Boisse, P., & Ducret, M. (2020). Validated Finite Element Models of Premolars: A Scoping Review. *Materials (Basel)*, *13*(15).
82. Roewer-Despres, F., Khan, N., & Stavness, I. (2018). Towards finite element simulation using deep learning. 15th international symposium on computer methods in biomechanics and biomedical engineering,
83. Schneider, J., Geiger, M., & Sander, F.-G. (2002). Numerical experiments on long-time orthodontic tooth movement. *American journal of orthodontics and dentofacial orthopedics*, *121*(3), 257-265.
84. Schwab, K. (2017). *The fourth industrial revolution*. Currency.
85. Shahbazian, M., Jacobs, R., Wyatt, J., Willems, G., Pattijn, V., Dhoore, E., C, V. A. N. L., & Vinckier, F. (2010). Accuracy and surgical feasibility of a CBCT-based stereolithographic surgical guide aiding autotransplantation of teeth: in vitro validation. *J Oral Rehabil*, *37*(11), 854-859.
86. Solle, D., Hitzmann, B., Herwig, C., Pereira Remelhe, M., Ulonska, S., Wuerth, L., Prata, A., & Steckenreiter, T. (2017). Between the Poles of Data-Driven and Mechanistic Modeling for Process Operation. *Chemie Ingenieur Technik*, *89*(5), 542-561.
87. Suenaga, H., Chen, J., Yamaguchi, K., Li, W., Sasaki, K., Swain, M., & Li, Q. (2015). Mechanobiological bone reaction quantified by positron emission tomography. *Journal of dental research*, *94*(5), 738-744.
88. Sulaiman, T. A. (2020). Materials in digital dentistry—A review. *Journal of Esthetic and Restorative Dentistry*, *32*(2), 171-181.
89. Szabó, B., & Babuška, I. (2021). Finite Element Analysis: Method, Verification and Validation.
90. Tajima, K., Chen, K.-K., Takahashi, N., Noda, N., Nagamatsu, Y., & Kakigawa, H. (2009). Three-dimensional finite element modeling from CT images of tooth and its validation. *Dental materials journal*, *28*(2), 219-226.
91. Tekin, S., Değer, Y., & Demirci, F. (2019). Evaluation of the use of PEEK material in implant-supported fixed restorations by finite element analysis. *Nigerian journal of clinical practice*, *22*(9), 1252-1258.

92. Tuna, M., Sunbuloglu, E., & Bozdog, E. (2014). Finite element simulation of the behavior of the periodontal ligament: a validated nonlinear contact model. *J Biomech*, 47(12), 2883-2890.
93. Ueda, N., Takayama, Y., & Yokoyama, A. (2017). Minimization of dental implant diameter and length according to bone quality determined by finite element analysis and optimized calculation. *J Prosthodont Res*, 61(3), 324-332.
94. Van Dyke, T., Hasturk, H., Kantarci, A., Freire, M., Nguyen, D., Dalli, J., & Serhan, C. (2015). Proresolving nanomedicines activate bone regeneration in periodontitis. *Journal of dental research*, 94(1), 148.
95. Van Noort, R. (2012). The future of dental devices is digital. *Dental Materials*, 28(1), 3-12.
96. von Arx, T., Jensen, S. S., Hänni, S., & Friedman, S. (2012). Five-year longitudinal assessment of the prognosis of apical microsurgery. *Journal of endodontics*, 38(5), 570-579.
97. von Arx, T., Maldonado, P., & Bornstein, M. M. (2021). Occurrence of vertical root fractures after apical surgery: a retrospective analysis. *Journal of endodontics*, 47(2), 239-246.
98. Wang, C., Han, J., Li, Q., Wang, L., & Fan, Y. (2014). Simulation of bone remodelling in orthodontic treatment. *Computer methods in biomechanics and biomedical engineering*, 17(9), 1042-1050.
99. Wang, Q., Liu, Y., Wang, Z., Yang, T., Liang, Y., Gao, Z., Fang, C., & Zhang, Y. (2020). Effect of Access Cavities and Canal Enlargement on Biomechanics of Endodontically Treated Teeth: A Finite Element Analysis. *J Endod*, 46(10), 1501-1507.
100. Wang, Q., Liu, Y., Wang, Z., Yang, T., Liang, Y., Gao, Z., Fang, C., & Zhang, Y. (2020). Effect of access cavities and canal enlargement on biomechanics of endodontically treated teeth: a finite element analysis. *Journal of endodontics*, 46(10), 1501-1507.
101. Wong, L. B., Yap, A. U., & Allen, P. F. (2021). Periodontal disease and quality of life: Umbrella review of systematic reviews. *J Periodontal Res*, 56(1), 1-17.
102. Xu, X., Liu, C., & Zheng, Y. (2018). 3D tooth segmentation and labeling using deep convolutional neural networks. *IEEE transactions on visualization and computer graphics*, 25(7), 2336-2348.
103. Yang, Z. (2019). *Finite element analysis for biomedical engineering applications*. CRC Press.
104. Yu, S. H., Saleh, M. H. A., & Wang, H. L. (2023). Simultaneous or staged lateral ridge augmentation: A clinical guideline on the decision-making process. *Periodontol 2000*, 93(1), 107-128.

105. Zarone, F., Apicella, D., Sorrentino, R., Ferro, V., Aversa, R., & Apicella, A. (2005). Influence of tooth preparation design on the stress distribution in maxillary central incisors restored by means of alumina porcelain veneers: a 3D-finite element analysis. *Dental materials*, *21*(12), 1178-1188.
106. Zupancic Cepic, L., Frank, M., Reisinger, A., Pahr, D., Zechner, W., & Schedle, A. (2022). Biomechanical finite element analysis of short-implant-supported, 3-unit, fixed CAD/CAM prostheses in the posterior mandible. *International Journal of Implant Dentistry*, *8*(1), 8.
107. Zysset, P., Qin, L., Lang, T., Khosla, S., Leslie, W. D., Shepherd, J. A., Schousboe, J. T., & Engelke, K. (2015). Clinical use of quantitative computed tomography-based finite element analysis of the hip and spine in the management of osteoporosis in adults: the 2015 ISCD official positions—part II. *Journal of clinical densitometry*, *18*(3), 359-392.





DEVELOPMENT AND VALIDATION STUDIES



## CHAPTER III | Artificial Intelligence for Fast and Accurate 3-Dimensional Tooth Segmentation on Cone-beam Computed Tomography

*This chapter is based on the following publication: **Lahoud P, EzEldeen M, Beznik T, Willems H, Leite A, Van Gerven A, Jacobs R.** Artificial intelligence for fast and accurate 3-dimensional tooth segmentation on cone-beam computed tomography. *Journal of Endodontics*. 2021 May 1;47(5):827-35.*

### Affiliations

1. OMFS-IMPACT Research Group, Department of Imaging and Pathology, Faculty of Medicine, KU, Leuven, Belgium
2. Department of Oral and Maxillofacial Surgery, University Hospitals Leuven, Leuven, Belgium
3. Department of Oral Health Sciences, KU Leuven and Paediatric Dentistry and Special Dental Care, University Hospitals Leuven, Leuven, Belgium
4. Relu, Leuven, Belgium
5. Department of Dentistry, Faculty of Health Sciences, University of Brasília, Brasília, Brazil
6. Department of Dental Medicine, Karolinska Institute, Stockholm, Sweden

# Artificial Intelligence for Fast and Accurate 3-Dimensional Tooth Segmentation on Cone-beam Computed Tomography

*Lahoud P, EzEldeen M, Beznik T, Willems H, Leite A, Van Gerven A,  
Jacobs R*

## **ABSTRACT**

**Aim(s):** This study aimed to develop and validate an artificial intelligence (AI)-driven tool for automated tooth segmentation on CBCT imaging.

**Materials and Methods:** A total of 433 Digital Imaging and Communications in Medicine images of single- and double-rooted teeth randomly selected from 314 anonymized CBCT scans were imported and manually segmented. An AI-driven tooth segmentation algorithm based on a feature pyramid network was developed to automatically detect and segment teeth, replacing manual user contour placement. The AI-driven tool was evaluated based on volume comparison, intersection over union, the Dice score coefficient, morphologic surface deviation, and total segmentation time.

**Results:** Overall, AI-driven and clinical reference segmentations resulted in very similar segmentation volumes. The mean intersection over union for full-tooth segmentation was 0.87 (60.03) and 0.88 (60.03) for semiautomated (SA) (clinical reference) versus fully automated AI-driven (F-AI) and refined AI-driven (R-AI) tooth segmentation, respectively. R-AI and F-AI segmentation showed an average median surface deviation from SA segmentation of 9.96 mm (659.33 mm) and 7.85 mm (669.55 mm), respectively. SA segmentations of single- and double-rooted teeth had a mean total time of 6.6 minutes (676.15 seconds), F-AI segmentation of 0.5 minutes (68.64 seconds, 12 times faster), and R-AI segmentation of 1.2 minutes (633.02 seconds, 6 times faster).

**Conclusion(s):** This study showed a unique fast and accurate approach for AI-driven automated tooth segmentation on CBCT imaging. These results may open doors for AI-driven applications in surgical and treatment planning in oral health care.

## INTRODUCTION

Dentistry excels in the delivery of personalized healthcare, traditionally through fabrication of dental fillings, crowns and prostheses. The last two decades have seen an exponential rise in the field of three-dimensional (3D) image analysis and printing techniques leading to multiple digital dentistry (DD) applications. Amongst the most frequent applications are 3D-guided implant surgery (Van Assche et al., 2012), guided-endodontics and apical surgeries (Byun et al., 2015; Torres et al., 2019) CBCT-based planning and fabrication of donor teeth replicas and surgical guides for successful tooth autotransplantation (TAT) (EzEldeen et al., 2019), digital orthodontic applications (Cui et al., 2019) and virtual orthognathic surgery planning (Shaheen et al., 2017).

DD relies primarily on acquisition and segmentation of 3D imaging modalities. The current trend of image acquisition in this field relies primarily on cone beam computed tomography (CBCT), which offers highly accurate volumetric data on jaw bones and teeth with relatively low radiation doses and cost, (EzEldeen et al., 2017; Jacobs et al., 2018; Ludlow et al., 2006).

Image segmentation is a process of dividing an image into different meaningful regions and is utilized in structural identification and quantitative assessment of dental structures for various imaging modalities (EzEldeen et al., 2015; Nguyen et al., 2020). Tooth segmentation is vital for accurate diagnosis, treatment planning and direct surgical assistance for a wide variety of DD applications as abovementioned.

Nevertheless, teeth segmentation on CBCT remains a labour-intensive and challenging task, primarily related to the lack of Hounsfield units (HUs) and the limited differential contrast between cementum, dentin and bone with only 200  $\mu\text{m}$ -wide periodontal ligament space. Meanwhile these images also suffer from artefacts in the jaw bone area, making fully automated tooth segmentation by merely relying on intensity variation of (CB)CT images unreliable (Cui et al., 2019).

Convolutional neural networks (CNN/ConvNet) are a special type of deep learning (DL) algorithms made of multilayer neural networks, specifically aimed at the recognition of visual patterns from pixelized images with minimal pre-processing (Saha, 2018). Several CNNs have been described with different architectures depending on the application (Kyong Hwan et al., 2017; Lakhani et al., 2018). CNNs sparked tremendous interest over the past few years, and have become relevant tools for image processing and segmentation (Litjens et al., 2017; Nguyen et al., 2020), such as the use of U-Net and V-Net for automated level set-based tooth segmentation (Chen et al., 2020; Lee et al., 2020). The architecture of a CNN is analogous to that of the connectivity pattern of neurons in the human brain; mainly inspired by the organization of the visual cortex. A CNN “learns” intrinsic statistical patterns in data to eventually cast predictions on unseen data (Schwendicke et al., 2020). Implementation of a CNN in a tooth segmentation tool could help improving the results, given that the algorithm could be taught how to behave for challenging – yet highly common – cases, including complicated root anatomy, heavy scattering, immature teeth and metal artefacts. Such tool could bridge the gap between accuracy and time consumption for tooth segmentation, and potentially simplify digital dentistry applications and surgical planning to a broader audience of practitioners.

Frequently used tooth segmentation software mainly relies on thresholding, template-based fitting methods (TbFM) and level set methods to segment individual tooth from dental CBCT images.

However, thresholding may not work if underlying shading distorts the image and may have difficulties finding the threshold minimum (Toennies, 2017b), especially with CBCT grey values. TbFM lacked robustness with multi-rooted teeth and complex anatomy (Chen et al., 2020), while the level set method needs to perform numerous mathematical operations, yielding relatively slow results (Akhoondali et al., 2009) and may be problematic in regards to partial volume effects, especially when the intensity variation in the background is higher than in the foreground (Toennies, 2017a). Also, the use of such

automated methods could struggle with images of low quality, metal artefacts and immature tooth segmentation.

The overall aim of this study was to develop and validate a clinically operational AI-driven tooth segmentation tool capable of minimizing manual interventions and yielding fast, accurate and consistent results essential for clinical use.

## **MATERIALS AND METHODS**

### **Data Acquisition and Training Database**

CBCCT scans were randomly collected from two previous study databases, described in supplemental S1. All teeth were segmented manually by experts in the field of dentomaxillofacial radiology using a dedicated tool developed in MeVisLab (MeVis Research, Bremen, Germany) and validated for accurate tooth/root and canal space segmentation as previously described (EzEldeen et al., 2015) with an integrated time monitoring module. Briefly, the imaging analysis tool applies a semi-interactive livewire boundary extraction (Barrett & Mortensen, 1997) to create a set of orthogonal contours, followed by a variational interpolation algorithm that reconstructs the surface of an object with energy-minimizing, smoothing and implicit functions (Heckel et al., 2011). Segmentations resulted in a total of 433 DICOM (digital imaging and communications in medicine) images of teeth randomly selected from the CBCCT scans – including upper and lower incisors, canines and premolars – accounting for 2924 slice images of teeth sampled in axial, sagittal or coronal direction and an associated binary mask identifying the region of the image belonging to the tooth. Each binary mask was generated based on a contour segmentation object file (CSO file) of the tooth, that were annotated on the 2D slices. Contours were filled and exported as portable network graphics (PNG) images, while the corresponding slice was extracted from the 3D DICOM image and exported to a grayscale PNG image. These 2D image

pairs were then divided into three datasets: training (2095 samples, 71.6%), optimization (501 samples, 17.2%) and validation set (328 samples, 11.2%). Datasets included single and double rooted teeth (with mature and immature cases), various artefacts, fillings, metal posts, low resolution images, various voxel sizes, heavy and low scattering as well as other segmentation-challenging cases.

## **Machine Learning**

### ***Dataset pre-processing and augmentation***

Data augmentation techniques were used on the training set in order to increase the generalization and robustness of the model, as detailed in supplemental S2.1.

### ***Network Architecture of the ConvNet***

The architecture used was a Feature Pyramid Network (FPN) (Kirillov et al., 2018). Network architecture is demonstrated in figure 1. Detailed description is provided in supplemental S2.2.

### ***AI driven tooth segmentation***

An AI-driven tooth segmentation algorithm trained with the above described dataset was developed for automated detection and segmentation of tooth structure replacing manual user contour placement implemented in the previously validated tooth segmentation method (EzEldeen et al., 2015). Moreover, the possibility of user interaction was preserved with the ability to modify, add, or delete the AI suggested contours (figure 2).

### ***Validation Dataset***

Forty-six randomly selected cases were chosen for the validation of the tool. These cases accounted for 10% of the whole database (433 DICOMs) and were unseen by the algorithm during the training phase. The validation set

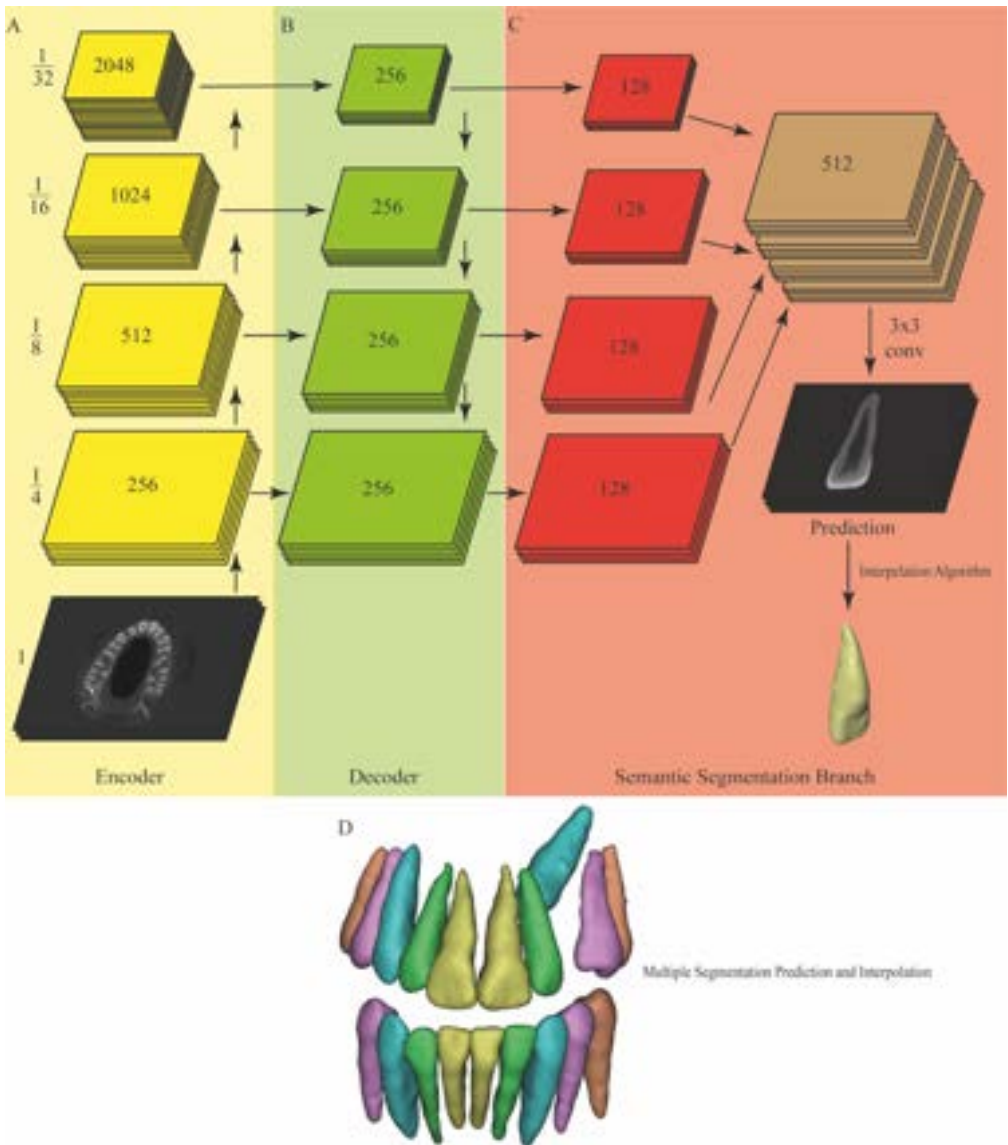


**Figure 1.** Architecture of the Feature Pyramid Network used. (A) The encoder extracts the interesting features from the input image, (B) the decoder generates a dense segmentation mask of the input and (C) the semantic segmentation branch combines the feature maps from all the layers of the decoder into one single output. (D) shows the result of multiple segmentation predictions and interpolations.

consisted of 19 incisors, 17 canines and 17 premolars, equally proportional to the full database tooth-type distribution. All 46 cases were segmented using three segmentation protocols: (1) semi-automated segmentation (SA) – performed manually by experts in the field of oral radiology and medical imaging and serving as the clinical reference – which relied on the use of livewire contour based segmentation as described earlier (EzEldeen et al., 2015) and without AI assistance, (2) fully automated AI-driven segmentation (F-AI) – where no user interaction was performed following the AI-computation and contour placement; and (3) refined AI-driven segmentation (R-AI) – where expert users refine what was judged under- or over-estimated following computation suggested by the AI-algorithm.

## **Assessment and Validation of the tool**

### ***Voxel-based performance metrics***

Binarized segmentation results were used for volume calculation and subsequent assessment. The binary images were fed to an Intersection-Over-Union (*IoU*) algorithm to test for the accuracy of overlap (Rahman & Wang, 2016). The module plotted F-AI and R-AI groups against SA in order to evaluate the performance of the AI-tool. An *IoU* score lower than 0.5 is considered as failure (Cop, 2018). Further, the Dice similarity coefficient (*DSC*) was calculated for each tooth/protocol (F-AI & R-AI) versus the reference image (SA).

*IoU* is employed as a loss function in foreground and background classification tasks of object in an image (Rahman & Wang, 2016). Detailed calculation steps are available in supplemental S3.

### ***3D Reconstruction and Morphologic Surface Analysis***

After segmentation, the 3D triangle-based surface of the tooth was reconstructed as a Standard Tessellation Language file (STL). All STL files were then imported in the 3-matic software (Materialise NV, Leuven,

Belgium) to perform a signed morphologic surface comparison between the 3D model for each tooth/protocol (F-AI & R-AI) versus the 3D model from the reference image (SA), allowing for positive and negative differentiation with regard to the reference image (figure 2-L/M). A cutoff value for accuracy was set at 200 $\mu$ m median surface deviation from the reference image (Jacobs, 2011; Shahbazian et al., 2010).

### **Statistical Analysis**

Results from the metrics calculated during and after segmentation were evaluated in regard to three distinct groups: (1) Full dataset analysis, (2) mature and immature tooth analysis, and (3) tooth-types dependent analysis (for incisors, canines and premolars separately). Statistical analysis was performed using GraphPad Prism for MacOS, version 9.0. (GraphPad Software, La Jolla California, USA). Volume variation between the three groups as well as between the different tooth types and condition (mature and immature) was reported in a descriptive fashion. The systematic volume deviation between F-AI, R-AI and SA segmentations was evaluated using the method of Bland and Altman (Bland & Altman, 1986) in MedCalc for Windows, version 15.0 (MedCalc Software, Ostend, Belgium). Detailed timing was recorded and compared between the three groups using repeated measures Analysis of Variance (ANOVA) method with Tukey's correction. To examine if AI segmentations were not inferior to the SA segmentations (dentist-operated) two metrics were evaluated as follows: 1- the *IoU* scores for F-AI and R-AI were tested using a one-sample t-test (an *IoU* score lower than 0.5 is considered as failure), 2- average surface deviation using a one-sample t-test against a cut-off value of 200  $\mu$ m. A two-way ANOVA test with Tukey's correction was used to evaluate the effect of tooth type (incisors, canines, and premolars) and apex maturation on the *IoU* score of F-AI as well as R-AI. All measurements were calculated for the overall tooth as well as for crown and root separately.

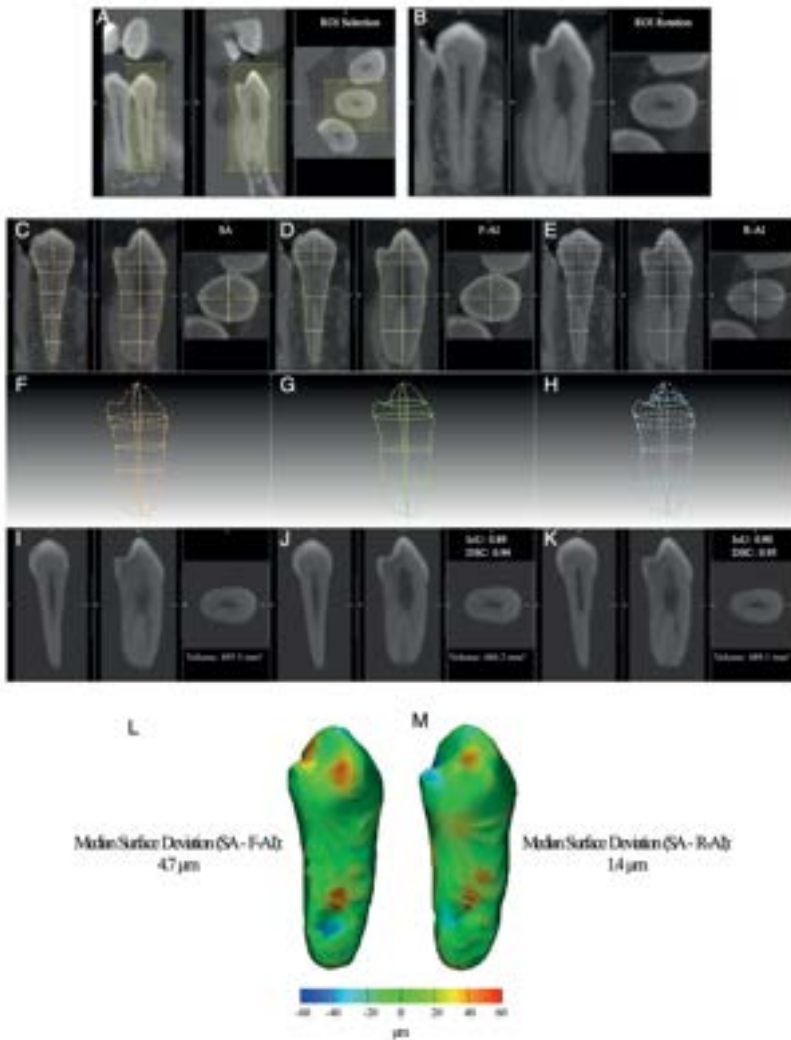


**Figure 2.** Workflow of the segmentation methods used. (A) and (B) represent ROI selection and rotation. (C) (D) and (E) show seeds and contour placement according to the three segmentation methods relying on semi-automated user segmentation (SA), Fully Automated AI-driven Segmentation (F-AI) and Refined AI-driven Segmentation (R-AI). (F) (G) and (H) show a 3D representation of CSOs contours. (I) (J) and (K) illustrate segmentation results for each method. (L) and (M) represent an example of a surface deviation map of F-AI (L) and R-AI (M) compared with the clinical reference (SA).

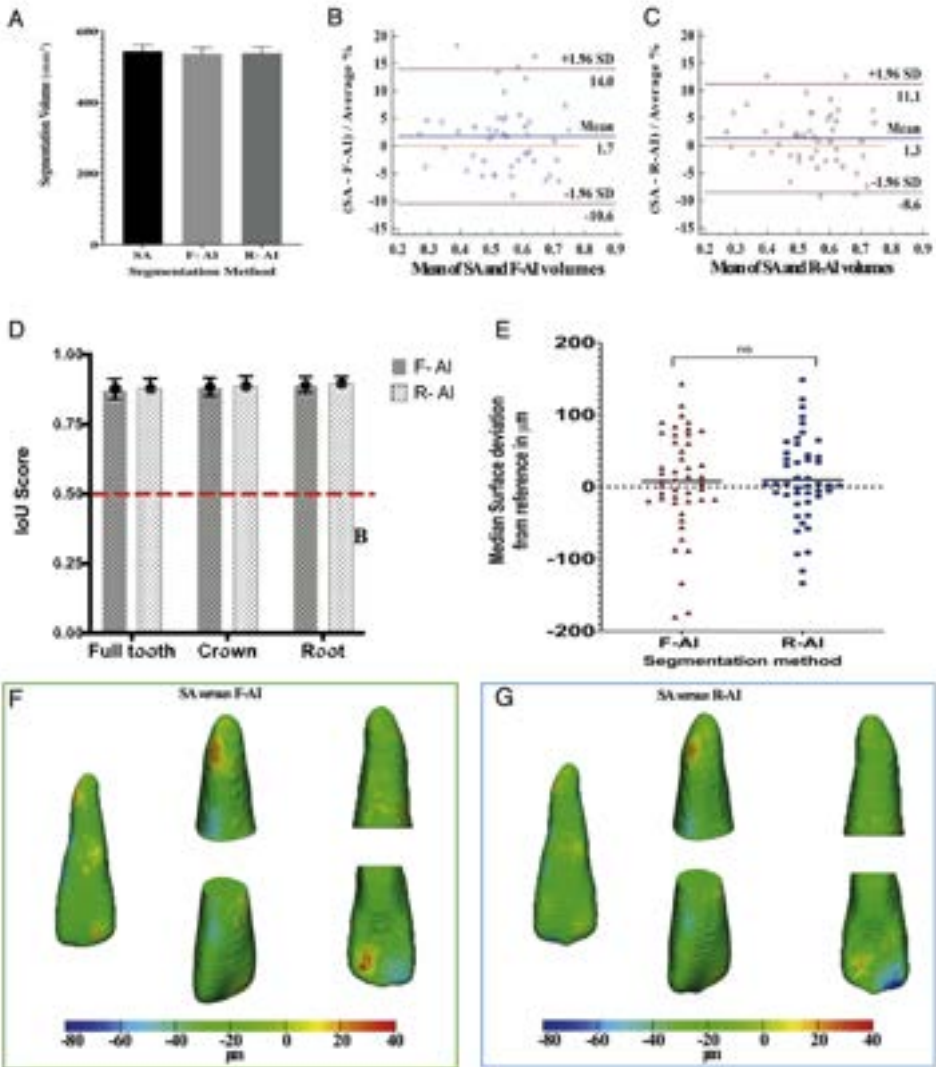


**Figure 3.** (A) a plot comparison between segmented volumes in mm<sup>3</sup> for SA, F-AI and R-AI. (B and C) Bland-Altman plots between tooth segmented volumes for F-AI (B) and R-AI (C) versus the clinical reference (SA) (the difference between the measurements is plotted against their mean). (D) IoU score comparison between F-AI and R-AI for Full tooth, crown and root segmentation (represented as mean with SD). (E) Median surface deviation from the clinical reference of F-AI and R-AI. (F and G) Morphologic surface comparison analysis of SA versus F-AI (F) and R-AI (G).

## RESULTS

Overall, AI-driven and clinical reference segmentations resulted in very similar segmentation volumes (figure 3A). The mean segmentation volume for the SA (clinical reference) was  $544 \text{ mm}^3 (\pm 121)$ , while this was  $536 \text{ mm}^3 (\pm 121)$  and  $538 \text{ mm}^3 (\pm 123)$  for the F-AI and the R-AI methods, respectively. The deviation in segmented volumes between F-AI and R-AI versus SA (clinical reference) was evaluated using the Bland-Altman method showing a systematic decrease in segmentation volume 1.7% for F-AI and 1.3% for R-AI (figure 3B-C).

The mean *IoU* for full tooth segmentation was  $0.87 (\pm 0.03)$  and  $0.88 (\pm 0.03)$  for SA vs F-AI and R-AI respectively. Both F-AI and R-AI performed as good as the human operator ( $p < 0.0001$ ), without any failure cases (*IoU* score below 0.5) (figure 4D). The mean DSC  $0.93$  was  $(\pm 0.02)$  and  $0.94 (\pm 0.02)$  for SA vs F-AI and R-AI respectively.

There was a significant effect on the *IoU* score at the  $p < 0.05$  for tooth types included in this study (incisors, canines and premolars) [F (2, 88) = 21.9,  $p < 0.0001$ ]. Post hoc comparisons using the Tukey test indicated that the mean *IoU* score for incisors (full tooth and crown segmentations) was significantly different than canines and premolars in both the F-AI and R-AI groups. Detailed *IoU* results are shown in table 1. While, there was no significant effect on the *IoU* score at the  $p < 0.05$  for the tooth apex maturation (mature vs. immature) [F (1, 89) = 0.1145,  $p = 0.73$ ].

A morphologic surface comparison between SA versus F-AI and R-AI showed an average median surface deviation of  $7.85 \mu\text{m} (\pm 69.55)$  and  $9.96 \mu\text{m} (\pm 59.33)$  (figure 3E). Both F-AI and R-AI performed as good as the human operator ( $p < 0.0001$ ), without average surface deviation higher than the cut-off value of  $200 \mu\text{m}$  (figure 3E, F and G).

There was a significant effect on the total time consumed at the  $p < 0.05$  for the three segmentation methods [F (2, 144) = 847,  $p < 0.0001$ ]. Post hoc comparisons using the Tukey test indicated that the SA segmentations time

(mean = 6.6 mins  $\pm$ 76.2s) was significantly different from the F-AI (mean = 0.5 mins  $\pm$ 8.6s) and R-AI (mean = 1.2 mins  $\pm$ 33.0s) segmentations. This difference demonstrated a 12.5- and 6.5-fold decrease in the segmentation time for the F-AI and R-AI respectively. The difference in segmentation time between F-AI and R-AI was statistically significant ( $p$ -value  $<$ 0.05). The aforementioned total time accounted for region of interest (ROI) selection, rotation, seeds/contour placement and image saving (figure 2). In case of AI-driven segmentations (F-AI / R-AI), the average time needed by the user for ROI selection, rotation and saving was 29.7 seconds ( $\pm$ 8.6s), and the average time needed by the algorithm to cast segmentation predictions on slices had a mean of 1.7 seconds ( $\pm$ 0.04s). Additional user interactions for R-AI segmentations then took an average of 55 seconds ( $\pm$ 2.5s).

**Table 1:** Mean IoU/DSC performance comparison depending on tooth part, condition and type for SA, F-AI and R-AI.

	SA vs F-AI Full tooth	SA vs R-AI Full tooth	SA vs F-AI Crown	SA vs R-AI Crown	SA vs F-AI Root	SA vs R-AI Root	SA vs F-AI Mature teeth	SA vs R-AI Mature teeth
<b>I</b> <b>o</b> <b>U</b>	0.877 ( $\pm$ 0.037)	0.881 ( $\pm$ 0.036)	0.887 ( $\pm$ 0.032)	0.889 ( $\pm$ 0.036)	0.894 ( $\pm$ 0.03)	0.898 ( $\pm$ 0.026)	0.876 ( $\pm$ 0.039)	0.881 ( $\pm$ 0.038)
<b>D</b> <b>S</b> <b>C</b>	0.934 ( $\pm$ 0.02)	0.937 ( $\pm$ 0.02)	0.940 ( $\pm$ 0.018)	0.941 ( $\pm$ 0.02)	0.944 ( $\pm$ 0.017)	0.946 ( $\pm$ 0.014)	0.934 ( $\pm$ 0.023)	0.937 ( $\pm$ 0.021)
	SA vs F-AI Immature teeth	SA vs R-AI Immature teeth	SA vs F-AI Incisors	SA vs R-AI Incisors	SA vs F-AI Canines	SA vs R-AI Canines	SA vs F-AI Premolars	SA vs R-AI Premolars
<b>I</b> <b>o</b> <b>U</b>	0.879 ( $\pm$ 0.032)	0.884 ( $\pm$ 0.031)	0.877 ( $\pm$ 0.038)	0.881 ( $\pm$ 0.035)	0.898 ( $\pm$ 0.027)	0.906 ( $\pm$ 0.029)	0.891 ( $\pm$ 0.025)	0.890 ( $\pm$ 0.022)
<b>D</b> <b>S</b> <b>C</b>	0.935 ( $\pm$ 0.018)	0.938 ( $\pm$ 0.018)	0.934 ( $\pm$ 0.024)	0.937 ( $\pm$ 0.022)	0.949 ( $\pm$ 0.012)	0.954 ( $\pm$ 0.013)	0.942 ( $\pm$ 0.011)	0.94 ( $\pm$ 0.0078)

## DISCUSSION

This study reports on the development and validation of a novel tool for automated tooth segmentation based on AI. The presented data confirms the positive impact of implementing AI technology in the field of radiology in general and segmentation in particular, highlighting the high accuracy and low time-consumption gained from AI integration.

Despite the heterogeneity of the dataset used in terms of age, image quality, voxel size and artefacts, no failure cases ( $IoU < 0.5$ ) were recorded and no cases showed an  $IoU$  rate below 0.77 – illustrating the wide array of clinical cases to which this tool can be applied. It must be stated that the  $IoU$  penalizes just a slight shift in overlap quite heavily. Therefore, a good overlap has an  $IoU > 0.6$ , and an excellent overlap has an  $IoU$  of  $> 0.9$  (Cop, 2018).

AI integration for tooth segmentation bridges the gap between automated segmentation and challenging cases such as immature teeth, teeth with fillings and metal induced artefacts. Previous studies applying automated segmentation methods using techniques such as the level-set or template-based fitting method for tooth segmentation (Cui et al., 2019), showed drawbacks obtaining highly accurate results on such challenging clinical cases, yet highly common in daily clinical practice.

CNNs have been introduced by (LeCun et al., 1989) in the early 1990's. They rely on hidden layers responsible of feature extraction and classification and have showed excellent results in detection and classification tasks (Zeiler & Fergus, 2014). In the current study a feature pyramid networks architecture was selected (Kirillov et al., 2018), since it is part of the state-of-the-art of semantic segmentation and because it showed from our preliminary results an acceptable inference time of approximately 1.6 seconds. As for the encoder, an efficientnet-b7 was used, as it achieves superior performances on the ImageNet dataset, while using less operations than other encoders such as ResNet (Tan & Le, 2019).

To date, few attempts of bridging AI and tooth segmentation were reported. Cui et al. (Cui et al., 2019) relied on a 2-stage approach with two 3D networks, requiring specialized software and advanced hardware to run efficiently. The sample size used in the study was relatively small (12 images for training and 8 for validation). Timing and comparison with manual segmentations were not reported, and no cases with artefacts were used. Moreover, DSC reached at most 0.921. Chen et al. (Chen et al., 2020) used a multi-task 3D fully convolutional network (V-Net) based on 3D operation to predict tooth region and surface. This approach had a maximum DSC of 0.94 ( $\pm 0.01$ ) and similar to the Cui et al.'s relies on a 3D approach, requiring heavy processing.

Lee et al.'s (Lee et al., 2020) used a 2D U-Net to label slice-by-slice, yet relied on mapping Grey values to HUs, which has been proven to be unreliable on CBCT even after normalization (Pauwels et al., 2015).

None of the approaches discussed reported the possibility of manual corrections or user interaction to enhance the AI-driven segmentations. Further, editing a 3D label-map is computationally demanding, as it requires going through the slices and editing on a voxel basis. Such methods may yield relatively slow results and require GPU to efficiently operate, complicating accurate user-interaction and manual corrections. Therefore, the aforementioned approaches might struggle with complex images, heavy scattering and other compromising radiological artefacts. In contrast to the 2D slice correction and interpolation approach applied in the current study.

This present study tackled these issues by exposing the algorithm to a large dataset with 314 CBCT scans, yielding 2924 fully segmented CSO paths for the study and diverse cases such as root shape variation, heavy scattering, restorations, orthodontic brackets, artefacts and resorptions. The method applied in the current study also allows for smooth user-interaction with the dentist in mind as an end-user. The operator is able to correct what is judged under- or over-estimated in a user-friendly and highly intuitive interface, given that the segmentations rely on CSOs seed points and contours on 2D images, which can easily be adjusted to precise locations, as well as having more

seeds/contours added or removed – according to the operator’s judgment. To the best of our knowledge, this is the first attempt of AI-driven tooth segmentation based on CSOs and 2D slices, that is combined with a previously validated interpolation algorithm for accurate 3D teeth segmentation (EzEldeen et al., 2015). This tool can be operated without GPU and therefore on personal computers and could also be implemented as a cloud-based service, serving a wider audience for DD applications.

It is fair to mention that this study has its own limitations. The AI algorithm was not trained to segment molars yet (figure 1). It can therefore segment from second premolar to second premolar in both the maxilla and mandible. The tool can also segment one tooth at a time and require a manual ROI selection and rotation, however both will be automated in the near future. Nevertheless, the results obtained are unique showing the effectiveness of this technique in terms of fully automated segmentations and provide the best results to date in terms of accuracy and time consumption for AI-driven teeth segmentations. The developed tool has a direct clinical application in guided-endodontics, CBCT-based TAT and orthodontic treatment planning and follow-up. Moreover, in research, the tool will simplify studying the 3D tooth root tissue changes after regenerative endodontic procedures (Austah et al., 2018; EzEldeen et al., 2015; Meschi et al., 2018), TAT (EzEldeen et al., 2019) and orthodontic tooth movement. Studying the 3D patterns of tissue deposition or resorption could offer valuable insights into the treatment outcomes and influence clinical decision making.

## **CONCLUSION**

The present study demonstrated a novel approach for using CNNs for accurate and fast automated 3D tooth segmentation. The aforementioned results may open doors for AI-driven applications in surgical and treatment planning for improving efficiency and accuracy of various procedures in oral surgery, orthodontics, guided-endodontics, tooth autotransplantation.

## **Supplemental Appendix S1. Data Acquisition and Training Database**

M3BE (mean age  $25 \pm 11$  years old) (Ethical Committee Research UZ/KU Leuven B322201525552) and CBCT-guided tooth autotransplantation (mean age  $13 \pm 2$  years old) (Ethics Committee Research UZ/KU Leuven - B322201317710). A total of 314 CBCT scans were taken by 3D Accuitomo 170 (Morita, Kyoto, Japan), ProMax 3D MAX (Planmeca, Helsinki, Finland), and NewTom VGI EVO (QR Verona, Cefla, Verona, Italy) devices (Supplemental appendix table 1), anonymized and imported into MeVisLab (MeVis Research, Bremen, Germany) for manual segmentation of the training dataset.

*Supplemental Appendix Table 1. Acquisition devices and parameters*

<b>CBCT Device</b>	<b>Voxel Size (<math>\mu\text{m}</math>)</b>	<b>Field of View (FOV) (mm x mm)</b>	<b>Number of Cases</b>
<b>Accuitomo 170</b>	80	40x40	12
<b>Accuitomo 170</b>	125	60x60	8
<b>ProMax 3D MAX</b>	150	100x90	2
<b>ProMax 3D MAX</b>	150	50x55	2
<b>Accuitomo 170</b>	160	80x80	114
<b>NewTom VGI evo</b>	200	100x100	11
<b>ProMax 3D MAX</b>	200	100x90	2
<b>NewTom VGI evo</b>	200	120x80	96
<b>NewTom VGI evo</b>	200	50x50	2
<b>ProMax 3D MAX</b>	200	50x55	1
<b>NewTom VGI evo</b>	200	80x50	2
<b>NewTom VGI evo</b>	200	80x80	43
<b>Accuitomo 170</b>	200	80x80	2
<b>NewTom VGI evo</b>	250	100x100	1
<b>NewTom VGI evo</b>	250	150x120	6
<b>NewTom VGI evo</b>	250	160x160	1
<b>Accuitomo 170</b>	250	80x80	3
<b>NewTom VGI evo</b>	300	240x190	2
<b>ProMax 3D MAX</b>	400	100x90	3
<b>ProMax 3D MAX</b>	400	50x55	1
			<b>314</b>

## **Supplemental Appendix S2**

### **Supplemental Appendix S2.1 Dataset pre-processing and augmentation**

The input images were normalized to the range 0-1 and resized to 192 by 192 pixels. Data augmentation techniques were used on the training set in order to increase the generalization and robustness of the model, with random combination of additive Gaussian noise, sharpening, Gaussian blur, multiplication, addition, X and Y scaling, rotation, horizontal and vertical flipping, as well as cropping.

### **Supplemental Appendix S2.2. Network Architecture of the ConvNet**

The architecture used is a Feature Pyramid Network (FPN) with an efficientnet-b7 encoder, which was pre-trained on the ImageNet dataset.

A hyper parameter search was performed for ConvNet selection, where the UNet architecture was investigated, as well as other pretrained encoders. The ConvNet that achieved the best accuracy, with an acceptable processing (i.e. inference) time was then selected. The FPN architecture was therefore chosen based on the validation set, that helps choose an appropriate network and aid in evaluating the progress with the training phase – preventing from overfitting the model. The FPN consists of three parts: an encoder, a decoder and a semantic segmentation branch. The encoder extracts the interesting features from the input image using convolutions, rectified linear unit (ReLU) operation and max pooling. The image is then down-sampled by 4 after each layer of the encoder resulting in a final feature map containing global information about the image, without local information. The decoder used is

symmetric to the encoder - but instead of down-sampling the image, it up-samples it in order to generate a dense segmentation mask of the input. To improve localization of the network, skip connections were added to combine the feature maps from the decoder with the ones of the encoder. A semantic segmentation branch then combines the feature maps from all the layers of the decoder into one single output. Feature maps are up-sampled to the same size - using convolutions, group norm, ReLU and bilinear up-sampling – and then combined using element-wise summing.

The hyper-parameters used for this study consisted of a depth of 5 layers, 2D dropout with probability of 20%, 256 channels for the feature pyramid of the decoder, 128 channels for the segmentation head, 1 input channel (grayscale) and 1 output channel (binary) (figure 1).

### **Supplemental Appendix S2.3. Hardware Considerations**

The study and validation were performed on a workstation loaded with 95.3GB of shared GPU memory, 8.0 GB of dedicated GPU memory, 2.3 GHz of CPU and 191 GB of usable memory RAM. A medical-grade screen display (Barco, Kortrijk, Belgium) was used for segmenting and evaluating the obtained results.

### **Supplemental Appendix S3. Intersection over Union (IoU) and Dice**

#### **Similarity Coefficient (DSC) assessment**

*IoU* is employed as a loss function in foreground and background classification tasks of object in an image.

The formula for the IoU is:

$$IoU(A, B) = \frac{|A \wedge B|}{|A \vee B|}$$

**Equation 1.** *IoU equation*

in which A and B are binary images of a tooth segmented by an expert and a tooth segmented by the software, respectively. The outcome yields an accuracy of overlap.

To relate *IoU* to the Dice similarity coefficient (*DSC*), another statistical, tool positively correlated to *IoU* and used for measuring the similarity between two sets of data for the validation of image segmentation algorithm created with AI, the following formulas were used:

$$IoU = \frac{\text{Area of Overlap}}{\text{Area of Union}} = \frac{TP}{(TP + FP + FN)}$$

**Equation 2.** *IoU in terms of TP, FP and FN*

The area of overlap between human and AI results is where the algorithm identifies pixels that exactly match the annotated ground truth segmentation. These pixels are known as true positives (TP). The pixels erroneously segmented by the CNN are known as false positives (FP) and the pixels that the CNN failed to segment are known as false negatives (FN).

The Dice Score can be expressed in terms of TP, FP and FN as follows:

$$DSC = \frac{2 \times TP}{(TP + FP) + (TP + FN)}$$

**Equation 3.** *Dice similarity coefficient (DSC) in terms of TP, FP and FN*

This yields the following equivalence relation between *IoU* and *DSC*:

$$IoU = \frac{DSC}{2 - DSC}$$

**Equation 4.** *IoU/Dice equivalence relation*

## REFERENCES

1. Akhoondali, H., Zoroofi, R. A., & Shirani, G. (2009). Rapid automatic segmentation and visualization of teeth in CT-scan data. *J. Applied Sci.*, 9(11), 2031-2044.
2. Austah, O., Joon, R., Fath, W. M., Chrepa, V., Diogenes, A., Ezeldeen, M., Couve, E., & Ruparel, N. B. (2018). Comprehensive Characterization of 2 Immature Teeth Treated with Regenerative Endodontic Procedures. *J Endod*, 44(12), 1802-1811.
3. Barrett, W. A., & Mortensen, E. N. (1997). Interactive live-wire boundary extraction. *Med Image Anal*, 1(4), 331-341.
4. Bland, J. M., & Altman, D. G. (1986). Statistical methods for assessing agreement between two methods of clinical measurement. *The Lancet*, 1, 307-310.
5. Byun, C., Kim, C., Cho, S., Baek, S. H., Kim, G., Kim, S. G., & Kim, S. Y. (2015). Endodontic Treatment of an Anomalous Anterior Tooth with the Aid of a 3-dimensional Printed Physical Tooth Model. *J Endod*, 41(6), 961-965.
6. Chen, Y., Du, H., Yun, Z., Yang, S., Dai, Z., Zhong, L., Feng, Q., & Yang, W. (2020). Automatic Segmentation of Individual Tooth in Dental CBCT Images From Tooth Surface Map by a Multi-Task FCN. *IEEE Access*, 8, 97296-97309.
7. Cop, R. (2018). Automatic teeth thresholding in cone beam CT with convolutional neural networks and tooth segmentation with the watershed transform University of Groningen. The Netherlands.
8. Cui, Z., Li, C., & Wang, W. (2019, 06/2019). *ToothNet: Automatic Tooth Instance Segmentation and Identification From Cone Beam CT Images* 2019 IEEE/CVF Conference on Computer Vision and Pattern Recognition (CVPR), Long Beach, CA, USA.
9. EzEldeen, M., Stratis, A., Coucke, W., Codari, M., Politis, C., & Jacobs, R. (2017). As Low Dose as Sufficient Quality: Optimization of Cone-beam Computed Tomographic Scanning Protocol for Tooth Autotransplantation Planning and Follow-up in Children. *J Endod*, 43(2), 210-217.
10. EzEldeen, M., Van Gorp, G., Van Dessel, J., Vandermeulen, D., & Jacobs, R. (2015). 3-dimensional analysis of regenerative endodontic treatment outcome. *J Endod*, 41(3), 317-324.
11. EzEldeen, M., Wyatt, J., Al-Rimawi, A., Coucke, W., Shaheen, E., Lambrechts, I., Willems, G., Politis, C., & Jacobs, R. (2019). Use of CBCT Guidance for Tooth Autotransplantation in Children. *J Dent Res*, 98(4), 406-413.
12. Heckel, F., Konrad, O., Karl Hahn, H., & Peitgen, H.-O. (2011). Interactive 3D medical image segmentation with energy-minimizing implicit functions. *Computers & Graphics*, 35(2), 275-287.

13. Jacobs, R. (2011). Dental cone beam CT and its justified use in oral health care. *JBR-BTR*, 94(5), 254-265.
14. Jacobs, R., Salmon, B., Codari, M., Hassan, B., & Bornstein, M. M. (2018). Cone beam computed tomography in implant dentistry: recommendations for clinical use. *BMC Oral Health*, 18(1), 88.
15. Kirillov, A., He, K., Girshick, R., Rother, C., & Dollar. (2018). *Panoptic Feature Pyramid Networks* The IEEE Conference on Computer Vision and Pattern Recognition (CVPR).
16. Kyong Hwan, J., McCann, M. T., Froustey, E., & Unser, M. (2017). Deep Convolutional Neural Network for Inverse Problems in Imaging. *IEEE Trans Image Process*, 26(9), 4509-4522.
17. Lakhani, P., Gray, D. L., Pett, C. R., Nagy, P., & Shih, G. (2018). Hello World Deep Learning in Medical Imaging. *J Digit Imaging*, 31(3), 283-289.
18. LeCun, Y., Boser, B., Denker, J. S., Henderson, D., Howard, R. E., Hubbard, W., & Jackel, L. D. (1989). Backpropagation Applied to Handwritten Zip Code Recognition. *Neural Comput*, 1(4), 541-551.
19. Lee, S., Woo, S., Yu, J., Seo, J., Lee, J., & Lee, C. (2020). Automated CNN-Based Tooth Segmentation in Cone-Beam CT for Dental Implant Planning. *Ieee Access*, 8, 50507-50518.
20. Litjens, G., Kooi, T., Bejnordi, B. E., Setio, A. A. A., Ciompi, F., Ghafoorian, M., van der Laak, J., van Ginneken, B., & Sanchez, C. I. (2017). A survey on deep learning in medical image analysis. *Med Image Anal*, 42, 60-88.
21. Ludlow, J. B., Davies-Ludlow, L. E., Brooks, S. L., & Howerton, W. B. (2006). Dosimetry of 3 CBCT devices for oral and maxillofacial radiology: CB Mercuray, NewTom 3G and i-CAT. *Dentomaxillofac Radiol*, 35(4), 219-226.
22. Meschi, N., EzEldeen, M., Torres Garcia, A. E., Jacobs, R., & Lambrechts, P. (2018). A Retrospective Case Series in Regenerative Endodontics: Trend Analysis Based on Clinical Evaluation and 2- and 3-dimensional Radiology. *J Endod*, 44(10), 1517-1525.
23. Nguyen, K. C. T., Duong, D. Q., Almeida, F. T., Major, P. W., Kaipatur, N. R., Pham, T. T., Lou, E. H. M., Noga, M., Punithakumar, K., & Le, L. H. (2020). Alveolar Bone Segmentation in Intraoral Ultrasonographs with Machine Learning. *J Dent Res*, 99(9), 1054-1061.
24. Pauwels, R., Jacobs, R., Singer, S. R., & Mupparapu, M. (2015). CBCT-based bone quality assessment: are Hounsfield units applicable? *Dentomaxillofac Radiol*, 44(1), 20140238.
25. Rahman, M. A., & Wang, Y. (2016). Optimizing Intersection-Over-Union in Deep Neural Networks for Image Segmentation. In *Advances in Visual Computing* (pp. 234-244). Springer.
26. Saha, S. (2018). A Comprehensive Guide to Convolutional Neural Networks — the ELI5 way.
27. Schwendicke, F., Samek, W., & Krois, J. (2020). Artificial Intelligence in Dentistry: Chances and Challenges. *J Dent Res*, 99(7), 769-774.

28. Shahbazian, M., Jacobs, R., Wyatt, J., Willems, G., Pattijn, V., Dhoore, E., C, V. A. N. L., & Vinckier, F. (2010). Accuracy and surgical feasibility of a CBCT-based stereolithographic surgical guide aiding autotransplantation of teeth: in vitro validation. *J Oral Rehabil*, 37(11), 854-859.
29. Shaheen, E., Khalil, W., Ezeldeen, M., Van de Castele, E., Sun, Y., Politis, C., & Jacobs, R. (2017). Accuracy of segmentation of tooth structures using 3 different CBCT machines. *Oral Surg Oral Med Oral Pathol Oral Radiol*, 123(1), 123-128.
30. Tan, M., & Le, Q. V. (2019). *EfficientNet: Rethinking Model Scaling for Convolutional Neural Networks* 36th International Conference on Machine Learning, Long Beach, California.
31. Toennies, K. D. (2017a). The Level Set Model. In *Guide to Medical Image Analysis - Methods and Algorithms* (2 ed., Vol. 1, pp. 311-360). Springer.
32. Toennies, K. D. (2017b). Segmentation and Basic Techniques. In *Guide to Medical Image Analysis - Methods and Algorithms* (2 ed., Vol. 1, pp. 208-247). Springer.
33. Torres, A., Shaheen, E., Lambrechts, P., Politis, C., & Jacobs, R. (2019). Microguided Endodontics: a case report of a maxillary lateral incisor with pulp canal obliteration and apical periodontitis. *Int Endod J*, 52(4), 540-549.
34. Van Assche, N., Vercauysen, M., Coucke, W., Teughels, W., Jacobs, R., & Quirynen, M. (2012). Accuracy of computer-aided implant placement. *Clin Oral Implants Res*, 23 Suppl 6, 112-123.
35. Zeiler, M. D., & Fergus, R. (2014). Visualizing and Understanding Convolutional Networks. In D. Fleet, T. Pajdla, B. Schiele, & T. Tuytelaars, *Computer Vision – ECCV 2014*.



## **CHAPTER IV | Development and validation of a novel artificial intelligence driven tool for accurate mandibular canal segmentation on CBCT**

*This chapter is based on the following publication: **Lahoud P, Diels S, Niclaes L, Van Aelst S, Willems H, Van Gerven A, Quirynten M, Jacobs R.** Development and validation of a novel artificial intelligence driven tool for accurate mandibular canal segmentation on CBCT. *Journal of dentistry.* 2022 Jan 1;116:103891.*

### Affiliations

1. OMFS-IMPACT Research Group, Department of Imaging and Pathology, Faculty of Medicine, KU, Leuven, Belgium
2. Department of Oral and Maxillofacial Surgery, University Hospitals Leuven, Leuven, Belgium
3. Department of Oral Health Sciences, Periodontology and Oral Microbiology, University Hospitals of Leuven, Belgium
4. Relu, Leuven, Belgium
5. Department of Dental Medicine, Karolinska Institute, Stockholm, Sweden

# Development and validation of a novel artificial intelligence driven tool for accurate mandibular canal segmentation on CBCT

*Lahoud P, Diels S, Niclaes L, Van Aelst S, Willems H, Van Gerven A, Quirynen M, Jacobs R.*

## **ABSTRACT**

**Aim(s):** The objective of this study is the development and validation of a novel artificial intelligence driven tool for fast and accurate mandibular canal segmentation on cone beam computed tomography (CBCT).

**Materials and Methods:** A total of 235 CBCT scans from dentate subjects needing oral surgery were used in this study, allowing for development, training and validation of a deep learning algorithm for automated mandibular canal (MC) segmentation on CBCT. Shape, diameter and direction of the MC were adjusted on all CBCT slices using a voxel-wise approach. Validation was then performed on a random set of 30 CBCTs - previously unseen by the algorithm - where voxel-level annotations allowed for assessment of all MC segmentations.

**Results:** Primary results show successful implementation of the AI algorithm for segmentation of the MC with a mean IoU of 0.636 ( $\pm 0.081$ ), a median IoU of 0.639 ( $\pm 0.081$ ), a mean Dice Similarity Coefficient of 0.774 ( $\pm 0.062$ ). Precision, recall and accuracy had mean values of 0.782 ( $\pm 0.121$ ), 0.792 ( $\pm 0.108$ ) and 0.99 ( $\pm 7.64 \times 10^{-5}$ ) respectively. The total time for automated AI segmentation was 21.26 s ( $\pm 2.79$ ), which is 107 times faster than accurate manual segmentation.

**Conclusion(s):** Given the importance of adequate pre-operative mandibular canal assessment, Artificial Intelligence could help relieve practitioners from the delicate and time-consuming task of manually tracing and segmenting this structure, helping prevent per- and post-operative neurovascular complications.

## INTRODUCTION

The last two decades have seen a shift towards full digital workflows for pretreatment diagnostics, treatment planning and follow-up (Jacobs, 2011; Ludlow et al., 2006). In this regard, Cone Beam Computed Tomography (CBCT) has gained a prominent position in this workflow, considering the low costs and compact size of such machines, meanwhile providing essential 3D anatomical details with high spatial resolution and low radiation dose (Carter et al., 2016; Ludlow et al., 2006). CBCT allows visualization of critical anatomical structures, such as the mandibular canal (MC), housing the vital mandibular neurovascular bundle (Agbaje et al., 2017; Jacobs et al., 2014). Knowledge of the exact position of the MC and its relation to adjacent structures is crucial to help avoiding mild to severe life-altering conditions (Agbaje et al., 2017; Ghaemina et al., 2011; Jacobs et al., 2014) during implant placement (Agbaje et al., 2017; Jacobs et al., 2014), sagittal split osteotomy (Agbaje et al., 2017; Friedland et al., 2008), cyst removal (Agbaje et al., 2017; Leung & Cheung, 2011) and tooth extraction (Agbaje et al., 2017; Friedland et al., 2008; Jacobs et al., 2014; Ueda et al., 2012). Such injuries are relatively common (incidence from 0.2 to 8.4%) (Pogrel & Goldman, 2004; Ueda et al., 2012), and could lead to (semi)-permanent paresthesia, anesthesia or dysesthesia of the innervated structures of the affected side (such as lip, jaw, teeth, tongue, mucosa, gingiva) (Agbaje et al., 2017; Leung & Cheung, 2011). Iatrogenic trigeminal damage could also significantly impact quality of life, lifestyle and psychosocial outcomes (Van der Cruyssen et al., 2020).

Accurate pre-operative assessment of the MC and any potential anatomical variation of this structure is thus crucial to avoid post-operative complications and damage to the inferior alveolar nerve (Agbaje et al., 2017; Friedland et al., 2008). Yet, precise and automatic delineation of the MC remains challenging. Several CBCT-guided planning software tools allow for visualization of the MC after manual placement of marks at different locations

across the canal's path with interpolation into a fixed diameter cylinder, providing a virtual depiction the MC, denoted as MC tracing.

Nevertheless, this approach yields certain inherent inaccuracies given the fully manual nature of the tracing (Gerlach et al., 2014; Gerlach et al., 2010), coupled with the inherent limitations of CBCTs in terms of low image contrast, increased noise, artefacts and the lack of Hounsfield units. All of this adds to the complexity of achieving - manually or automatically – an accurate assessment of this structure (Carter et al., 2016; Pauwels et al., 2015).

For these reasons, the introduction of Convolutional Neural Networks (CNNs) and Artificial Intelligence (AI) in medical imaging segmentation tasks has been seen as an apparent solution for countering such problems: CNNs, which are at the core of AI technologies, are computational processing systems heavily inspired by how the occipital cortex operates. They are comprised of neurons that self-optimize through learning, consisting of an input and an output layer, with multiple hidden layers in between. They are primarily used in the field of patterns recognition within images (O'Shea & Nash, 2015).

CNNs and AI have proven to counter various limitations previously met with manual and automatic segmentation methods (Popovic et al., 2007; Ronneberger et al., 2015; Toennies, 2017), which could in our case allow for accurate automated segmentation of the MC, in spite of localized morphological variations such as bifid canals and localized canal enlargement, assisting clinicians in accurate presurgical MC assessment; thus lowering the risk of per-and postoperative complications.

Therefore, the aim of this study is twofold: 1. development and validation of a novel tool for accurate voxel-wise segmentations, capable of adjusting to variations in MC shape and width MC; 2. training and automation of such a tool for fast and accurate result generation. The hypothesis is that such AI-driven tool might provide MC segmentations for clinical use, that are much faster and at least as accurate as the expert's segmentations.

## MATERIALS AND METHODS

### Data Acquisition and Training Database

A random collection of CBCT scans from the M3BE database (Ethical Committee Research UZ/KU Leuven B322201525552) was initially gathered, yielding a total of 235 CBCT scans from dentate patients needing oral surgical procedures (mean age  $25 \pm 11$  years old). Scans were acquired using the 3D Accuitemo 170 (Morita, Kyoto, Japan), ProMax 3D MAX (Planmeca, Helsinki, Finland), Scanora 3Dx (Soredex, Tuusula, Finland) and NewTom VGI EVO (QR Verona, Cefla, Verona, Italy) devices (table 1). An initial anonymization of the image dataset was subsequently performed.

The initially collected dataset was divided as follow: 166 cases for training (70.64%), 39 cases for testing (16.59%) and 30 cases for final validation of the algorithm (12.77%). All three subsets included a random distribution of CBCT scans from the four scanning devices, having various acquisition parameters and degrees of artefacts.

The testing dataset allowed to test several CNNs and opt for the one that showed the best results for the various parameters, such as speed and accuracy (Balki et al., 2019).

Next, the chosen CNNs were trained using a large number of cases (training dataset). To tackle maximum variability and increase robustness of the algorithm, included CBCTs relied on a variety of field of view (FOV) dimensions, various voxel sizes, presence of different types of artefacts in the scans, low- and high-resolution images, many levels of scattering and different degrees of mandibular canal cortication. The trained model was finally tested for validation using a set of unseen cases by the algorithm – being the validation dataset.

As for the training of the algorithm, 40 random CBCT scans were initially imported into Romexis® version 5.2.1.R (Planmeca, Helsinki, Finland) for

tracing of the MC – going from the mandibular foramen until the mental foramen – using the built-in tool in Romexis® for nerve annotation (Figure 1.A). The MC tracings were performed and verified by two experts in dentomaxillofacial radiology. The tool required the user to specify control points for the canal, followed by an automated interpolation of the pathway of the MC, based on the control points (Jaskari et al., 2020). A uniform cylinder of 2.50 mm was then fixed to simulate the width of the mandibular canal (Tsuji et al., 2005) (Figure 1.B). This initial training set allowed for the development of an initial version of a Deep Learning (DL) algorithm, Virtual Patient Creator (Relu BV, Leuven, Belgium), capable of performing accurate voxel-wise MC segmentations. 126 new random CBCT scans were then imported into the DL tool (Figure 1.C), where two experts in dentomaxillofacial radiology accurately segmented the limits of the MC on cross-sectional slices, with a voxel-wise segmentation approach (Figure 1.D).

The performed segmentations were double checked jointly by the experts and adjustments were made when deemed necessary. Segmentations were then used to train and refine the DL algorithm and allow for the development of a refined and robust algorithm (Figure 1.E).

**Table 1.** Acquisition devices and parameters of the study's database

<b>CBCT Device</b>	<b>Voxel Size <math>\mu\text{m}</math></b>	<b>Field of View (FOV) mm x mm</b>	<b>Number of Cases</b>
<b>NewTom VGI evo</b>	100	80 x 80	4
<b>NewTom VGI evo</b>	125	120 x 80	7
<b>NewTom VGI evo</b>	150	80 x 80	5
<b>NewTom VGI evo</b>	150	120 x 80	4
<b>NewTom VGI evo</b>	200	120 x 80	61
<b>NewTom VGI evo</b>	200	100 x 100	26
<b>NewTom VGI evo</b>	250	150 x 120	24
<b>NewTom VGI evo</b>	300	240 x 190	51
<b>NewTom VGI evo</b>	300	160 x 160	3
<b>ProMax 3D MAX</b>	250	130 x 90	5
<b>ProMax 3D MAX</b>	400	230 x 260	7
<b>ProMax 3D MAX</b>	200	130 x 130	5
<b>Accuitomo 170</b>	250	140 x 165	16
<b>Accuitomo 170</b>	200	140 x 100	7
<b>Accuitomo 170</b>	125	100 x 100	5
<b>Scanora 3Dx</b>	160	140 x 100	2
<b>Scanora 3Dx</b>	250	170 x 120	3
			<b>235</b>

### **Dataset pre-processing and augmentation**

Various types of data augmentation strategies were applied to artificially increase the dataset and improve on generalizability and robustness of the model (Figure 1.B, D). These strategies included affine transformations such as scaling, rotation, shear, mirroring, translation, elastic deformations and random cropping. These techniques were randomly applied during the training phase.

### **Network Architecture of the ConvNet**

In this study, two CNNs worked together in order to produce a full-resolution segmentation output. The first CNN performed a coarse segmentation of the MC, while the second CNN performed in turn a fine segmentation on the region around the coarse segmentation.

Based on the test set – which is used to optimize the network architecture by minimizing the error on this dataset (Larsen et al., 1996) – the architecture used for MC segmentation was a 3D U-Net (Çiçek et al., 2016; Ronneberger et al., 2015). The U-Net is an encoder-decoder fully convolutional network with skip connections, that has been successfully applied in various medical segmentation problems. The encoder extracted the interesting features from the input image using convolutions, rectified linear unit (ReLU) operation and max pooling. The images were then down-sampled, resulting in a final feature map containing global information about the image. The decoder used is symmetric to the encoder and helps generate a dense segmentation mask of the input.

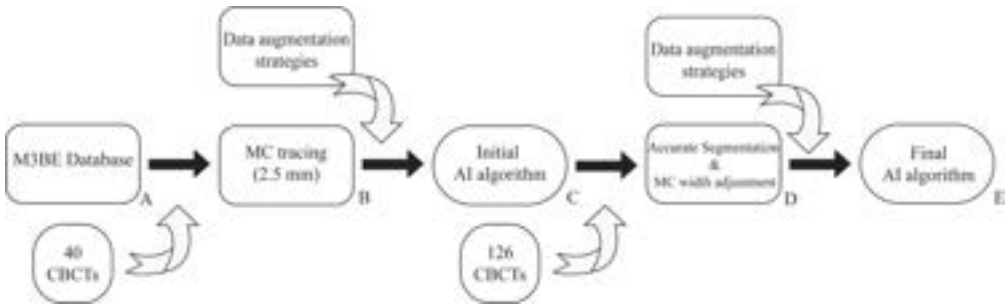


**Figure 1.** Workflow of the methodology used for the development and training of an AI-driven algorithm for mandibular canal segmentation on CBCT.

To improve localization of the network, skip connections were added to combine the feature maps from the decoder with the ones of the encoder. A semantic segmentation branch subsequently combined the feature maps from all the layers of the decoder into one single output. Feature maps were up-sampled to the same size using convolutions, group norm, ReLU and bilinear up-sampling – and then combined using element-wise summing. The model was trained on full resolution patches with Binary Cross Entropy loss and early stopping (Figure 2).

### AI driven MC segmentation

A 3D U-Net CNN (Çiçek et al., 2016), trained with the above described dataset was developed for automated detection and segmentation of the MC. The tool relied on automatically detecting the path of the MC using a voxel-wise probability approach.

Moreover, the possibility of user interaction was preserved with the ability to modify the path of the canal as well as its shape and width. Over- and under-estimations could therefore be adjusted, if deemed necessary by the operator.

## Validation Dataset

AI study validation relied on 30 randomly selected CBCT scans, where AI-driven segmentation of the MC was performed (Figure 3).

Results were saved as Digital Imaging and Communications in Medicine (DICOM) files and as Standard Tessellation Language file (STL). Expert manual segmentations were then conducted, allowing for further objective accuracy assessment between AI-driven versus expert manual MC segmentations.

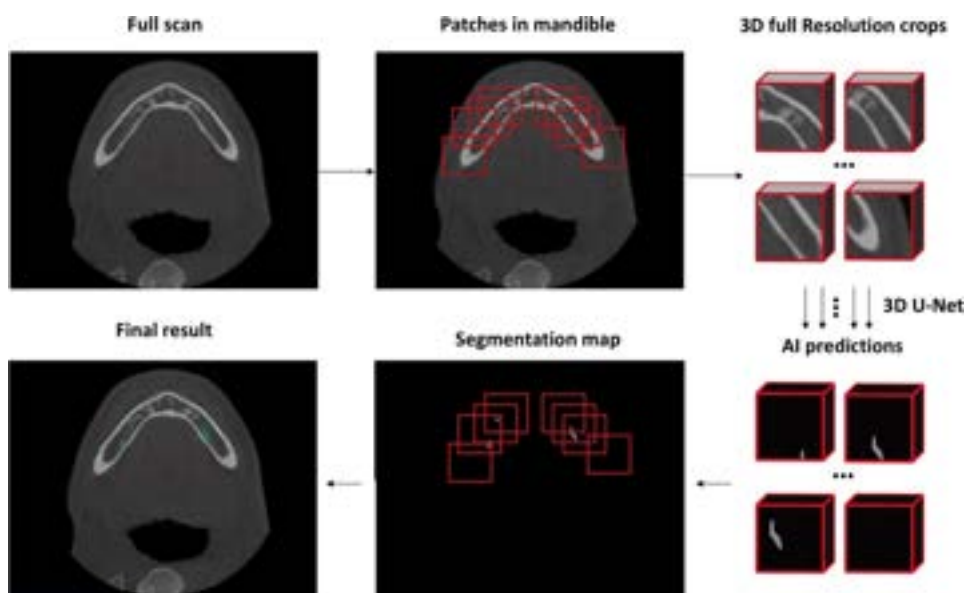


Figure 2. Workflow of the 3D U-Net Convolutional Neural Network.

## Assessment and Validation of the algorithm

Voxel-level annotations were performed on the validation set to assess the accuracy and performance of the AI-driven segmentations. Firstly, the intersection-over-union (IoU) score was assessed: IoU is a standard performance measure for the object category segmentation problem. For a

given object, the IoU measures the similarity between the predicted object and its ground-truth counterpart. It is defined by the following equation:

$$(1) \quad IoU = \frac{TP}{FP + TP + FN}$$

where, TP, FP, and FN denote the true positive, false positive and false negative pixel counts, respectively (Rahman & Wang, 2016). The area of overlap between expert-user and AI-algorithm results is where the algorithm identifies which voxels exactly match the annotated ground truth segmentation. These voxels are known as TP. The voxels erroneously segmented by the CNN are known as FP and the pixels that the CNN failed to segment are known as FN.

Furthermore, the Dice Similarity Coefficient (*DSC*), which relates to the amount of intersection between two segmented objects (Popovic et al., 2007; Rahman & Wang, 2016), is defined by the following equation:

$$(2) \quad DSC = \frac{2 \times TP}{(TP + FP) + (TP + FN)}$$

Hausdorff Distance (HD) was used as an indicator of the largest segmentation error (Karimi & Salcudean, 2020). HD indicates the longest distance given from a point in the first segmented entity (manual expert segmentation) to its closest point in the other entity (AI-computed segmentation). HD is therefore computed between boundaries of the AI-computed and ground-truth segmentations, which consist of curves in 2D and surfaces in 3D (Beauchemin et al., 1998; Karimi & Salcudean, 2020). HD is defined by:

$$HD(A, B) = \max [hd(A, B), hd(B, A)]$$

Where the function  $hd(A, B)$  is referred to as the directed Hausdorff distance from  $A$  to  $B$ . It ranks each point of  $A$  according to its distance to the nearest point of  $B$ . The largest of these distances determines the value of  $hd(A, B)$  (Beauchemin et al., 1998).

The precision and recall measures characterize the agreement between the oriented boundary edge elements of region boundaries of two segmentations (Monteiro & Campilho, 2006). They are therefore calculated based on overlapping regions. Two aspects related to overlapping regions are stated prior to experimentation: the matching direction and the corresponding criteria. The matching direction for the precision measure is defined as a reference-to-segment directional correspondence (Zhang et al., 2015). Precision and recall measures relate to the following equations:

$$Precision = \frac{TP}{TP + FP}$$

$$Recall = \frac{TP}{TP + FN}$$

Accuracy is a weighted arithmetic mean which explicitly takes into account the classification of negatives, and is expressible both as a weighted average of Precision and Inverse Precision and as a weighted average of Recall and Inverse Recall (Powers, 2011). It is defined as follows:

$$Accuracy = \frac{TP + TN}{TP + TN + FP + FN}$$

Time was also recorded by from the moment the algorithm received the DICOM of the scan, until a segmentation map was outputted.

### **Part comparison analysis of MC segmentation versus tracing**

In order to further elaborate on the advantages of the development of a MC segmentation tool as opposed to MC tracing – where a fixed diameter is used to simulate the whole path of the neuro-vascularization, a part comparison analysis was performed based on the two methods: For the AI-driven automatic MC segmentation method, the DICOM files were imported into the

cloud-based tool, where the AI-driven algorithm yielded stereolithography (STL) files of the segmented MC. The same DICOM files were then loaded into Romexis® version 5.2.1.R, where accurate manual MC tracing was performed, relying on a 2.5 mm fixed diameter and a 2.0 mm slice thickness between the different points of the tracing. After export, STLs were imported into 3-Matic (Materialise, Leuven, Belgium), where a signed part comparison analysis (PCA) was performed.

PCA allows to calculate the volumetric deviation between two structures: in this case between AI-driven segmentations and manual MC tracing (Figure 4).

## RESULTS

Results of IoU, DSC, Precision, Recall, Accuracy and HD can be found in **table 2**. The mean IoU of the 30 cases was 0.636 ( $\pm 0.081$ ), the median IoU 0.639 ( $\pm 0.081$ ), the mean DSC was 0.782 ( $\pm 0.062$ ). HD had a mean value of 0.705mm ( $\pm 0.389$ ), while Precision, Recall and Accuracy had mean values of 0.782 ( $\pm 0.121$ ), 0.792 ( $\pm 0.108$ ) and 0.99 ( $\pm 9.52 \times 10^{-05}$ ) respectively Total time from uploading until result visualization was 21.26 s ( $\pm 2.79$ ), while the average time for expert manual segmentation was 37.9 minutes ( $\pm 9.11$ ).

Furthermore, a part comparison analysis from the registration of the AI-driven MC segmentation on the expert manual segmentations shows high agreement between the two methods at the level of first and second molars, as well as at the distal level of the second molar, mesial to the first molar and at the level of the mandibular foramen, with a mean deviation of 0.382 mm ( $\pm 0.860$ ) between AI-driven automated segmentations and manual tracing of the MC (figure 4).

**Table 2.** Results of the intersection-over-union (IoU), Dice Similarity Coefficient (DSC), Precision, Recall, Accuracy and Hausdorff distance (HD) (mm) measures are presented for all 30 CBCTs of the validation dataset. The mean and standard deviation (SD) of the results are shown in the last two rows.

	<b>IoU</b>	<b>DSC</b>	<b>Precision</b>	<b>Recall</b>	<b>Accuracy</b>	<b>HD</b>
<b>1</b>	0.716	0.835	0.834	0.835	0.999	0.559
<b>2</b>	0.785	0.880	0.915	0.846	0.999	0.346
<b>3</b>	0.652	0.789	0.916	0.694	0.999	0.600
<b>4</b>	0.688	0.815	0.750	0.892	0.999	0.400
<b>5</b>	0.672	0.804	0.719	0.912	0.999	0.447
<b>6</b>	0.698	0.822	0.888	0.765	0.999	0.400
<b>7</b>	0.504	0.670	0.577	0.799	0.999	1.095
<b>8</b>	0.695	0.820	0.709	0.972	0.999	0.400
<b>9</b>	0.637	0.778	0.923	0.673	0.999	0.559
<b>10</b>	0.449	0.620	0.708	0.551	0.999	2.163
<b>11</b>	0.634	0.776	0.788	0.765	0.999	0.600
<b>12</b>	0.519	0.683	0.549	0.906	0.999	1.637
<b>13</b>	0.547	0.707	0.852	0.605	0.999	0.938
<b>14</b>	0.630	0.773	0.732	0.818	0.999	0.632
<b>15</b>	0.640	0.781	0.889	0.696	0.999	0.600
<b>16</b>	0.780	0.876	0.915	0.841	0.999	0.490
<b>17</b>	0.595	0.746	0.600	0.987	0.999	0.490
<b>18</b>	0.513	0.678	0.545	0.896	0.999	0.825
<b>19</b>	0.546	0.706	0.579	0.906	0.999	1.020
<b>20</b>	0.589	0.741	0.757	0.727	0.999	0.938
<b>21</b>	0.664	0.798	0.814	0.783	0.999	0.500
<b>22</b>	0.698	0.822	0.828	0.816	0.999	0.490
<b>23</b>	0.626	0.770	0.841	0.710	0.999	0.849
<b>24</b>	0.673	0.805	0.757	0.858	0.999	0.490
<b>25</b>	0.614	0.761	0.846	0.691	0.999	0.600
<b>26</b>	0.643	0.783	0.731	0.843	0.999	0.896
<b>27</b>	0.752	0.859	0.858	0.859	0.999	0.447
<b>28</b>	0.724	0.840	0.924	0.770	0.999	0.400
<b>29</b>	0.598	0.748	0.969	0.609	0.999	0.748
<b>30</b>	0.591	0.743	0.758	0.729	0.999	0.600
<b>Mean</b>	<b>0.636</b>	<b>0.774</b>	<b>0.782</b>	<b>0.792</b>	<b>0.999</b>	<b>0.705</b>
<b>SD</b>	<b>0.081</b>	<b>0.062</b>	<b>0.121</b>	<b>0.108</b>	<b>9.52x10<sup>-5</sup></b>	<b>0.389</b>

## DISCUSSION

Accurate MC assessment for procedures similar to tooth extraction, implant placement, bone grafting and orthognathic surgeries have proven to be of high clinical relevance (Gerlach et al., 2014; Jaskari et al., 2020; Kwak et al., 2020). Assessing structures using imaging modalities, such as CBCTs can be done through segmentation.

However, limitations of conventional segmentation techniques for surgical assessment in both the medical and dental fields have led in the last few years to a surge in DL technologies for classification and segmentation purposes (Lahoud et al., 2021; Leite, Gerven, et al., 2020). CNNs have shown great potential in generating accurate results, given their capabilities of learning from contextual information within image slices of complex 3D anatomical structures (Leite, Vasconcelos, et al., 2020). Nowadays, CNNs have proven to outperform conventional approaches in many computer-vision and image segmentation tasks (Çiçek et al., 2016; Lahoud et al., 2021; Leite, Gerven, et al., 2020). While current limitations were mainly centered around GPU and hardware technicalities, current progresses - as is the case in this study - allow to run DL algorithms on the cloud, relieving clinicians and researchers from having to invest and maintain complex and expensive hardware equipment.

This study reports on development and validation of a novel tool for MC segmentation based on DL and AI technologies. In this study, the algorithm successfully detected the presence of the MC bilaterally on all CBCTs. Despite the heterogeneity of the dataset used in terms of CBCT devices, FOVs, voxel sizes, presence of artefacts and the various degrees of cortication of the MC, a high level of accuracy was achieved by the algorithm, with only one case from the validation subset displaying an IoU  $< 0.5$  (supplemental figure 1). Regarding accuracy metrics, it must be stated that the IoU penalizes slight shifts in overlap quite heavily, with a good overlap having an IoU  $> 0.60$  (DSC  $> 0.75$ ) (Cop, 2018).

Kwak et al. in (Kwak et al., 2020) tested several CNNs for mandibular canal detection and obtained a mean IoU of 0.577 using a 3D U-Net. Their study however shows a lack of variability in the acquisition parameters of the training set, whereas all CBCT scans were acquired using the same device, with relatively similar acquisition parameters. This issue was tackled in the present study, where variability was greatly introduced in the training, testing and validation datasets, as well as by the used of data augmentation strategies, which resulted in a highly robust algorithm with an increased generalizability and performance of the model. As for the study published by Jaskari et al. in (Jaskari et al., 2020), results showed a mean DSC of 0.570, well below the acceptable DSC score of 0.75 (Cop, 2018).

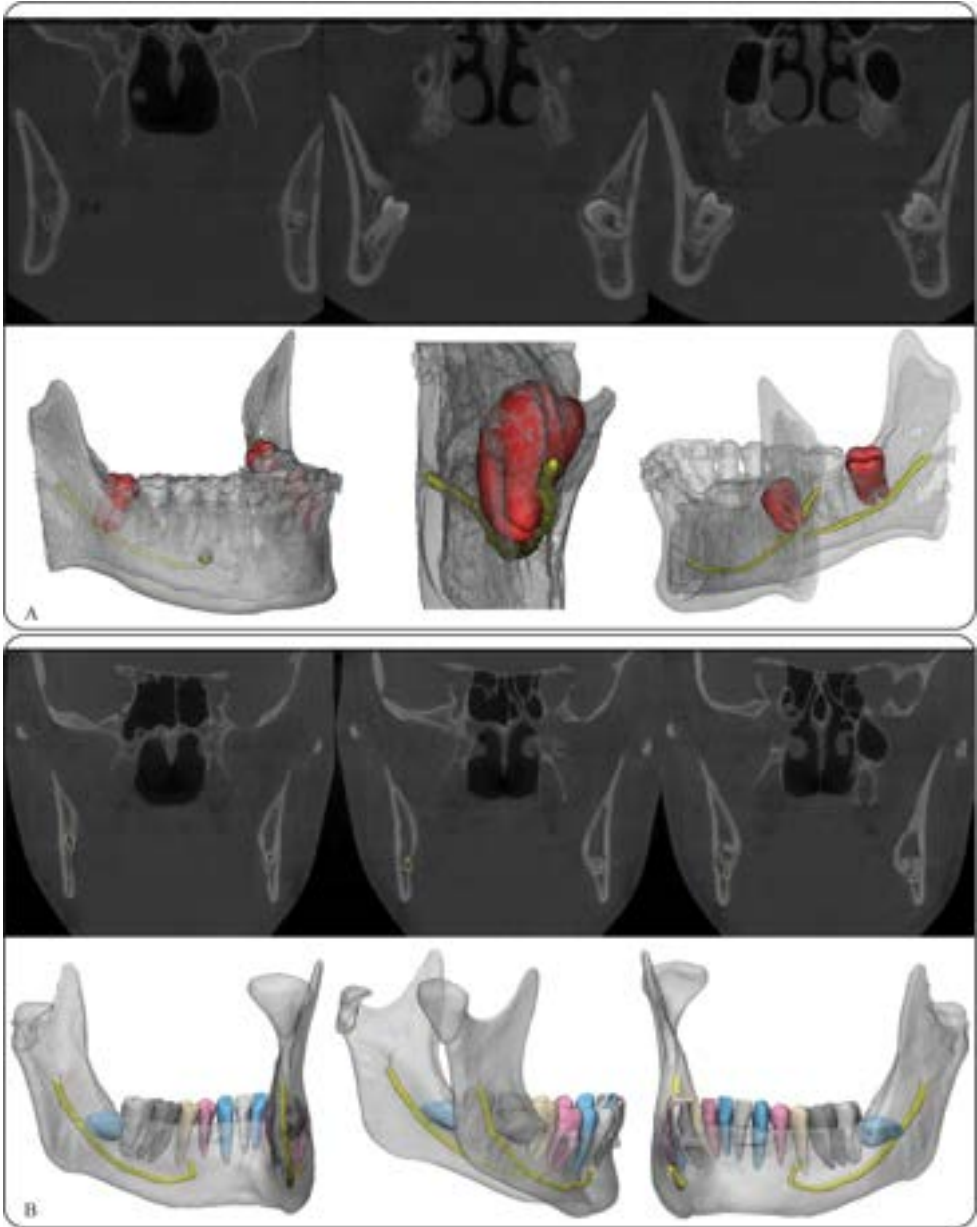


**Figure 3.** 3-Dimensional simulation of an AI-driven mandibular canal segmentation on CBCT, where the proximity between the mandibular canal and third molar can be visualized and assessed preoperatively (A), as well as its relation with all dental structures in the mandible (B).

With a DSC score of  $0.774 (\pm 0.061)$ , this study relates to the first AI-driven tool for MC segmentation to pass the barrier of clinically acceptable accuracy and allows for its potential use in surgical planning scenarios.

To achieve such results, accurate manual segmentations took expert operators on average  $37.9 (\pm 9.11)$  minutes per CBCT. Presently, AI-driven automated segmentations of the MC take on average  $21.26 \text{ s} (\pm 2.79)$  – 107 times faster than accurate expert-manual segmentation of this bilateral structure.

It is also important to mention that the state-of-the-art approach used in this study relies on accurate MC segmentation as opposed to MC tracing – the latter being the current standard for both manual and automated approaches. MC segmentation allows for more accurate results and the ability to detect and adapt to morphological variations, such as localized canal enlargement and bifid canals.

While a part comparison analysis further confirmed the high agreement in terms of accuracy between MC tracing and MC segmentation (mean deviation of  $0.38 \text{ mm} (\pm 0.86)$ ), it interestingly illustrated that most deviations happened at the level of the third molar and between first and second premolars. In this context, it is clinically very relevant to highlight that AI-driven segmentations seemed to better adjust in cases where a lack of clear cortication of the MC was observed and in cases of proximity between the roots of the mandibular third molar and the MC when compared to other MC tracing modalities (Jaskari et al., 2020). To further tackle this issue during training, the radiologists cross-checked manual segmentations until reaching a consensus regarding the path of the mandibular canal, before feeding the data to the deep learning algorithm. This allowed to limit potential errors in the training dataset and improve the performance of the algorithm, given that those regions remain of utmost importance for both oral and maxillofacial surgeries, where small anatomical variations might cause mild to severe per- and postoperative complications (Agbaje et al., 2017; Ghaemini et al., 2011; Jacobs et al., 2014) (see also figures 3-4).

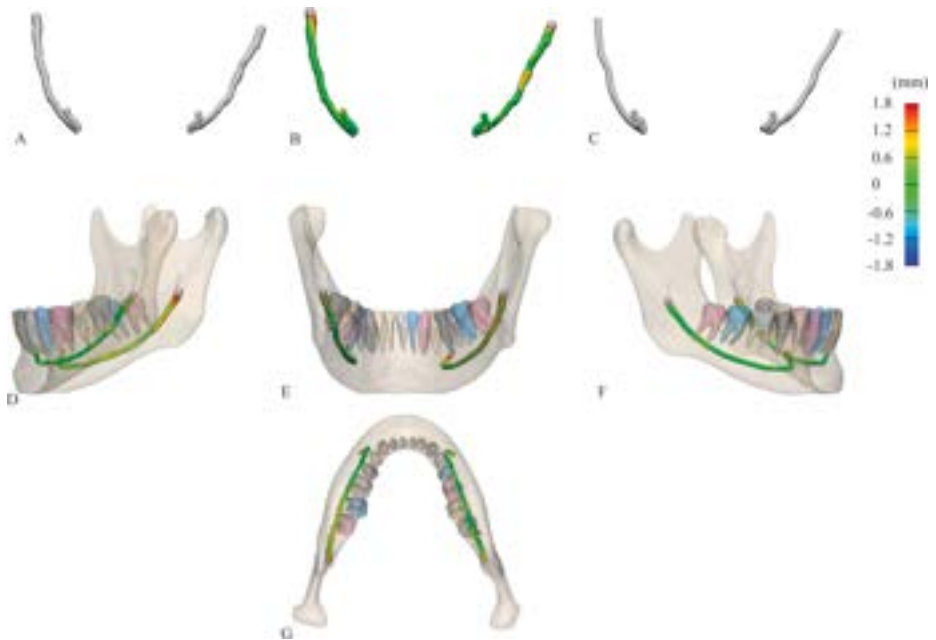


**Figure 4.** 3-Dimensional part comparison analysis (B) between mandibular canal segmentations (A) and mandibular canal tracing (C). Lateral (D, F), frontal (E) and inferio-superior (G) views of the part comparison analysis highlight areas of deviation between the two scenarios, due to local variation of the width of the mandibular canal, inferior or superior to 2.5 mm.

Blind to the device or acquisition parameters used – the algorithm seemed to perform best on CBCTs, where a higher degree of cortication was observed; from which the algorithm could accurately detect the presence of the mandibular canal on slices where cortication is visible, and subsequently accurately interpolate the position of the canal in between. Higher degrees of cortication of the MC were observed on CBCTs acquired using a High Resolution (HR) acquisition protocol; a finding that was further supported by Zaki et al. (Zaki et al., 2021).

This study therefore introduces two novel concepts for MC assessment: segmentation using adjustable diameters and shapes for accurate segmentation, as well as automation using AI. This opens new doors in the

field of digital dentistry – be it for implant placement, tooth extraction and/or orthognathic surgeries – where future research could help segment anterior branches of the mandibular neuro-vascular bundle up to the mandibular symphysis. Furthermore, AI could assist in automatically classifying and notifying clinicians of any potential proximity and risk associated with a given procedure.

Despite the mandibular canal being one of the most challenging structures to segment on CBCT (Kwak et al., 2020), results obtained in this study point to the benefits AI and DL technologies could bring to both researchers and practitioners in terms of high precision, low time-consumption and user-friendliness for diagnostics, surgical planning and patients' follow-up.

While AI may never fully replace experienced clinicians in their assessments, current results confirm its positive role in assisting both experienced and novice practitioners in their diagnoses, presurgical planning and daily patient management.

This study does however have some limitations: since dealing with Artificial Intelligence requires a great deal of variability, predictions cannot be made as for how the algorithm will perform outside scans taken from the CBCT devices used for training and testing of this study, as well as outside the acquisition parameters used. Anatomical variations are also another aspect where rigorous testing remains needed given the scarcity, yet crucial importance of assessing such variations. Future prospective of this study will focus on tackling these issues as well as on the subsequent segmentation of the anterior portion of the mandibular canal and on scans of adolescent patients presenting mixed dentition.

This will in turn allow for the clinical usability of such a tool in planning oral and maxillofacial surgeries, helping avoid neuro-vascular complications and potentially help in the diagnosis of pathological processes affecting the neurovascular mandibular bundle.

## **CONCLUSION**

The present study introduced development and validation of a novel AI-driven tool for fast and accurate mandibular canal segmentation on CBCT. The results obtained in this study could help improving pre-surgical planning procedures, such as for implant placement, bone grafting, orthognathic surgery and tooth extraction. The developed technique may open further doors for advanced AI development to automatically visualize accessory canals, anatomical variations as well as neurovascularisation in the symphyseal area of the mandible.

## REFERENCES

1. Agbaje, J. O., de Castele, E. V., Salem, A. S., Anumendem, D., Lambrichts, I., & Politis, C. (2017). Tracking of the inferior alveolar nerve: its implication in surgical planning. *Clin Oral Investig*, *21*(7), 2213-2220.
2. Balki, I., Amirabadi, A., Levman, J., Martel, A. L., Emersic, Z., Meden, B., Garcia-Pedrero, A., Ramirez, S. C., Kong, D., Moody, A. R., & Tyrrell, P. N. (2019). Sample-Size Determination Methodologies for Machine Learning in Medical Imaging Research: A Systematic Review. *Can Assoc Radiol J*, *70*(4), 344-353.
3. Beauchemin, M., Thomson, K. P. B., & Edwards, G. (1998). On the Hausdorff Distance Used for the Evaluation of Segmentation Results. *Canadian Journal of Remote Sensing*, *24*(1), 3-8.
4. Carter, J. B., Stone, J. D., Clark, R. S., & Mercer, J. E. (2016). Applications of Cone-Beam Computed Tomography in Oral and Maxillofacial Surgery: An Overview of Published Indications and Clinical Usage in United States Academic Centers and Oral and Maxillofacial Surgery Practices. *J Oral Maxillofac Surg*, *74*(4), 668-679.
5. Çiçek, Ö., Abdulkadir, A., Lienkamp, S. S., Brox, T., & Ronneberger, O. (2016). 3D U-Net: learning dense volumetric segmentation from sparse annotation. Proceedings of the Medical Image Computing and Computer-Assisted Intervention,
6. Cop, R. (2018). *Automatic teeth thresholding in cone beam CT with convolutional neural networks and tooth segmentation with the watershed transform* [University of Groningen]. The Netherlands.
7. Friedland, B., Donoff, B., & Dodson, T. B. (2008). The use of 3-dimensional reconstructions to evaluate the anatomic relationship of the mandibular canal and impacted mandibular third molars. *J Oral Maxillofac Surg*, *66*(8), 1678-1685.
8. Gerlach, N. L., Ghaemina, H., Bronkhorst, E. M., Berge, S. J., Meijer, G. J., & Maal, T. J. (2014). Accuracy of assessing the mandibular canal on cone-beam computed tomography: a validation study. *J Oral Maxillofac Surg*, *72*(4), 666-671.
9. Gerlach, N. L., Meijer, G. J., Maal, T. J., Mulder, J., Rangel, F. A., Borstlap, W. A., & Berge, S. J. (2010). Reproducibility of 3 different tracing methods based on cone beam computed tomography in determining the anatomical position of the mandibular canal. *J Oral Maxillofac Surg*, *68*(4), 811-817.

10. Ghaemina, H., Meijer, G. J., Soehardi, A., Borstlap, W. A., Mulder, J., Vlijmen, O. J., Berge, S. J., & Maal, T. J. (2011). The use of cone beam CT for the removal of wisdom teeth changes the surgical approach compared with panoramic radiography: a pilot study. *Int J Oral Maxillofac Surg*, 40(8), 834-839.
11. Jacobs, R. (2011). Dental cone beam CT and its justified use in oral health care. *JBR-BTR*, 94(5), 254-265.
12. Jacobs, R., Quirynen, M., & Bornstein, M. M. (2014). Neurovascular disturbances after implant surgery. *Periodontology 2000*, 66(1), 188-202.
13. Jaskari, J., Sahlsten, J., Jarnstedt, J., Mehtonen, H., Karhu, K., Sundqvist, O., Hietanen, A., Varjonen, V., Mattila, V., & Kaski, K. (2020). Deep Learning Method for Mandibular Canal Segmentation in Dental Cone Beam Computed Tomography Volumes. *Sci Rep*, 10(1), 5842.
14. Karimi, D., & Salcudean, S. E. (2020). Reducing the Hausdorff Distance in Medical Image Segmentation With Convolutional Neural Networks. *IEEE Trans Med Imaging*, 39(2), 499-513.
15. Kwak, G. H., Kwak, E. J., Song, J. M., Park, H. R., Jung, Y. H., Cho, B. H., Hui, P., & Hwang, J. J. (2020). Automatic mandibular canal detection using a deep convolutional neural network. *Sci Rep*, 10(1), 5711.
16. Lahoud, P., EzEldeen, M., Beznik, T., Willems, H., Leite, A., Van Gerven, A., & Jacobs, R. (2021). Artificial intelligence for fast and accurate 3D tooth segmentation on CBCT. *J Endod*.
17. Larsen, J., Hansen, L. K., Svarer, C., & Ohlsson, M. (1996). Design and regularization of neural networks: the optimal use of a validation set. Proceedings of the 1996 IEEE Signal Processing Society Workshop.
18. Leite, A. F., Gerven, A. V., Willems, H., Beznik, T., Lahoud, P., Gaeta-Araujo, H., Vranckx, M., & Jacobs, R. (2020). Artificial intelligence-driven novel tool for tooth detection and segmentation on panoramic radiographs. *Clin Oral Investig*.
19. Leite, A. F., Vasconcelos, K. F., Willems, H., & Jacobs, R. (2020). Radiomics and Machine Learning in Oral Healthcare. *Proteomics Clin Appl*, 14(3), e1900040.
20. Leung, Y. Y., & Cheung, L. K. (2011). Risk factors of neurosensory deficits in lower third molar surgery: an literature review of prospective studies. *Int J Oral Maxillofac Surg*, 40(1), 1-10.
21. Ludlow, J. B., Davies-Ludlow, L. E., Brooks, S. L., & Howerton, W. B. (2006). Dosimetry of 3 CBCT devices for oral and maxillofacial radiology: CB Mercuray, NewTom 3G and i-CAT. *Dentomaxillofac Radiol*, 35(4), 219-226.

22. Monteiro, F. C., & Campilho, A. C. (2006). Performance Evaluation of Image Segmentation. In A. C. Campilho & M. Kamel (Eds.), *Image Analysis and Recognition* (pp. 248-259). Springer.
23. O'Shea, K., & Nash, R. (2015). An Introduction to Convolutional Neural Networks. *Computing Research Repository*.
24. Pauwels, R., Jacobs, R., Singer, S. R., & Mupparapu, M. (2015). CBCT-based bone quality assessment: are Hounsfield units applicable? *Dentomaxillofac Radiol*, *44*(1), 20140238.
25. Pogrel, M. A., & Goldman, K. E. (2004). Lingual flap retraction for third molar removal. *J Oral Maxillofac Surg*, *62*(9), 1125-1130.
26. Popovic, A., de la Fuente, M., Engelhardt, M., & Radermacher, K. (2007). Statistical validation metric for accuracy assessment in medical image segmentation. *International Journal of Computer Assisted Radiology and Surgery*, *2*(3-4), 169-181.
27. Powers, D. M. W. (2011). Evaluation: From Precision, Recall and F-Factor to ROC, Informedness, Markedness & Correlation. *Journal of Machine Learning Technologies*, *2*, 37-63.
28. Rahman, M. A., & Wang, Y. (2016). Optimizing Intersection-Over-Union in Deep Neural Networks for Image Segmentation. In *Advances in Visual Computing* (pp. 234-244). Springer.
29. Ronneberger, O., Fischer, P., & Brox, T. (2015). U-Net: Convolutional Networks for Biomedical Image Segmentation. In *Medical Image Computing and Computer-Assisted Intervention – MICCAI 2015* (pp. 234-241).
30. Toennies, K. D. (2017). Segmentation and Basic Techniques. In *Guide to Medical Image Analysis - Methods and Algorithms* (2 ed., Vol. 1, pp. 208-247). Springer.
31. Tsuji, Y., Muto, T., Kawakami, J., & Takeda, S. (2005). Computed tomographic analysis of the position and course of the mandibular canal: relevance to the sagittal split ramus osteotomy. *Int J Oral Maxillofac Surg*, *34*(3), 243-246.
32. Ueda, M., Nakamori, K., Shiratori, K., Igarashi, T., Sasaki, T., Anbo, N., Kaneko, T., Suzuki, N., Dehari, H., Sonoda, T., & Hiratsuka, H. (2012). Clinical significance of computed tomographic assessment and anatomic features of the inferior alveolar canal as risk factors for injury of the inferior alveolar nerve at third molar surgery. *J Oral Maxillofac Surg*, *70*(3), 514-520.
33. Van der Cruyssen, F., Peeters, F., Gill, T., De Laat, A., Jacobs, R., Politis, C., & Renton, T. (2020). Signs and symptoms, quality of life and psychosocial data in 1331 post-traumatic trigeminal neuropathy patients

- seen in two tertiary referral centres in two countries. *J Oral Rehabil*, 47(10), 1212-1221.
34. Zaki, I. M., Hamed, W. M., & Ashmawy, M. S. (2021). Effect of CBCT dose reduction on the mandibular canal visibility: ex vivo comparative study. *Oral Radiol*, 37(2), 282-289.
  35. Zhang, X., Feng, X., Xiao, P., He, G., & Zhu, L. (2015). Segmentation quality evaluation using region-based precision and recall measures for remote sensing images. *ISPRS Journal of Photogrammetry and Remote Sensing*, 102, 73-84.



## **CHAPTER V | Developing Advanced Patient-Specific In Silico Models: A New Era in Biomechanical Analysis of Tooth Autotransplantation**

*This chapter is based on the following publication: **Lahoud P, Jacobs R, Elahi SA, Ducret M, Lauwers W, van Lenthe GH, Richert R, EzEldeen M. Developing advanced patient-specific in silico models: a new era in biomechanical analysis of tooth autotransplantation. Journal of Endodontics. 2024 Jun 1;50(6):820-6.***

### Affiliations

1. Department of Oral and Maxillofacial Surgery & Imaging and Pathology, OMFS-IMPATh Research Group, University Hospitals Leuven, KU Leuven, Belgium.
2. Division of Periodontology & Oral Microbiology, Department of Oral Health Sciences-University Hospitals Leuven, KU Leuven, Belgium.
3. Department of Dental Medicine, Karolinska Institute, Stockholm, Sweden.
4. Department of Movement Sciences, Human Movement Biomechanics Research Group, KU Leuven, Leuven, Belgium.
5. Department of Mechanical Engineering, KU Leuven, Leuven, Belgium.
6. Laboratoire de Biologie Tissulaire et Ingénierie thérapeutique, UMR 5305 CNRS/Université Claude Bernard Lyon 1, UMS 3444 BioSciences Gerland-Lyon Sud, Lyon, France.
7. Service d'Odontologie, Hospices Civils de Lyon, Lyon, France.
8. Université de Lyon, INSA Lyon, CNRS, LaMCoS, UMR5259, Villeurbanne, France.
9. Paediatric Dentistry and Special Dental Care, University Hospitals Leuven, KU Leuven, Leuven, Belgium.

# Developing Advanced Patient-Specific In Silico Models: A New Era in Biomechanical Analysis of Tooth Autotransplantation

*Lahoud P, Jacobs R, Elahi SA, Ducret M, Lauwers W, van Lenthe GH,  
Richert R, EzEldeen M*

## **ABSTRACT**

**Aim(s):** As personalized medicine advances, there is an escalating need for sophisticated tools to understand complex biomechanical phenomena in clinical research. Recognizing a significant gap, this study pioneers the development of patient-specific in silico models for tooth autotransplantation (TAT), setting a new standard for predictive accuracy and reliability in evaluating TAT outcomes.

**Materials and Methods:** Development of the models relied on 6 consecutive cases of young patients (mean age 11.66 years  $\pm$  0.79), all undergoing TAT procedures. The development process involved creating detailed in silico replicas of patient oral structures, focusing on transplanting upper premolars to central incisors. These models underpinned finite element analysis simulations, testing various masticatory and traumatic scenarios.

**Results:** The models highlighted critical biomechanical insights. The finite element models indicated homogeneous stress distribution in control teeth, contrasted by shape-dependent stress patterns in transplanted teeth. The surface deviation in the postoperative year for the transplanted elements showed a mean deviation of 0.33 mm ( $\pm$ 0.28), significantly higher than their contralateral counterparts at 0.05 mm ( $\pm$ 0.04).

**Conclusion(s):** By developing advanced patient-specific in silico models, we are ushering in a transformative era in TAT research and practice. These models are not just analytical tools; they are predictive instruments capturing patient uniqueness, including anatomical, masticatory, and tissue variables, essential for understanding biomechanical responses in TAT. This foundational work paves the way for future studies, where applying these models to larger cohorts will further validate their predictive capabilities and influence on TAT success parameters.

## INTRODUCTION

Over the past half-century, the dental field has experienced remarkable advancements, including three-dimensional imaging with cone-beam computed tomography (CBCT) and the rise of Computer-Aided Design and Manufacturing (CAD-CAM). These strides in digital dentistry are attributed to progress in oral and maxillofacial radiology, along with advancements in computer hardware and software technologies (Patel et al., 2009). Breakthroughs in machine learning (ML) and computer vision have also played a significant role. Together, these achievements have laid the foundation for the digitalization of dentistry. As a result, complex technologies can now be combined to simulate, plan, and analyze clinical cases with unprecedented accuracy (Leite et al., 2020; Patel et al., 2009; Schwendicke et al., 2020).

One procedure revitalized by the digitalization revolution is tooth autotransplantation (TAT). TAT provides children and adolescents with a viable biological tooth replacement option (EzEldeen et al., 2019). However, it remains a relatively complex surgery due to the variability in dental root shape, recipient site dimensions, and overall procedure predictability. Recent advancements in precision and personalized medicine have enabled clinicians to transition from the conventional TAT approach to the CBCT-guided TAT (EzEldeen et al., 2019; Shahbazian et al., 2010). Furthermore, the integration of AI has streamlined several steps of this once-cumbersome procedure (Lahoud, Diels, et al., 2022; Lahoud et al., 2021).

Despite significant advancements in dentistry, accurately assessing oral biomechanics remains a major challenge. The analysis of oral biomechanics is crucial in everyday clinical practice due to its substantial impact on the success of various procedures in areas such as prosthodontics (Kirmali et al., 2022; Li et al., 2005; Richert et al., 2020), endodontics (Bucchi et al., 2019; Richert et al., 2020), oral implantology (Atieh et al., 2013; Galbusera et al., 2014; Macedo et al., 2017; Marcian et al., 2018) and orthodontics (Lahoud,

Jacobs, et al., 2022; Liao et al., 2016). Yet, comprehensive research into the biomechanical responses of TAT and their effects on treatment outcomes remains surprisingly scarce (Kirmali et al., 2022; Richert et al., 2020). Furthermore, while precise tools for evaluating and addressing occlusal biomechanics do exist (Manfredini et al., 2012) — playing a vital role in comprehensive treatment planning — their patient-specific application in routine clinical practice is still not a reality. This gap highlights a significant area for potential research and development, aiming to bridge the divide between advanced tools and their practical implementation in patient care.

Simultaneously, Finite Element (FE) models have experienced a recent resurgence and are proving to be highly effective in studying and predicting complex bio-mechanical phenomena (Erdemir et al., 2012; Lahoud, Jacobs, et al., 2022). FE models are tools engineered to analyze the mechanics of objects with different material properties and irregular shapes (Li et al., 2019; Richert et al., 2020; Tuna et al., 2014).

Consequently, this study aimed to develop and apply accurate patient-specific in-silico modeling to investigate the influence of oral biomechanics on tooth autotransplantation outcomes, which has not been done so far.

## **MATERIALS AND METHODS**

### **Database Constitution**

Ethical approval was obtained from the ethical board (S55287, University Hospitals, KU Leuven) in compliance with the Helsinki Declaration. From the University Hospitals of Leuven (UZ Leuven)'s database, patients were retrospectively screened according to the following inclusion criteria:

- Patients of less than 15 years of age.
- Having undergone TAT from the upper pre-molar region to an upper central incisor recipient site (EzEldeen et al., 2019).

- Presence of a recent pre-operative CBCT from before TAT (T1).
- Presence of a CBCT 1 year after TAT (T2).
- Absence of orthodontic treatments during the 1-year follow-up period.

From the patients that aligned with the aforementioned inclusion criteria, six consecutive patients were included to develop and test for further modeling and biomechanical analysis.

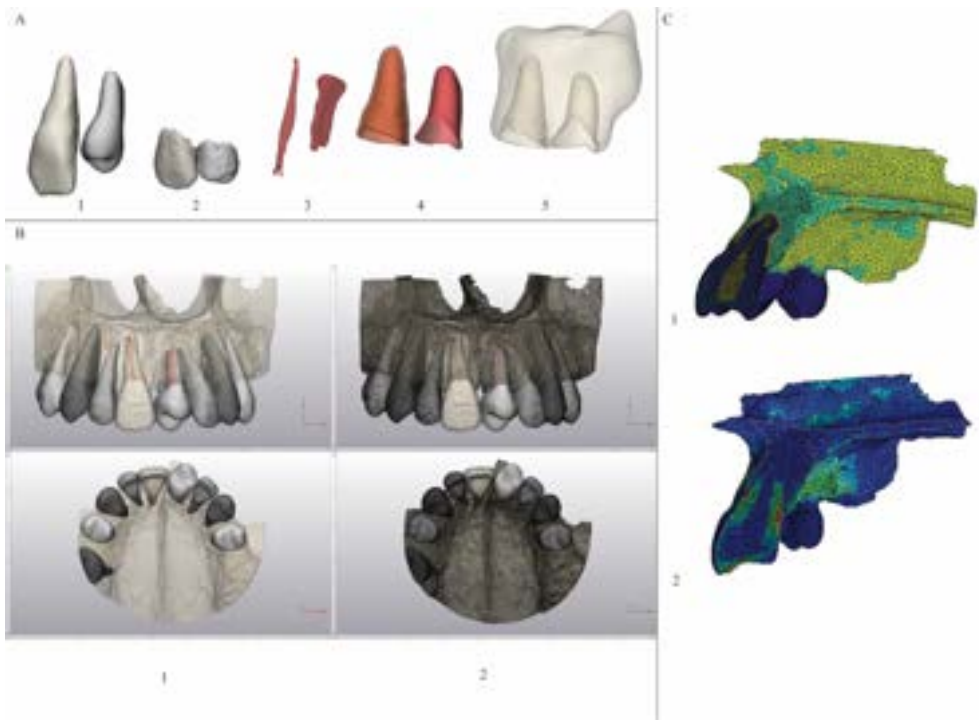


**Figure 1.** Workflow of the in-silico modeling procedure: (A) Segmentation of the different oral and maxillofacial structures, ranging from segmentation of the (A-1) teeth, (A-2) enamel, (A-3) pulp, (A-4) periodontal ligament and (A-5) surrounding maxillary bone. (B-1) The different structures are then combined into a patient-specific in-silico model and (B-2, C-1) meshed for further (C-2) finite element analysis.

## **Data Pre-Processing and Image Segmentation**

CBCT scans of the included patients were processed as detailed in S1.1 and shown in Figure 1.

## **Meshing and Finite Element Analyses**

Following previously validated and published protocols, all segmented surfaces were imported and meshed using DESK software (Figure 1, B) (Jacinto et al., 2012). The models were then imported into Abaqus 2022 software (Dassault Systèmes, Vélizy-Villacoublay, France), where the nodes of the zygomatic process were constrained to prevent displacement of the Finite Element (FE) models (Richert et al., 2020). All dental materials were assumed to be homogeneous and linearly elastic except for the periodontal ligament, which was assumed hyper-elastic. The attributed material properties were referenced from the literature (Table 1) (Richert et al., 2020).

Two clinical situations - physiologic mastication and dental trauma - were simulated, and a given force was applied on the transplanted donor tooth as well as on the contralateral upper central incisor, which served as the control tooth. For masticatory force simulation, a unique load of 240 N was applied on the incisal edge of both the transplanted element and its contralateral counterpart, with an angle of 120° to the long axis of the tooth. A unique load of 300 N was applied perpendicular to the vestibular face of the tooth to simulate a traumatic scenario, as described by Bucchi and co-workers (Bucchi et al., 2019).

The direct post-operative situation models following TAT were made based on the pre-operative CBCT scan and segmentations, combined with the coordinate of the 1-year follow-up elements (control and transplanted teeth). This resulted in the T1 models. T2 models were based on the 1-year follow-up CBCT scan and the resulting segmentation models.

Furthermore, static explicit analysis was conducted in Abaqus software for FE analysis (Figure 1, C). After that, the mechanical behavior of both the transplanted teeth (Figure 2) and the contra-lateral control one (Figure 3) were

evaluated by comparing all FE models' stress distribution patterns and Von Mises values.

The selected physical and mechanical properties of the different structures were based on a review of various studies investigating the mechanical properties of dental tissues, suggesting the isotropic elastic behavior of dental tissues favors using the von Mises stress distributions for accurate simulation in FE models (Bucchi et al., 2019). Finally, each FE model was verified using a mesh convergence test and the Zienkiewicz- Zhu error indicator (Richert et al., 2020).

### **Statistical Methods and Analyses**

Data were evaluated for normality using the Kolmogorov-Smirnov and Shapiro-Wilk tests, followed by an analysis of variance (ANOVA) test was used to assess stress values at T1 and T2.

A surface part comparison analysis (SPCA) was then performed to study and quantify the volumetric changes happening at the level of the dental root after TAT (Suppl. Fig. 1). Finally, a wall thickness analysis (WTA) allowed us to quantify the thickness of the dental roots at both T1 (Suppl. Fig. 1E) and T2 (Suppl. Fig. 1F) based on the patient-specific segmentations.

## **RESULTS**

This study utilized in-silico modeling to analyze six consecutive TAT cases (mean age 11.66 years  $\pm$  0.79), followed over a mean period of 13 months ( $\pm$  0.94). Under masticatory forces, homogeneous stress distribution characterized the control teeth (Figure 3C), contrasting sharply with their transplanted counterparts that exhibited a notably heterogeneous stress pattern (Figure 2B, D), particularly at the dental root apical third (Figure 2 & 3). This distinction was statistically significant ( $p < 0.001$ ) and emphasized the

variability in stress adaptation between transplanted and natural dental structures.

A detailed stress comparison revealed a 56% variation in mean stress values between different transplants at T2, underscoring the influence of individual anatomical factors. Specifically, transplants **2**, **3**, and **5** encountered higher stress concentrations at the root apical third, correlating with a substantial gain in tooth structure at T2 (Figure 2 & Suppl. Fig. 1C-D).

Interestingly, stress values under masticatory forces at T2 were predominantly higher than at T1, except for transplant **3** ( $p < 0.001$ ) (Figure 2B). This trend was particularly pronounced for teeth with shorter roots or apical root curvature, indicating a relationship between root morphology and stress distribution (Figure 2).

Response to simulated trauma showed an overall decrease in stress values at T2 across all cases ( $p < 0.001$ ) (Figure 2I). Notably, transplants **2**, **3**, and **4** exhibited the most significant stress reduction, pointing to possible differences in biomechanical adaptation post-TAT. Also, statistically significant differences in biomechanical behavior were noted between the contralateral upper central incisor (control) and the transplanted upper premolar donor tooth, as well as between the T1 and T2 models of the transplanted elements. The surface part comparison analysis revealed a mean surface deviation between T1 and T2 models of 0.33 mm ( $\pm 0.28$ ) for the transplanted element, significantly differing from the 0.05 mm ( $\pm 0.04$ ) observed for the contralateral central incisor. This finding was accompanied by a pronounced difference in dental wall thickness between transplanted and control elements at both T1 and T2 (Suppl. Fig. 1D, E, F), highlighting the structural adaptations occurring post-transplantation.

**Table 1.** Material Properties of the different structures used for Finite Element Analysis.

<b>Material</b>	<b>Model</b>
Dentine	Linear elastic isotropic E= 18600 MPa v=0.31
Enamel	Linear elastic isotropic E= 84000 MPa v=0.33
Pulp	Linear elastic isotropic E= 69 MPa v=0.45
Periodontal Ligament	Hyper-elastic Ogden order 1 $\mu = 0,12$ MPa $\alpha = 20,9$ MPa D = 10
Trabecular bone	Linear elastic isotropic E= 1300 MPa v=0.30
Cortical bone	Linear elastic isotropic E= 13000 MPa v=0.30

E: Young's modulus | v: Poisson's ratio.

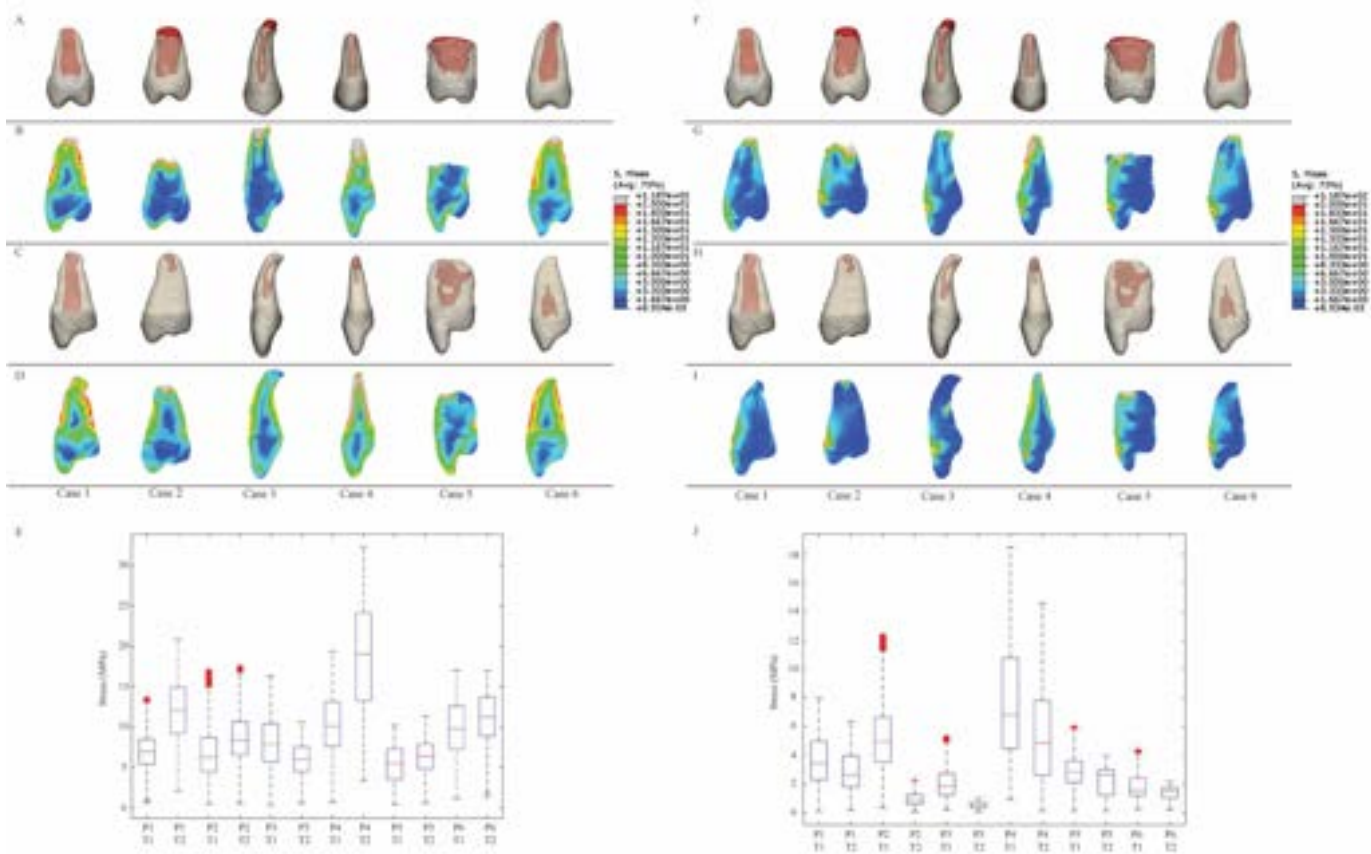


**Figure 2.** 3D modeling of the included TAT cases under masticatory forces, showing (A) 3D segmentation of dental structures at the moment of the transplantation (T1), (B) von Mises stress distributions (MPa) at T1s following masticatory force simulation. (C) shows 3D segmentation of dental structures at 1-year follow-up (T2), with (D) von Mises stress distributions at T2, following masticatory force simulation. (E) Boxplot showing differences in stress distribution between all six cases (P1 to P6) at (T1) and (T2) following masticatory force simulation. (F) segmentation of dental structures at (T1), (G) stress distributions at (T1) following traumatic force simulation. (H) segmentation of dental structures at (T2), with (I) stress distributions at (T2), following traumatic force simulation. (J) Boxplot showing differences in stress distribution between all six cases at (T1) and (T2) following traumatic force simulation.

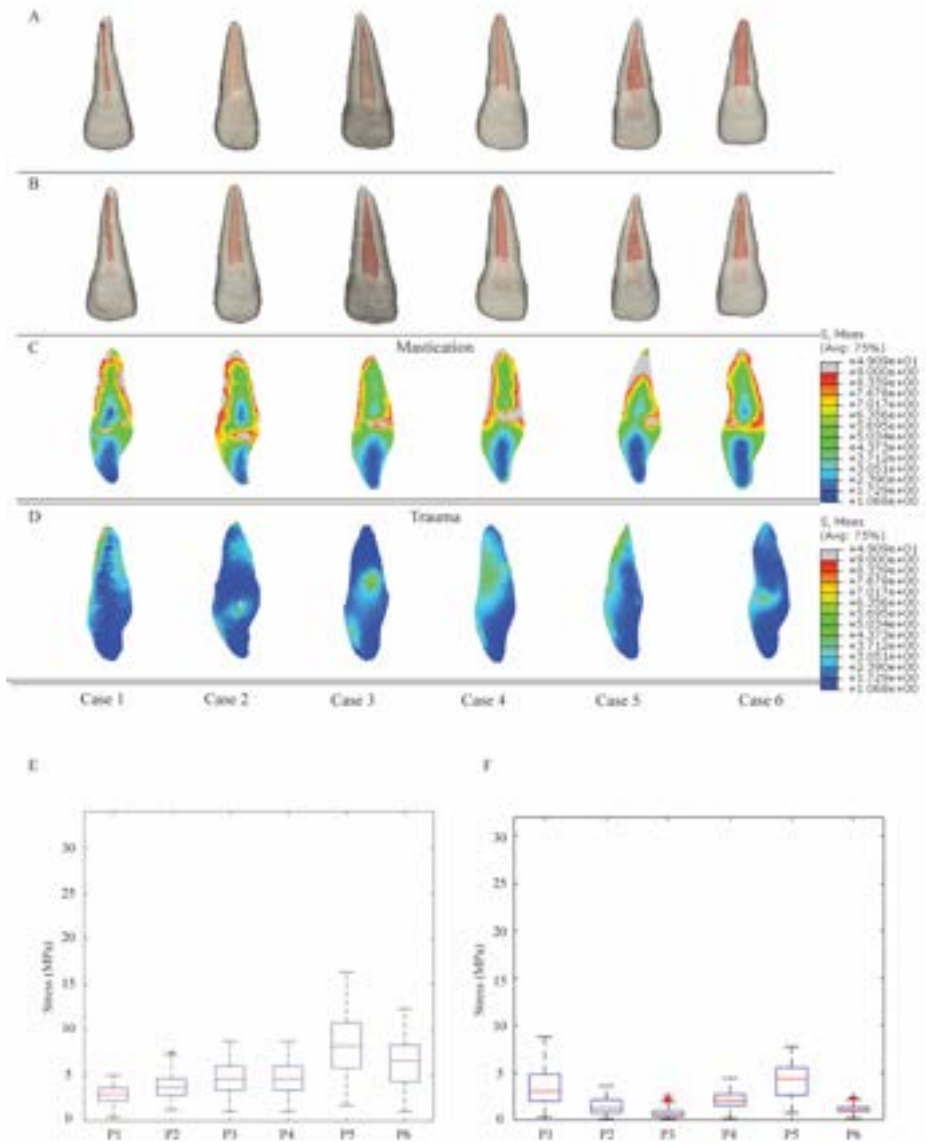
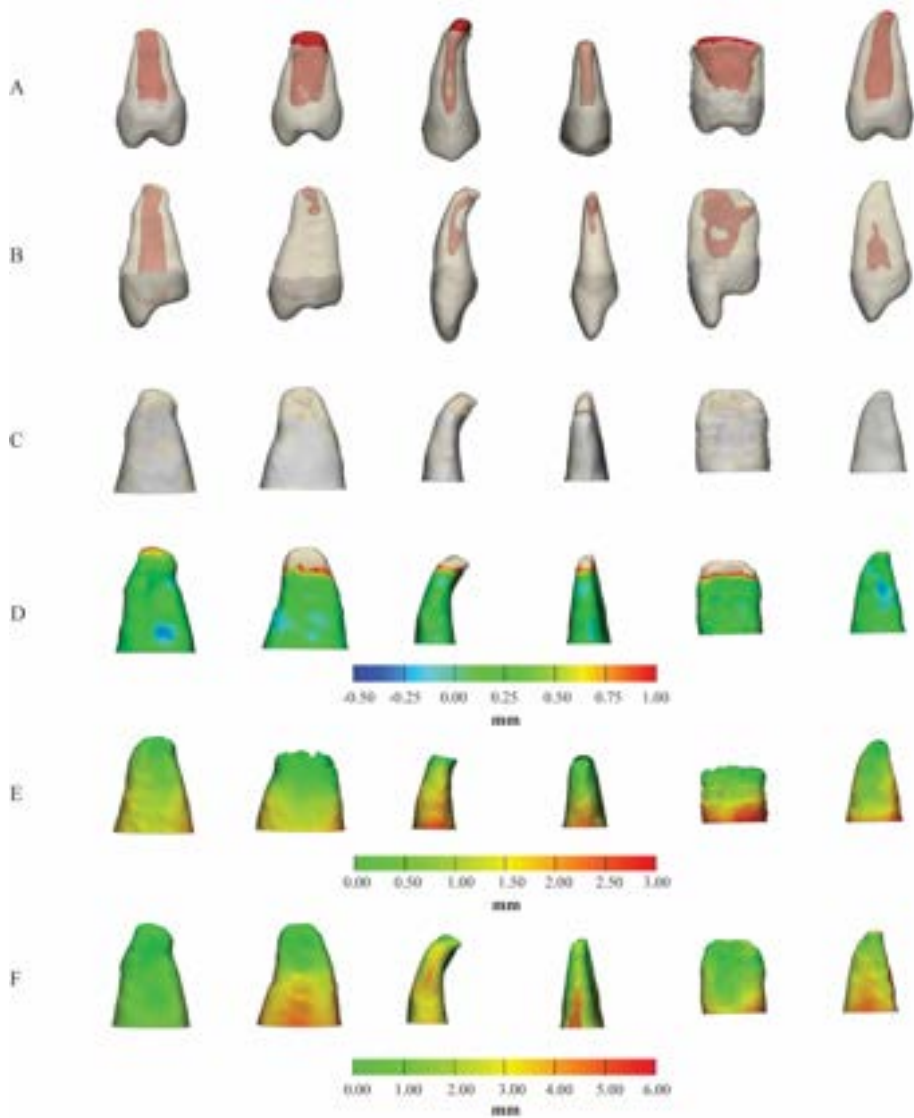


**Figure 3.** 3-Dimensional modeling of the contra-lateral central incisor showing (A) the 3D segmentation of the dental structures at the moment of the transplantation (T1), (B) the 3D segmentation of the dental structures at the 1-year follow-up (T2), following transplantation, (C) the von Mises stress distributions following masticatory force simulation and (D) the von Mises stress distributions following a simulated trauma. (E) Boxplot showing the differences in stress distribution (MPa) between all six cases (P1 to P6) for the contra-lateral central incisor following masticatory force simulation and (F) following a simulated trauma.



**Supplemental Figure 1 (Suppl. Fig. 1).** 3D modeling of the transplanted elements (A) before and (B) 1 year after TAT surgery, followed by (C) a surface-based registration of the pre-operative (grey) and 1-year follow-up (beige) surfaces of the root of the TAT elements, for which (D) a surface part comparison analysis (SPCA) was performed between the 2 studied time points, followed by a dental wall thickness analysis (WTA) (E) pre-operatively and (F) at the 1-year follow-up.

## DISCUSSION

In this study, we focused on creating accurate patient-specific in-silico models to better understand the role of oral biomechanics in tooth autotransplantation (TAT) outcomes. We analyzed stress distributions and biomechanical responses following TAT by employing detailed imaging and computational methods, contributing valuable insights to personalized dental medicine.

The introduction of computer-aided surgical planning in TAT has revolutionized pre-operative assessments, melding surgical precision with individual anatomical consideration for optimized functional and aesthetic outcomes (EzEldeen et al., 2019; Shahbazian et al., 2010). Despite these advancements, the post-operative biomechanical milieu remains a relatively uncharted domain (Kirmali et al., 2022; Richert et al., 2020), necessitating a more profound exploration into occlusal biomechanics integral to comprehensive treatment planning (Manfredini et al., 2012). Studies have, for example, documented different root-healing patterns following TAT. More specifically, EzEldeen and co-workers reported in a CBCT-based study of 50 transplanted teeth four radiographic patterns of root-healing following TAT of immature premolars. These patterns included differences in the mean and maximum dentin wall thickness and the root hard tissue volume, translating into differences in the tissue deposition timeframe on the internal root surface and the overall root maturation and remodeling (EzEldeen et al., 2019). But could these differences in tissue changes following TAT be associated with different risks of post-operative complications and/or failures - such as ankyloses, root resorption, and/or inflammatory reactions?

Von Mises stress was used as it is often preferred in dental studies (Kahler et al., 2003; Rekow, 2020) over principal stress due to its ability to accurately predict failure and damage in dental materials, including dentin. Indeed, von Mises stress is a scalar value derived from the stress components in three dimensions and represents the equivalent stress that would cause the same

amount of deformation as the combined normal and shear stresses. In contrast, principal stress inherently neglects multiaxial stress states, which, in the presence of complex loading conditions and varying stress distributions, can make the analysis based solely on maximum principal stress less comprehensive (Rekow, 2020). The maximum principal stress criterion may also overlook stress concentrations at specific locations, such as sharp corners or material interfaces, highly common in dental tissues, leading to a less accurate representation of the results (Ateyah, 2013; Bucchi et al., 2019). Indeed, principal stresses represent the maximum and minimum values of stress in the material, which may not adequately capture the stress state in dentin, especially in areas with complex loading conditions (Ateyah, 2013). Von Mises stress, on the other hand, considers all stress components and provides a single value that reflects the overall stress state, making it more suitable for capturing the complex nature of dentin, especially when the accurate differentiation in fracture-toughening mechanisms between hydrated versus dehydrated dentin is taken into account (Kahler et al., 2003). Additionally, it has the advantage of considering both tension and compression. It provides a more accurate representation of the results by considering the combined effect of all stress components by accurately representing the stress state, providing a more comprehensive assessment of the potential damage in the dental tissues during FE simulations (Rekow, 2020).

The heterogeneity in stress distributions post-TAT, particularly in contrast to control incisors, accentuates the individualistic biomechanical responses dictated by factors such as root configuration and crown morphology (Choy et al., 2000; Kirmali et al., 2022). These observations not only corroborate previous studies but also amplify the call for patient-specific modeling in predicting TAT outcomes (Lahoud, Jacobs, et al., 2022).

While our study assumed homogeneity, isotropy, and linear elasticity for oral and maxillofacial structures, the periodontal ligament (PDL) was an

exception, modeled as hyper-elastic to reflect its unique mechanical properties (Li et al., 2005; Tuna et al., 2014; Ueda et al., 2017). Stress distributions were mainly located on the apical and lateral parts of the dental roots and on the PDL, which seems to play a crucial protective role by enabling homogeneous transmission of the occlusal forces to the surrounding bony structures by the mean of its hyper-elastic properties (Richert et al., 2020; Tuna et al., 2014).

For trauma, stress values were significantly lower after root maturation at the follow-up evaluation compared to the day of transplantation, which confirms previous conclusions related to the frequency of cervical dental fractures based on the level of root development, where the highest decreases in stress value were reported for teeth presenting the highest root development (Cvek, 1992). It's, however, interesting to note that stress values were sometimes higher after root maturation at the 1-year follow-up, suggesting different biomechanical behaviors. This could be explained by patient-specific differences between structures, such as dental root anatomy, and therefore emphasizes the need for accurate in-silico-based studies with larger sample sizes and accurate patient-specific models instead of generic morphological representations of oral and maxillofacial structures.

However major limitations of such FE studies remain linked to the large sample size needed to build prediction models, given the technical complexity and high time consumption needed to generate and analyze such models, and the clinical validation of the models.

This research highlights the utility of patient-specific in-silico modeling in understanding the biomechanical aspects following TAT. Looking ahead, methodologies such as Extended Finite Element Analysis (E-FEA) and model order reduction concepts (Lahoud et al., 2023) hold promise for further exploration. Such approaches could unveil deeper correlations between procedural timing and success rates, potentially guiding clinical decisions on optimal stages for intervention based on fracture risks and tooth development

stages. By bridging current knowledge gaps, this study catalyzes future research, with the prospective integration of these advanced models into routine clinical practice, enhancing TAT success rates within personalized dental healthcare frameworks.

## **CONCLUSION**

In-silico modeling, particularly in complex procedures like Tooth Autotransplantation (TAT), offers a significant advancement in understanding patient-specific biological responses. This study demonstrates its effectiveness in revealing biomechanical variations due to individual anatomical and tissue differences. Furthermore, the integration of Deep Learning and Artificial Intelligence into clinical practice holds promise for enhancing treatment outcomes, leveraging data-driven insights for improved healing and surgical precision.

## REFERENCES

1. Ateyah, N. (2013). Mechanical behavior of water-aged nano-filled hybrid composite restoratives. *King Saud University Journal of Dental Sciences*, 4(1), 21-25.
2. Atieh, M. A., Alsabeeha, N. H., Faggion, C. M., Jr., & Duncan, W. J. (2013). The frequency of peri-implant diseases: a systematic review and meta-analysis. *J Periodontol*, 84(11), 1586-1598.
3. Bucchi, C., Marce-Nogue, J., Galler, K. M., & Widbiller, M. (2019). Biomechanical performance of an immature maxillary central incisor after revitalization: a finite element analysis. *Int Endod J*, 52(10), 1508-1518.
4. Choy, K., Pae, E.-K., Park, Y., Kim, K.-H., & Burstone, C. J. (2000). Effect of root and bone morphology on the stress distribution in the periodontal ligament. *American Journal of Orthodontics and Dentofacial Orthopedics*, 117(1), 98-105.
5. Cvek, M. (1992). Prognosis of luxated non-vital maxillary incisors treated with calcium hydroxide and filled with gutta-percha. A retrospective clinical study. *Endod Dent Traumatol*, 8(2), 45-55.
6. Erdemir, A., Guess, T. M., Halloran, J., Tadepalli, S. C., & Morrison, T. M. (2012). Considerations for reporting finite element analysis studies in biomechanics. *J Biomech*, 45(4), 625-633.
7. EzEldeen, M., Wyatt, J., Al-Rimawi, A., Coucke, W., Shaheen, E., Lambrechts, I., Willems, G., Politis, C., & Jacobs, R. (2019). Use of CBCT Guidance for Tooth Autotransplantation in Children. *J Dent Res*, 98(4), 406-413.
8. Galbusera, F., Taschieri, S., Tsesis, I., Francetti, L., & Del Fabbro, M. (2014). Finite element simulation of implant placement following extraction of a single tooth. *J Appl Biomater Funct Mater*, 12(2), 84-89.
9. Jacinto, H., Kéchichian, R., Desvignes, M., Prost, R. m., & Valette, S. b. (2012, Aug 2012). A web interface for 3D visualization and interactive segmentation of medical images. Web 3D 2012 - 17th International Conference on 3D Web Technology, Los Angeles, United States.
10. Kahler, B., Swain, M. V., & Moule, A. (2003). Fracture-toughening mechanisms responsible for differences in work to fracture of hydrated and dehydrated dentine. *Journal of Biomechanics*, 36, 229-237.
11. Kirmali, O., Turker, N., Akar, T., & Yilmaz, B. (2022). Finite element analysis of stress distribution in autotransplanted molars. *J Dent*, 119, 104082.

12. Lahoud, P., Badrou, A., Ducret, M., Farges, J. C., Jacobs, R., Bel-Brunon, A., EzEldeen, M., Blal, N., & Richert, R. (2023). Real-time simulation of the transplanted tooth using model order reduction. *Front Bioeng Biotechnol*, *11*, 1201177.
13. Lahoud, P., Diels, S., Niclaes, L., Van Aelst, S., Willems, H., Van Gerven, A., Quirynen, M., & Jacobs, R. (2022). Development and validation of a novel artificial intelligence driven tool for accurate mandibular canal segmentation on CBCT. *J Dent*, *116*, 103891.
14. Lahoud, P., EzEldeen, M., Beznik, T., Willems, H., Leite, A., Van Gerven, A., & Jacobs, R. (2021). Artificial intelligence for fast and accurate 3D tooth segmentation on CBCT. *J Endod*.
15. Lahoud, P., Jacobs, R., Boisse, P., EzEldeen, M., Ducret, M., & Richert, R. (2022). Precision medicine using patient-specific modelling: state of the art and perspectives in dental practice. *Clin Oral Investig*, *26*(8), 5117-5128.
16. Leite, A. F., Gerven, A. V., Willems, H., Beznik, T., Lahoud, P., Gaeta-Araujo, H., Vranckx, M., & Jacobs, R. (2020). Artificial intelligence-driven novel tool for tooth detection and segmentation on panoramic radiographs. *Clin Oral Investig*.
17. Li, H., Shi, M., Liu, X., & Shi, Y. (2019). Uncertainty optimization of dental implant based on finite element method, global sensitivity analysis and support vector regression. *Proc Inst Mech Eng H*, *233*(2), 232-243.
18. Li, W., Swain, M. V., Li, Q., & Steven, G. P. (2005). Towards automated 3D finite element modeling of direct fiber reinforced composite dental bridge. *J Biomed Mater Res B Appl Biomater*, *74*(1), 520-528.
19. Liao, Z., Chen, J., Li, W., Darendeliler, M. A., Swain, M., & Li, Q. (2016). Biomechanical investigation into the role of the periodontal ligament in optimising orthodontic force: a finite element case study. *Arch Oral Biol*, *66*, 98-107.
20. Macedo, J. P., Pereira, J., Faria, J., Pereira, C. A., Alves, J. L., Henriques, B., Souza, J. C. M., & Lopez-Lopez, J. (2017). Finite element analysis of stress extent at peri-implant bone surrounding external hexagon or Morse taper implants. *J Mech Behav Biomed Mater*, *71*, 441-447.
21. Manfredini, D., Castrolforio, T., Perinetti, G., & Guarda-Nardini, L. (2012). Dental occlusion, body posture and temporomandibular disorders: where we are now and where we are heading for. *J Oral Rehabil*, *39*(6), 463-471.
22. Marcian, P., Wolff, J., Horackova, L., Kaiser, J., Zikmund, T., & Borak, L. (2018). Micro finite element analysis of dental implants under different loading conditions. *Comput Biol Med*, *96*, 157-165.

23. Patel, V. L., Shortliffe, E. H., Stefanelli, M., Szolovits, P., Berthold, M. R., Bellazzi, R., & Abu-Hanna, A. (2009). The coming of age of artificial intelligence in medicine. *Artif Intell Med*, 46(1), 5-17.
24. Rekow, E. D. (2020). Digital dentistry: The new state of the art - Is it disruptive or destructive? *Dent Mater*, 36(1), 9-24.
25. Richert, R., Farges, J. C., Tamimi, F., Naouar, N., Boisse, P., & Ducret, M. (2020). Validated Finite Element Models of Premolars: A Scoping Review. *Materials (Basel)*, 13(15).
26. Schwendicke, F., Samek, W., & Krois, J. (2020). Artificial Intelligence in Dentistry: Chances and Challenges. *J Dent Res*, 99(7), 769-774.
27. Shahbazian, M., Jacobs, R., Wyatt, J., Willems, G., Pattijn, V., Dhoore, E., C, V. A. N. L., & Vinckier, F. (2010). Accuracy and surgical feasibility of a CBCT-based stereolithographic surgical guide aiding autotransplantation of teeth: in vitro validation. *J Oral Rehabil*, 37(11), 854-859.
28. Tuna, M., Sunbuloglu, E., & Bozdog, E. (2014). Finite element simulation of the behavior of the periodontal ligament: a validated nonlinear contact model. *J Biomech*, 47(12), 2883-2890.
29. Ueda, N., Takayama, Y., & Yokoyama, A. (2017). Minimization of dental implant diameter and length according to bone quality determined by finite element analysis and optimized calculation. *J Prosthodont Res*, 61(3), 324-332.



The background of the image is a complex marbled paper pattern. It features swirling, organic shapes in shades of deep blue, vibrant orange, and light cream. In the center, there is a dark, intricate silhouette of a tree with a thick trunk and a dense, branching canopy. The overall aesthetic is artistic and textured.

APPLICATION OF PATIENT-SPECIFIC MODELING  
IN PLANNING ORAL SURGICAL PROCEDURES



## CHAPTER VI | Real-time simulation of the transplanted tooth using model order reduction

*This chapter is based on the following publication: **Lahoud P**, Badrou A, Ducret M, Farges JC, Jacobs R, Bel-Brunon A, EzEldeen M, Blal N, Richert R. Real-time simulation of the transplanted tooth using model order reduction. *Frontiers in Bioengineering and Biotechnology*. 2023 Jun 29;11:1201177.*

### Affiliations

1 OMFS-IMPACT Research Group, Department of Imaging and Pathology, Faculty of Medicine, Leuven, Belgium.

2 Department of Oral and Maxillofacial Surgery, University Hospitals Leuven, Leuven, Belgium.

3 Division of Periodontology and Oral Microbiology, Department of Oral Health Sciences, KU Leuven, Leuven, Belgium.

4 Laboratoire de Mécanique Des Contacts Et Structures, CNRS/INSA, Villeurbanne, France.

5 Laboratoire de Biologie Tissulaire Et Ingénierie Thérapeutique, UMR5305 CNRS/UCBL, Lyon, France.

6 Hospices Civils de Lyon, Lyon, France.

7 Faculty of Odontology, Lyon 1 University, Lyon, France.

8 Department of Dental Medicine, Karolinska Institute, Stockholm, Sweden.

9 Department of Oral Health Sciences, KU Leuven and Paediatric Dentistry and Special Dental Care, University Hospitals Leuven, Leuven, Belgium.

# Real-time simulation of the transplanted tooth using model order reduction

*Lahoud P, Badrou A, Ducret M, Farges JC, Jacobs R, Bel-Brunon A, EzEldeen M, Blal N, Richert R.*

## **ABSTRACT**

**Aim(s):** The biomechanics of transplanted teeth remain poorly understood due to a lack of models. In this context, finite element (FE) analysis has been used to evaluate the influence of occlusal morphology and root form on the biomechanical behavior of the transplanted tooth, but the construction of a FE model is extremely time-consuming.

**Materials and Methods:** Model order reduction (MOR) techniques have been used in the medical field to reduce computing time, and the present study aimed to develop a reduced model of a transplanted tooth using the higher-order proper generalized decomposition method.

The FE model of a previous study was used to learn von Mises root stress, and axial and lateral forces were used to simulate different occlusions between 75 and 175N.

**Results:** The error of the reduced model varied between 0.1% and 5.9% according to the subdomain, and was the highest for the highest lateral forces. The time for the FE simulation varied between 2.3 and 7.2 h. In comparison, the reduced model was built in 17s and interpolation of new results took approximately 2.10-2s. The use of MOR reduced the time for delivering the root stresses by a mean 5.9 h.

**Conclusion(s):** The biomechanical behavior of a transplanted tooth simulated by FE models was accurately captured with a significant decrease of computing time. Future studies could include using jaw tracking devices for clinical use and the development of more realistic real-time simulations of tooth autotransplantation surgery.

## INTRODUCTION

Replacement of permanent teeth in case of trauma appears particularly challenging in children and adolescents due to bone growth and contraindication for the use of implants. Recently, tooth autotransplantation regained interest in the dental community thanks to advancements in medical imaging. With the advent of cone beam computed tomography (CBCT), it is now possible to simulate and utilize 3D printed replicas to prepare the donor site based on the segmentation of the donor tooth. This advancement has led to reduced extra-alveolar time and improved the success rate of the surgery (EzEldeen et al., 2019). However, the risk of root fracture or root resorption of transplanted teeth is still greater than that of non-transplanted ones, and numerous biomechanical processes still remain unclear (Zhu et al., 2014; Jang et al., 2016). It was reported that excessive occlusal forces could lead to root resorption but that occlusal stimuli also facilitate the regeneration of the periodontal ligament; understanding how occlusal forces will be distributed to the root appears therefore decisive (Mine et al., 2005; Wu et al., 2019). In this context, finite element (FE) analysis has been used to evaluate the influence of occlusal morphology and root form on the biomechanical behaviour of the transplanted tooth, but only in one study (Kırmalı et al., 2022), possibly because the construction of a FE model is extremely time-consuming (Liang et al., 2018).

Numerous methods, such as deep learning-based segmentation, have been developed to automate some parts of the FE analysis (Lahoud et al., 2021). However, the computing time remains long due to large meshes and non-linearity of the periodontal ligament. In the medical field, model order reduction (MOR) techniques (Calka et al., 2021), including the most recently described higher-order proper generalised decomposition (HOPGD) method (Modesto et al., 2015; Lu et al., 2018; Badrou et al., 2023), have been used to simplify the computational complexity of biological processes and allow, for example, to simulate the blood flow with

high accuracy or the displacement of the tongue. MOR techniques have yet to be employed in dentistry; herein we compared the results of a HOGPD reduced model to those of a traditional FEA approach.

## MATERIALS AND METHODS

### Numerical method

The CBCT scan of a transplanted tooth was chosen from a previous cohort study. Detailed clinical and radiographic examinations, as well as the protocol, were previously described (EzEldeen et al., 2019; Lahoud et al., 2021). All segmented volumes were then meshed with 786,558 tetrahedral elements using the computational geometry algorithms library (CGAL) meshing library after a convergence test (Jacinto et al., 2012). A 200  $\mu\text{m}$ - thick periodontal ligament was simulated using an Ogden first order hyper-elastic model around the root surface with thickness and all dental materials were supposed homogeneous and linearly elastic defined by the Young's modulus  $E$  and by the Poisson ratio  $\nu$ , for the latter (Chang et al., 2015). The strain energy function  $U$  for this law is defined as:

$$U = \frac{2\mu}{\alpha} (\bar{\lambda}_1^\alpha + \bar{\lambda}_2^\alpha + \bar{\lambda}_3^\alpha - 3) + \frac{1}{D} (J - 1)^2 \quad (1)$$

Where  $\mu$  and  $\alpha$  are material constants.  $D$  is an incompressible parameter.  $\lambda_i$  for  $i = 1, 2, 3$  have the relation  $\bar{\lambda}_i = J^{-1/3} \lambda_i$  where  $\lambda_i$  are the principal stretches of the left Cauchy-Green strain tensor and  $J$  is the total volume strain.

The attributed material properties were referenced from the literature (Richert et al., 2020). There was a perfect bonding between each component and the nodes of the lateral faces of the cortical bone were constrained to prevent displacement. A load was applied to the palatal face of the transplanted tooth to simulate masticatory forces. The FE analysis was

conducted using the Abaqus software 6.14 (Dassault Systèmes, Vélizy-Villacoublay, France) to evaluate the von Mises root stress (VMS) of the transplanted tooth (Figure 1A). The extreme von Mises stress value was then extracted from each FE model to create a response surface.

### **Model order reduction**

The general procedure follows a two-stage offline-online decomposition. In the offline stage (learning phase), snapshots (a set of results depending on space, time and model control parameters) are generated with high fidelity simulations (Figure 1B). In the online stage (in real-time), the results are interpolated with respect to the model parameters (Figure 1C).

An alternating fixed-point algorithm as proposed in (Modesto et al., 2015) can solve this minimisation problem. For a new set of parameters, the new functions were interpolated from the existing functions. In the present study, the discretisation of the parameters was conducted using uniform grids. The forces  $F_x$  and  $F_y$  were chosen as the two input parameters to simulate different occlusions ranging from an intensity from 50 to 200 N.

### **Performance and error estimation**

The time for delivering root stresses calculated by FE analysis and the reduced models were compared using an Intel 2 Xeon 2.30 GHz central processing unit (CPU; Intel, Santa Clara, CA, United States).

To evaluate the accuracy of the reduced model, evaluation points are considered at the centres of the subdomains defined by the snapshot grid in the parameter space (Figure 1D). For each of these evaluation points, an additional snapshot is computed using the set of parameters at this point and the results (VMS in the present study) are stored in a reference matrix  $U_{\text{ref}}$  containing the so-called high-fidelity results.

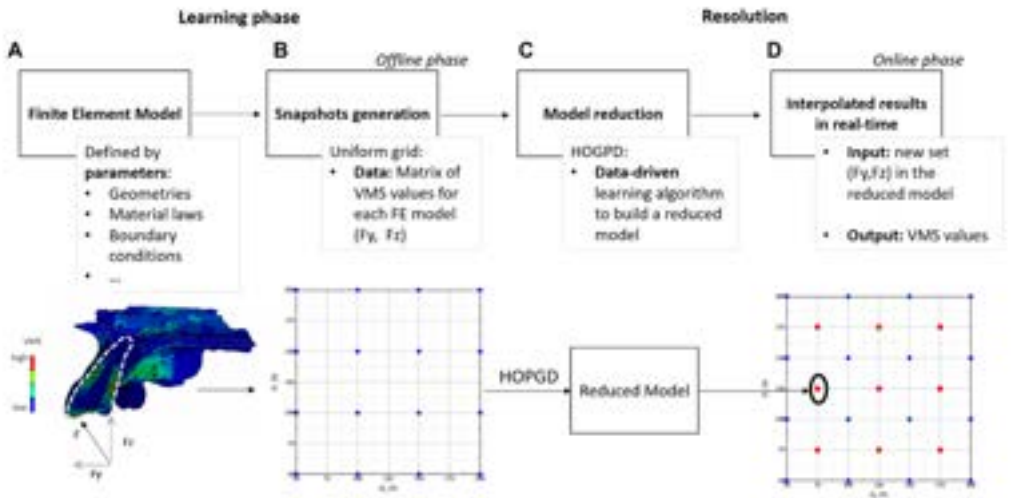


**Figure 1.** Workflow of the higher-order proper generalized decomposition (HOPGD) method. (A) A finite element (FE) model is created based on the anatomy of a transplanted tooth (indicated by a white dotted line). The von Mises stresses (VMS) are then calculated within the FE model under an oblique force  $F$  (represented by a black arrow), split into lateral force ( $F_y$ ) and axial force ( $F_z$ ). (B) The FE computations (blue dots) are generated in a second step using an uniform grid and VMS values for each computation are stored for data learning. In (C) the HOPGD algorithm is used to build a reduced model based on the previous results. (D) For a new set of input parameters within the parameter space (for example, the red dots in the center of each subdomain), the reduced model can provide real-time results.

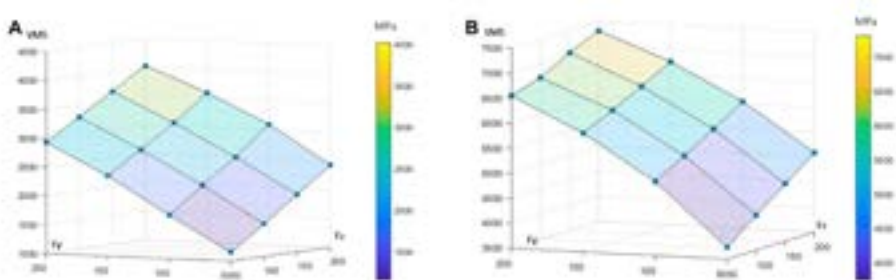


**Figure 2.** Outputs of the 16 finite element (FE) models summarised in response surfaces. Each blue node represents the extreme von Mises stress (VMS) in MPa for each of the 16 FE models. The influence of axial ( $F_z$ ) and lateral forces ( $F_y$ ) is presented for (A) the root and (B) the periodontal ligament.

The reduced model is used to interpolate the results using the same set of parameters and the stresses obtained are in turn stored in a matrix  $U$ . For the considered point, an error  $\delta$  is computed such that:

$$\delta = \frac{\|U - U_{ref}\|}{\|U_{ref}\|} \quad (2)$$

## RESULTS

For low-intensity lateral and axial loading, high stresses in the cervical part of the root and lower stresses in the center of the canal of FE models (Figure 1A). Considering the root stresses, the extreme VMS increased linearly by 109% between the lowest and highest axial load and by 152% between the lowest and highest lateral load (Figure 2A). Considering the periodontal ligament, the extreme VMS increased linearly by 32% between the lowest and highest axial load and quadratically by 73% between the lowest and highest lateral load (Figure 2B).

The error of the reduced model varied between 0.1% and 5.9% according to the subdomain and was the highest for the highest lateral forces (Figure 3).

The time for the FE simulation varied between 2.3 and 7.2 h. In comparison, the reduced model was built in 17 s and interpolation of new results took approximately  $2 \cdot 10^{-2}$ s (Table 1). The use of MOR reduced the time for delivering the root stresses by a mean 5.9 h.

**Table 1.** Comparison between data from the finite element analysis and those interpolated by the reduced model for the 9 sets of parameters at the centres of the subdomains

$F_y/F_z^a$ (N)	Finite element analysis (h)	Reduced model response time (s)	Error (%)
75/75	6.6	0.024	0.3
75/125	7.0	0.021	0.3
75/175	7.1	0.020	0.3
125/75	6.9	0.021	0.1
125/125	7.0	0.022	0.1
125/175	7.2	0.019	0.1
175/75	7.1	0.019	5.9
175/125	2.3	0.020	5.4
175/175	2.6	0.020	4.9

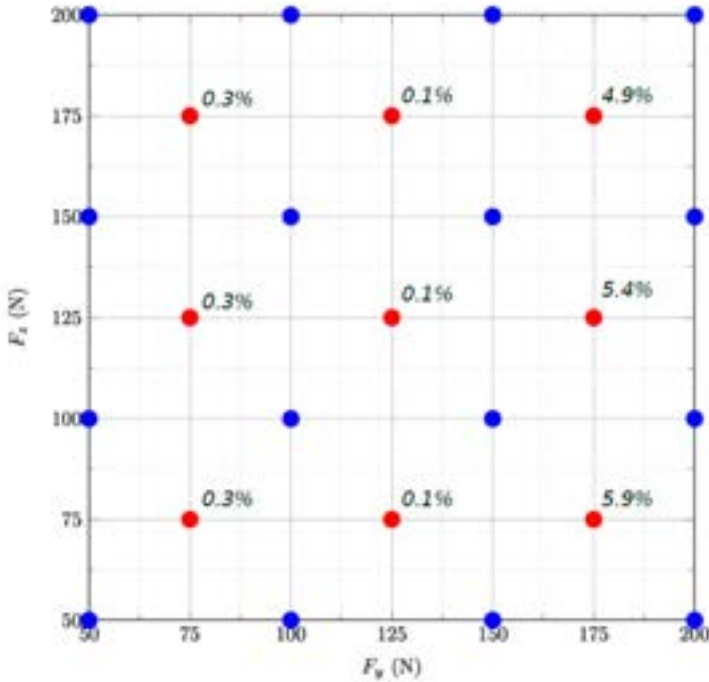


**Figure 3.** Grid representing the 2D parameter space for the two forces  $F_z$  and  $F_y$  applied on the tooth. The blue and red dots are the snapshots used to build the reduced model and those used to evaluate its accuracy using at the centres of the subdomains, respectively.

## DISCUSSION

This proof-of-concept study demonstrated that these biomechanical aspects simulated by FE models could be captured by MOR (HOPGD) with good accuracy and with a significant decrease in computing time.

The performance of the method reported herein is in accordance with previous studies reporting a reduction of CPU time, from approximately 3 h for FEA to <1 s for reduced models (i.e., a  $10^4$ -fold reduction) (Lu et al., 2018) and 5 min for FEA to  $10^{-5}$  s for reduced models (i.e., a  $10^7$ -fold reduction) (Badrou et al., 2023). In comparison, a proper orthogonal decomposition (POD) was used by Ng et al. for modeling the cardiac propagation and reported similar accuracy with a 10-fold reduction of computing time (Khan et al., 2020).

This difference of computing times might be explained by the difference of problems to learn. It is of particular importance to note that this method also requires snapshots in an offline phase and the resolution in a reduced basis online, however one of the limitations of POD is that the enrichment of the reduced basis can quickly become expensive for high dimensional problems (Chinesta et al., 2011). By considering uniform grids, the number of snapshots is exponential. For example, a uniform grid of snapshots in a space of eight parameters with 10 values to be considered in each axis requires  $10^8$  finite element snapshots. (Lu et al., 2018). Other approaches such as Proper Generalized Decomposition (PGD) based on the separation of variables, were used for haptic simulators (Quesada et al., 2018). However, the CPU time could increase by more than 100 depending on the number of modes required to construct the model (i.e., the accuracy required) (Quesada et al., 2018).

Furthermore, the PGD remains an intrusive method and might therefore appear less adapted to the use of commercial software. In the present study a limited number of snapshots was chosen, but the grid could be refined for

lateral forces where the error was higher. For example, a refinement strategy was recommended if the error is greater than 5% by adding snapshots along the axes of the most influential parameters in a regular grid (Lu et al., 2018). Furthermore, other approaches such as design of experiment could have been used as a first approach (Richert et al., 2022) as weakly non-linear responses were herein present. In comparison, MOR is mostly used for highly non-linear phenomena (Chinesta et al., 2011), but numerous non-linear factors were also neglected such as fatigue or contact between teeth for this first proof of concept and will be considered for future real-time simulations (Wakabayashi et al., 2008).

The root stresses were herein mostly influenced by the axis of loading, which confirms the conclusions of previous studies on the importance of occlusion (Lin et al., 2009; Hilgenfeld et al., 2019). For *in vitro*, as *in silico*, models only one occlusal situation is traditionally simulated (Richert et al., 2020), probably due to long computing times. As a consequence, our comprehension of biomechanical phenomena is limited to a particular clinical scenario (Ordinola-Zapata et al., 2022). However, understanding occlusion is fundamental as occlusal morphology was reported to be one of the most significant variables in stress distribution in dentin and cortical bone of the transplanted tooth (Kırmalı et al., 2022). An improper occlusion can reduce the survival of the restored tooth (Bhuva et al., 2021) or impact the dental support by transmitting excessive forces (Passanezi and Sant’Ana, 2000). Conversely, it may result in premature fracture of the crown and in extreme cases root fracture. Currently, occlusal evaluation is often done using articulation papers or virtual records, which are operator-dependent and do not provide a clear understanding of force transmission in the tooth or crown (Carey et al., 2007; Kerstein and Radke, 2014; O’Carroll et al., 2019; Fraile et al., 2022). It may therefore be interesting in the future to combine the reduced model presented herein with a jaw tracking device such as Modjaw (Modjaw, Villeurbanne, France) to better understand the

force transmission and adjust occlusion (Bapelle et al., 2021). Another perspective for pre-clinical students would be to use these real-time simulations with haptic simulators to better develop their surgical skills and timeliness as it was previously developed for the laparoscopic surgery (Quesada et al., 2018).

The study does have certain limitations; for instance, it is of particular importance to note that the current model was restricted to a single anatomy for a shorter learning time. Different anatomies should be tested but this appears to be complex as FE studies are currently based on a single anatomy (Richert et al., 2020). This limitation could be explained by the time needed to construct a FE model based on one tooth and future studies should evaluate how to automate this construction (Lahoud et al., 2021; Lahoud et al., 2022). In the future, it would be interesting to couple MOR with statistical shape analysis to learn also anatomic features as it has been successfully done for the aorta and the human liver (Lauzeral et al., 2019; Maquart et al., 2021). Another limitation is that the present study used simple occlusion without multiple dental contacts, as it is currently the case for most models that are limited to small deformations on relatively simple shapes and with restricted input forces (Mendizabal et al., 2020); future studies should evaluate how MOR could be adapted to learn complex occlusal schemes with multiple dental contacts. This is a major concern as computational cost could greatly increase with the complexity of the learned model.

## **CONCLUSION**

This study constitutes a first proof of concept to provide real-time stress values using MOR. The biomechanical behavior of a transplanted tooth simulated by FE models was accurately captured with a significant decrease of computing time.

## REFERENCES

1. Badrou, A., Duval, A., Szewczyk, J., Blanc, J., Tardif, N., Hamila, N., et al. (2023). Development of decision support tools by model order reduction for active endovascular navigation. *J. Theor. Comput. Appl. Mech.*, 1–33.
2. Bapelle, M., Dubromez, J., Savoldelli, C., Tillier, Y., and Ehrmann, E. (2021). Modjaw device: Analysis of mandibular kinematics recorded for a group of asymptomatic subjects. *Cranio* 6, 1–7.
3. Bhuva, B., Giovarruscio, M., Rahim, N., Bitter, K., and Mannocci, F. (2021). The restoration of root filled teeth: A review of the clinical literature. *Int. Endod. J.* 54, 509–535.
4. Calka, M., Perrier, P., Ohayon, J., Grivot-Boichon, C., Rochette, M., and Payan, Y. (2021). Machine-Learning based model order reduction of a biomechanical model of the human tongue. *Comput. Methods Programs Biomed.* 198, 105786.
5. Carey, J. P., Craig, M., Kerstein, R. B., and Radke, J. (2007). Determining a relationship between applied occlusal load and articulating paper mark area. *Open Dent. J.* 1, 1–7.
6. Chang, Y. H., Lee, H., and Lin, C. L. (2015). Early resin luting material damage around a circular fiber post in a root canal treated premolar by using micro-computerized tomographic and finite element sub-modeling analyses. *J. Mech. Behav. Biomed. Mat.* 51, 184–193.
7. Chinesta, F., Ladevèze, P., Cueto, E., Chinesta, F., Ladevèze, P., Cueto, E., et al. (2011). A short review on model order reduction based on proper generalized decomposition. *Arch. Comput. Methods Eng.* 18, 395–404.
8. Passanezi, E., and Sant’Ana, A. C. P. (2000), Role of occlusion in periodontal disease. *Periodontol* 79 (2019) 129–150.
9. EzEldeen, M., Wyatt, J., Al-Rimawi, A., Coucke, W., Shaheen, E., Lambrichts, I., et al. (2019). Use of CBCT guidance for tooth autotransplantation in children. *J. Dent. Res.* 98, 406–413.
10. Fraile, C., Ferreira, A., Romeo Rubio, M., Alonso, R., and Pradies Ramiro, G. (2022). Clinical study comparing the accuracy of interocclusal records, digitally obtained by three different devices. *Clin. Oral Investig.* 26, 4663–4668.
11. Hilgenfeld, T., Juerchott, A., Deisenhofer, U. K., Weber, D., Rues, S., Rammelsberg, P., et al. (2019). In vivo accuracy of tooth surface reconstruction based on CBCT and dental mri—a clinical pilot study.

- Clin. Oral Implants Res. 30, 920–927.
12. Jacinto, H., Kéchiçhian, R., Desvignes, M., Prost, R., and Valette, S. (2012). A web interface for 3D visualization and interactive segmentation of medical images, Proceedings of the Web3D 2012 - 17th Int. Conf. 3D Web Technol. 51–58.
  13. Jang, Y., Hong, H. T., Chun, H. J., and Roh, B. D. (2016). Influence of dentoalveolar ankylosis on the biomechanical response of a single-rooted tooth and surrounding alveolar bone: A 3-dimensional finite element analysis. *J. Endod.* 42, 1687–1692.
  14. Kerstein, R. B., and Radke, J. (2014). Clinician accuracy when subjectively interpreting articulating paper markings. *Cranio* 32, 13–23.
  15. Khan, R., Shahebul Hasan, A., and Ng, K. (2020). Reduced order method for finite difference modeling of cardiac propagation. *Curr. Diections Biomed. Eng.* 6, 107–110.
  16. Kırmalı, Ö., Türker, N., Akar, T., and Yılmaz, B. (2022). Finite element analysis of stress distribution in autotransplanted molars. *J. Dent.* 119, 104082.
  17. Lahoud, P., Jacobs, R., Boisse, P., EzEldeen, M., Ducret, M., and Richert, R. (2022). Precision medicine using patient-specific modelling: State of the art and perspectives in dental practice. *Clin. Oral Investig.* 26, 5117–5128.
  18. Lauzeral, N., Borzacchiello, D., Kugler, M., George, D., Rémond, Y., Hostettler, A., et al. (2019). A model order reduction approach to create patient-specific mechanical models of human liver in computational medicine applications. *Comput. Methods Programs Biomed.* 170, 95–106.
  19. Liang, L., Liu, M., Martin, C., and Sun, W. (2018). A deep learning approach to estimate stress distribution: A fast and accurate surrogate of finite-element analysis. *J. R. Soc. Interface.* 15, 20170844.
  20. Lin, C. L., Chang, W. J., Lin, Y. S., Chang, Y. H., and Lin, Y. F. (2009). Evaluation of the relative contributions of multi-factors in an adhesive MOD restoration using FEA and the Taguchi method. *Dent. Mat.* 25, 1073–1081.
  21. Lu, Y., Blal, N., and Gravouil, A. (2018). Adaptive sparse grid based HOPGD: Toward a nonintrusive strategy for constructing space-time welding computational vademecum. *Int. J. Numer. Methods Eng.* 114, 1438–1461.
  22. Maquart, T., Elguedj, T., Gravouil, A., and Rochette, M. (2021). 3D B-Rep meshing for real-time data-based geometric parametric analysis.

- Adv. Model. Simul. Eng. Sci. 8, 8–28.
23. Mendizabal, A., Márquez-Neila, P., and Cotin, S. (2020). Simulation of hyperelastic materials in real-time using deep learning. *Med. Image Anal.* 59, 101569–101611.
  24. Mine, K., Kanno, Z., Muramoto, T., and Soma, K. (2005). Occlusal forces promote periodontal healing of transplanted teeth and prevent dentoalveolar ankylosis: An experimental study in rats. *Angle Orthod.* 75, 637–644.
  25. Modesto, D., Zlotnik, S., and Huerta, A. (2015). Proper generalized decomposition for parameterized Helmholtz problems in heterogeneous and unbounded domains: Application to harbor agitation. *Comput. Methods Appl. Mech. Eng.* 295, 127–149.
  26. O’Carroll, E., Leung, A., Fine, P. D., Boniface, D., and Louca, C. (2019). The teaching of occlusion in undergraduate dental schools in the UK and Ireland. *Br. Dent. J.* 227, 512–517.
  27. Ordinola-Zapata, R., Lin, F., Nagarkar, S., and Perdigão, J. (2022). A critical analysis of research methods and experimental models to study the load capacity and clinical behaviour of the root filled teeth. *Int. Endod. J.* 1, 471–494.
  28. Lahoud, P., EzEldeen, M., Beznik, T., Willems, H., Leite, A., Van Gerven, A., et al. (2021), Artificial intelligence for fast and accurate 3-dimensional tooth segmentation on cone-beam computed tomography, *J. Endod.* 47 827–835.
  29. Quesada, C., Alfaro, I., González, D., Chinesta, F., and Cueto, E. (2018). Haptic simulation of tissue tearing during surgery. *Int. J. Numer. Method. Biomed. Eng.* 34, e2926–e2932.
  30. Richert, R., Farges, J. C., Maurin, J. C., Molimard, J., Boisse, P., and Ducret, M. (2022). Multifactorial analysis of endodontic microsurgery using finite element models. *J. Pers. Med.* 12, 1012.
  31. Richert, R., Farges, J. C., Tamimi, F., Naouar, N., Boisse, P., and Ducret, M. (2020). Validated finite element models of premolars: A scoping review. *Mater. (Basel)* 13, 3280.
  32. Wakabayashi, N., Ona, M., Suzuki, T., and Igarashi, Y. (2008). Nonlinear finite element analyses: Advances and challenges in dental applications. *Nonlinear finite Elem. analyses Adv. challenges Dent. Appl.* 36, 463–471.
  33. Wu, Y., Chen, J. M., Xie, F. P., Liu, H. H., Niu, G., and Lin, L. S. (2019). Simulation of postoperative occlusion and direction in autotransplantation of teeth: Application of computer-aided design and

- digital surgical templates. *Br. J. Oral Maxillofac. Surg.* 57, 638–643.
34. Zhu, Y., Yang, W., V Abbott, P., Martin, N., Wei, W., Li, J., et al. (2014). The biomechanical role of periodontal ligament in bonded and replanted vertically fractured teeth under cyclic biting forces. *Int. J. Oral Sci.* 7, 125–130.



## **CHAPTER VII | Individual "alveolar phenotype" limits dimensions of lateral bone augmentation**

*This chapter is based on the following publication: Quirynen M\*, **Lahoud P\***, Teughels W, Cortellini S, Dhondt R, Jacobs R, Temmerman A. Individual "alveolar phenotype" limits dimensions of lateral bone augmentation. *Journal of Clinical Periodontology*. 2023 Apr;50(4):500-10.*

### Affiliations

1 Division of Periodontology and Oral Microbiology, Department of Oral Health Sciences, KU Leuven, Leuven, Belgium.

2 OMFS-IMPACT Research Group, Department of Imaging and Pathology, Faculty of Medicine, Leuven, Belgium.

3 Department of Oral and Maxillofacial Surgery, University Hospitals Leuven, Leuven, Belgium.

4 Department of Dental Medicine, Karolinska Institute, Stockholm, Sweden.

# Individual "alveolar phenotype" limits dimensions of lateral bone augmentation

*Quirynten M\*, Lahoud P\*, Teughels W, Cortellini S, Dhondt R, Jacobs R, Temmerman A.*

## **ABSTRACT**

**Aim(s):** Alveolar ridge resorption following tooth extraction often renders a lateral bone augmentation inevitable. Some patients, however, suffer from severe early (during graft healing,  $E_{res}$ ) and/or late (during follow-up,  $L_{res}$ ) graft resorption. We explored the hypothesis that the "individual phenotypic dimensions" may partially explain the degree of such resorptions.

**Materials and Methods:** Patients who underwent a guided bone regeneration (GBR) procedure were screened for inclusion according to the following criteria: (1) a relatively symmetrical maxillary arch; (2) an intact contra-lateral alveolar bone dimension; (3) the availability of a pre-operative cone-beam CT (CBCT); (4) a CBCT taken immediately after GBR, and (5) at least one CBCT scan  $\geq 6$  months after surgery. CBCT scans from different timepoints were registered and imported into the Mimics software (Materialise, Leuven, Belgium). Bone dimensions of the contra-lateral site of the augmentation, representing the "individual phenotypical dimension" (IPD) of the alveolar crest, were superimposed on the augmented site and registered accordingly. As such,  $E_{res}$  and  $L_{res}$  could be measured over time, in relation to the IPD (in two dimensions; per millimetre apically from the alveolar crest, in the centre of the GBR), as well as in three dimensions (the entire GBR, 2 mm away from the mesial, distal, and apical border for standardization).

**Results:** A total of 17 patients (23 augmented sites) were included. After  $E_{res}$ , the outline of the augmentation was in general located  $\pm 1$  mm outside the IPD, but  $\geq 1.5$  years after GBR, it further moved towards the IPD (85% within 0.5 mm distance).

**Conclusion(s):** Within the limitations of this study, the results indicate that the dimensions of a lateral bone augmentation are defined by the "individual phenotypic bone boundaries" of the patient.

## INTRODUCTION

In patients desiring dental implants, an adequate alveolar ridge dimension is often lacking because of trauma or periodontitis, or as the consequence of tooth loss. To achieve an optimal three-dimensional (3D) position of dental implants, a variety of techniques have been proposed to reconstruct the alveolar ridge, including, but not limited to, guided bone regeneration (GBR), block grafting, shell technique, distraction osteogenesis, transplantation of autologous bone, alveolar ridge splitting, and the use of narrow-diameter implants (Elnayef et al., 2018; Naenni et al., 2019). The clinical outcome of implants following lateral bone augmentation seems to be similar to that of implants inserted into the pristine bone (Blanco et al., 2005; Donos et al., 2008; Jensen & Terheyden, 2009; Jung et al., 2013, Sanz-Sanchez et al., 2015; Benic, Bernasconi, et al., 2017; Benic, Thoma, et al., 2017; Elnayef et al., 2018).

While bone regeneration is a predictable procedure, short- and especially long-term data on implant peripheral bone stability after GBR remains scarce and of major concern. Most of the bone resorption and volumetric loss take place in the period immediately after the augmentation (during the integration/regeneration process, called early resorption,  $E_{res}$ ), but resorption (late resorption  $L_{res}$ ) does occur also afterwards (Benic, Bernasconi, et al., 2017; Benic, Thoma, et al., 2017; Naenni et al., 2019).

A recent systematic review (Naenni et al., 2019) including seven RCTs (Arújo, 2016; Chiapasco et al., 1999; Maiorana et al., 2005; Cordaro et al., 2011; Eskin et al., 2014; Mordenfeld et al., 2014; Thoma et al., 2018) reported small but non-significant differences between various treatment modalities for “primary” lateral bone augmentation, with and overall alveolar “bone width gain” of 3.5 mm (2.2–4.6) after graft healing (4–8 months, thus after  $E_{res}$ ). These data correspond well with those of other systematic reviews on  $E_{res}$ : 4.3 mm (3.7–4.9) for a simultaneous approach, 3.9 mm (3.5–4.3) for a staged approach (Sanz-Sanchez et al., 2015), 4.4 mm (0.1–7.7) for GBR with xenograft (de Azambuja Carvalho et al., 2019), 3.4 mm (2.8–4.0) for

block graft, and 2.4 mm (2.1–2.7) for GBR (Elnayef et al., 2018).

Some of the above-mentioned systematic reviews also verified the amount of graft resorption (first 4–8 months:  $E_{res}$ ). Naenni et al. (2019) reported a resorption of 1.5 mm (0.9–2.2) for a staged GBR, and Thoma et al. (2019) observed a graft resorption of 0.9 mm (0.2–2.2) for a GBR combined with immediate implant placement. Elnayef et al. (2018) compared the resorption between a block graft and a GBR procedure and reported 0.8 and 1.2 mm  $E_{res}$  (6 months of healing). Some recent studies have reported on 3D volumetric changes of the graft. Gultekin et al. (2017) compared a GBR with an iliac bone block (staged approach) and reported  $12\% \pm 2\%$  and  $36\% \pm 8\%$   $E_{res}$  and  $16\% \pm 2.0\%$  and  $42\% \pm 7\%$   $L_{res}$  ( $\pm 30$  months after augmentation). Li et al. (2019, 2020) reported an  $E_{res}$  for a GBR combined with immediate implant placement (6 months of healing) of 52% (ranging from 28% to 60%), with a linear resorption of 19% (3%–36%) at 2 mm distance from the implant shoulder. Mordini et al. (2020) examined the resorption of a freeze-dried bone allograft (FDBA) and a resorbable collagen membrane 4 and 6 months after GBR (thus  $E_{res}$ ) via stone cast models and observed a resorption of  $5\% \pm 4\%$ . The degree of graft resorption was higher when primarily non-contained defects were included (Benic et al., 2019). Under these conditions, a GBR procedure (combined with implant placement) showed an  $E_{res}$  of  $82\% \pm 27\%$  versus  $23\% \pm 31\%$  for a deproteinized bovine-derived bone mineral block. It is important to note that for these data, the ranges and standard deviations are very high.

Several factors seem to affect the predictability of lateral GBR. These factors range from defect morphology (Garaicoa et al., 2015) and biological principles (Wang & Boyapati, 2006) to the technique (Urban & Monje, 2019) and biomaterial employed (Elgali et al., 2017). But, to the best of our knowledge, no information is available on the impact of the “individual phenotypic dimension” (IPD), also called the “individual natural alveolar crest contour”—potentially representing “anatomical boundaries” limiting the alveolar bone augmentation. This study therefore aimed to evaluate the

volume stability of lateral augmentation using 3D virtual reconstruction and superimposition of cone-beam CT (CBCT) data, with the contra-lateral ridge dimensions as reference.

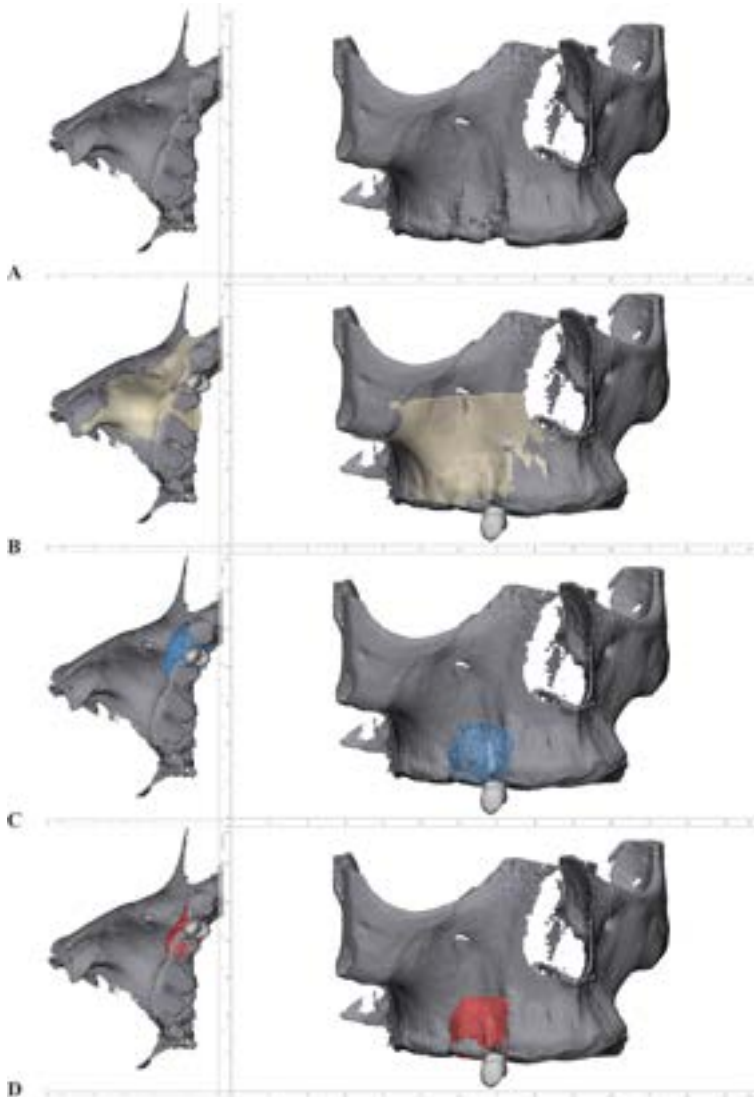


**Figure 1.** 3D modeling of consecutive CBCTs: (a) the pre-operative maxilla, (b) the superimposed contra-lateral side (beige), (c) augmentation following guided bone regeneration (blue), and (d) bone dimensions after Eres + Lres (red).

## MATERIALS AND METHODS

### Study population and image data set

A database of 112 patients who had undergone a bone augmentation procedure at the University Hospitals of Leuven (EC: S59813) was screened according to the following inclusion criteria:

- $\geq 18$  years of age
- maxillary GBR procedure
- a relatively symmetrical maxillary arch
- presence of an intact contra-lateral site (either pre-operatively or from an older CBCT scan)
- a CBCT procedure before GBR
- a CBCT immediately after the GBR procedure
- follow-up CBCT 6–8 months of healing after GBR (immediately before implant placement [staged approach, re-entry for implant insertion] to evaluate  $E_{res}$ ), and/or  $\geq 12$  months after implant placement (being  $\geq 18$  months after GBR) to measure the impact of  $E_{res} + L_{res}$ .

All CBCT images were pseudo-anonymized, and the study was performed according to local and international ethical standards and following the STROBE checklist for cohort studies.

### Image standardization, pre-processing, and segmentation procedures

CBCTs from different timepoints were registered using MeVisLab (MeVis Research, Bremen, Germany), where a validated semi-automatic network relying on mutual information and partial volume interpolation, with the number of iterations fixed at 50, allowed the matching of all post-operative CBCTs on the pre-operative scan, which was routinely used as the reference registration image.

The CBCTs were then imported into the Mimics software (Materialize, Leuven, Belgium), where a semi-automatic segmentation of the maxillary bone was performed using a combination of thresholding and region-growing, as previously validated by Verhelst and co-workers (Verhelst et al., 2021). Automatic interpolation was then applied, and the mask was subsequently transformed into a 3D object of the maxilla.

A symmetrical sagittal cut then allowed dividing the maxillary bone into its right and left portions, based on anatomical points taken at the level of the anterior nasal spine and the median palatine suture. This allowed the separation of the maxilla into its right and left portion, respectively. All parts were converted into ASCII Standard Tessellation Language (STL) files to allow spatial handling. The contra-lateral side of the augmentation was mirrored, and a two-step registration of the mirrored side was performed using a global registration approach, which helped counter small asymmetrical variations between the left and right loci. A semi-automatic registration further allowed the determination of the initial spatial position of the mirrored side with regard to the augmented maxillary side. This corrected potential rotational and translational movements during radiographic acquisition followed by a region of interest (ROI)-based registration to further refine the mirrored site's position, based on mutual information registration with regard to the specifically augmented locus.

### **Radiographic assessment**

After standardization, pre-processing, and segmentation of all CBCTs, the segmented jaw from different timepoints (pre-operative, post-GBR, healing, and/or follow-up) were imported into the Mimics software as STL files and color-coded based on their acquisition timepoint to facilitate measurements (Figure 1). Multi-planar reconstructions (MPRs) were performed to render the coronal, axial, and sagittal slices of the CBCT perpendicular to the bony contour of the jaw (Fernandes et al., 2014; Barreto et al., 2020) (Figure 2a). Linear measurements were then made on a medical display (Barco, Kortrijk,

Belgium), where the slice representing the middle of the graft was selected, and linear measurement were performed on the axial slices, beginning 2 mm apical to the most coronal part of the graft, with 1.0 mm interval, up to 10 mm apically.

### **Three-dimensional analysis of the central part of the graft**

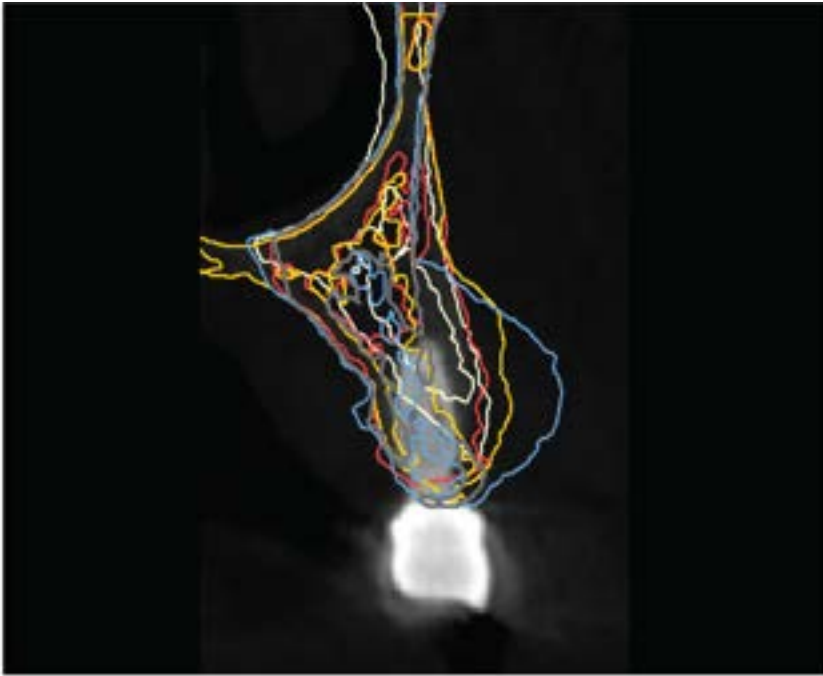
The 3D triangle-based surface of the bony envelope was reconstructed as STL files, and a signed part comparison analysis (SPCA) was performed in 3-Matic software (Materialize), which allowed the quantification of, based on approximately 3500 points per augmented site, the volumetric deviation between the mirrored-registered site, and the bony envelope following late resorption ( $E_{res} + L_{res}$ ) (Figure 2b).

This SPCA quantifies the morphological changes in 3D space coordinates by comparing the same individual points on each triangle from the 3D meshes (Chargo et al., 2019): bony envelope following late resorption compared to the superimposed mirrored site. From each comparison, raw coordinate data were generated that represented the deviations in three dimensions between each individual point on the follow-up and mirrored images, respectively.

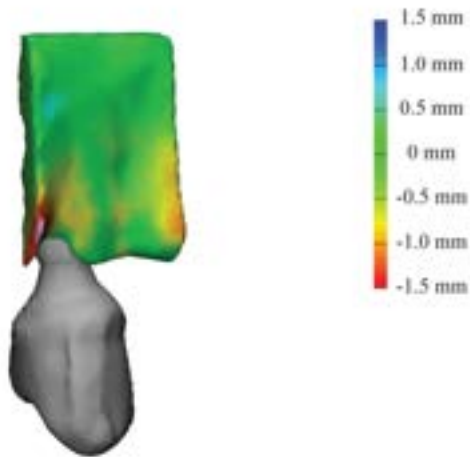
### **Statistical analyses**

For the 2D measurements, the distances between the mirrored line and the graft at different timepoints (before GBR, post GBR, after  $E_{res}$ , and/or after  $L_{res}$ ) were calculated, at 1 mm interval in the apical direction, together with the mean and standard deviation.

The relation between initial bone augmentation beyond the mirrored line and amount of bone resorption was modelled by a linear mixed model with patient as random factor, and the different measurement levels (1-mm interval from coronal to apical) and initial bone augmentation as fixed factors.



A



B

**Figure 2.** Modeling of consecutive CBCTs on (a) 2D cross-sectional visualization of the GBR-augmented site showing the pre-operative bony dimensions (grey), post-GBR bony volume (blue), the registered mirrored line (white), the bony envelope following early (yellow) and late resorption (red). (b) A part comparison analysis that quantifies the volumetric deviation between the mirrored-registered site and the bony envelope following late resorption (Eres + Lres).

Since there was no interaction, the mean line modeling the relation between bone augmentation beyond the mirrored line and bone resorption was evaluated. Residual analysis by means of a normal quantile plot and a residual dot plot showed that the basic assumptions of the linear mixed model were met.

The correlation between the distance of the graft outside the IPD and the amount of  $E_{res} + L_{res}$  was determined based on the CBCTs before GBR, immediately after GBR, at implant placement (6–8 months after GBR), and after >1 year of loading. For these data, the regression line was calculated together with a correlation coefficient and a  $p$ -value.

Finally, a surface part comparison analysis (SPCA) allowed us to generate measurements of the mean, median, standard deviation, minimum, maximum, and first and third quartiles of the distribution of the distances between each point on the 3D triangle-based surface of the patient's bony envelope following late resorption and the corresponding point on the registered mirrored model.

**Table 1.** Patient demographics and guided bone regeneration (GBR) specification per group (Group A: Patients with a cone-beam CT (CBCT) pre-GBR, post-GBR, and after 6–8 months of graft healing; Group B: With a CBCT pre-op, post-GBR, and  $\geq 1.5$  years after GBR; Group C: Patients with a CBCT pre and post GBR, 6–8 months after GBR, and  $\geq 1$  year later).

	Group A		Group B		Group C	
	Number of augmentation	Percentage (%)	Number of augmentation	Percentage (%)	Number of augmentation	Percentage (%)
Single tooth edentation	7	33.5	5	33.5	5	38.5
Posterior edentation	2	9.5	2	13.5	0	0.0
Bounded edentation	12	57.0%	8	53.0	8	61.5
L-PRF bone block	17	81.0	11	73.0	9	69.0
Composite block	4	19.0	4	27.0	4	31.0
Collagen membrane	21	100.0	15	100.0	13	100.0
FRIOS membrane tacks	21	100.0	15	100.0	13	100.0

## RESULTS

### Patient population

Twenty-three lateral bone augmentation sites from 17 different patients (10 females, 7 males) with a mean age at GBR of 51.8 ( $\pm 17.1$ ) years were enrolled (Table 1). Depending on the available CBCTs, three groups of data were considered:

**Group A:** patients with a CBCT pre-GBR, post-GBR, and after 6–8 months of healing (just prior to implant insertion), to evaluate  $E_{res}$

**Group B:** patients with a CBCT pre-GBR, post-GBR, and a follow-up CBCT  $\geq 1$  year after implant loading (two-stage procedure), being  $\geq 1.5$  years after GBR (mean  $33.7 \pm 10.9$  months), to estimate the total impact of  $E_{res} + L_{res}$  together

**Group C:** patients with a CBCT pre-GBR, post-GBR, 6–8 months post GBR, and  $\geq 1$  year afterwards to measure the relative impact of  $E_{res}$  and  $L_{res}$ , separately.

Patients with a CBCT 6–8 months after GBR and a later follow-up ( $\geq 1.5$  years after GBR) were included in both Group A and Group B, as well.

### GBR specifications

Twelve GBRs were performed on bounded edentulous zones; seven on of a single tooth span edentation, and four posterior to a last tooth. Nineteen GBRs were performed with an L-PRF bone block (a 50/50% mixture of chopped L-PRF membranes with xenograft [Bio-Oss, Geislich Pharma AG, Switzerland] glued together with liquid fibrinogen, as described by Cortellini et al. (2018), and four were treated with a composite bone block (50/50% mixture of a xenograft with autogenous bone chips), three of which were part of a randomized controlled trial (RCT) split-mouth study, where patients were treated on one side with an L-PRF bone block and on the other side with 50% Bio-Oss and 50% autogenous bone chips. In all cases, a collagen membrane (Bio-Guide) was used as the barrier, fixed with FRIOS membrane tacks (Densply Sirona, NC, USA).

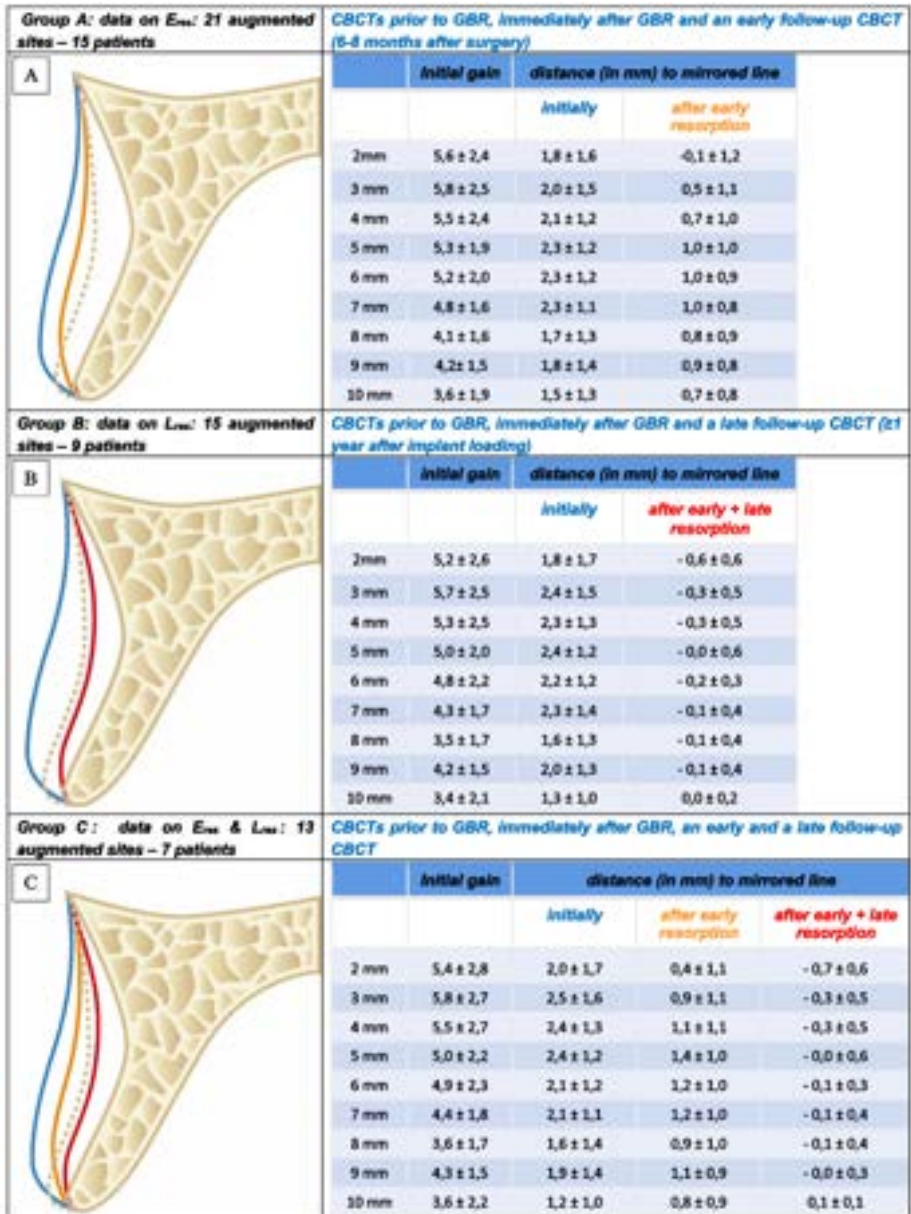


**Figure 3.** Resorption of graft after GBR over time. Images represent cross-section of alveolar bone, in the center of buccal cavity after tooth extraction, indicating the outline of the graft immediately after GBR (blue), after early resorption (6–8 months of healing, in orange), and/or at a later stage ( $\geq 12$  months later,  $\geq 18$  months after GBR, in red) for the three groups. The corresponding tables highlight the measurements (in the middle of the graft, 2–10 mm apically to the crest) at different occasions.

### **Two-dimensional measurement in the middle of the graft**

The linear measurements per millimeter in the apical direction are summarized in Figure 3, per group. Additional analyses were conducted to study dimensional differences between groups: L-PRF bone block versus composite bone block cases (Table S1), and self-contained versus non-self-contained defects (Table S2).

#### ***Group A: CBCTs pre-GBR, post-GBR, and after 6–8 months of healing ( $E_{res}$ )***

The overall mean initial horizontal bone gain (2–10 mm apical to the crest) was  $5.0 \pm 2.1$  mm ( $5.5 \pm 2.2$  mm from 2 to 6 mm). The grafts reached a mean value of  $2.0 \pm 1.3$  mm outside the IPD. After 6–8 months of healing, the augmentations shrank ( $E_{res}$ ) to a mean value of  $3.7 \pm 2.2$  mm, being  $0.7 \pm 1.0$  mm “outside” the IPD. The corresponding data for the area from 2 to 6 mm are  $4.0 \pm 2.4$  mm and  $0.6 \pm 1.1$  mm, respectively (Figure 3a).

#### ***Group B: CBCTs pre-GBR, post-GBR, and $\geq 1.5$ years after GBR (total of $E_{res} + L_{res}$ )***

The overall mean initial horizontal bone gain (2–10 mm apical to the crest) was  $4.7 \pm 2.2$  mm ( $5.2 \pm 2.3$  mm from 2 to 6 mm). The grafts reached a mean of  $2.1 \pm 1.3$  mm outside the IPD. At or more than 18 months later, the augmentations shrank ( $E_{res} + L_{res}$  together) to a mean of  $2.4 \pm 2.1$  mm, being  $0.2 \pm 0.5$  mm “inside” the IPD. The corresponding data for the area from 2 to 6 mm were  $2.7 \pm 2.4$  mm and  $0.3 \pm 0.5$  mm (“inside”), respectively (Figure 3b).

#### ***Group C: CBCTs pre-GBR, post-GBR, and 6–8 months ( $E_{res}$ ) and $\geq 1.5$ years after GBR (total of $E_{res} + L_{res}$ )***

The overall mean initial horizontal bone gain (2–10 mm apical to the crest) was  $4.8 \pm 2.3$  mm ( $5.3 \pm 2.5$  mm from 2 to 6 mm, respectively). Initially the grafts reached a mean of  $2.1 \pm 1.4$  mm outside the IPD. After 6–

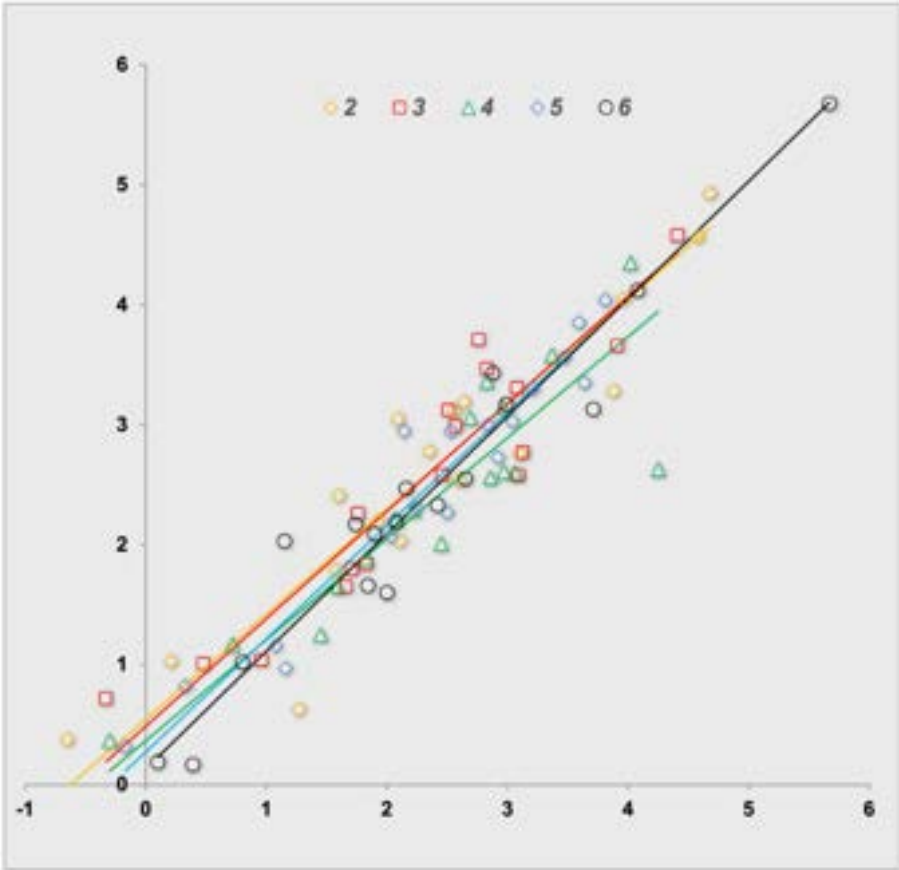
8 months of healing, the augmentations shrank ( $E_{res}$ ) to a mean of  $3.8 \pm 2.4$  mm, being  $1.0 \pm 1.0$  mm outside the IPD. However, at 1 year or later (adding  $L_{res}$ ), the gain reduced to  $2.5 \pm 2.2$  mm, and now the outline of the graft was  $0.3 \pm 0.5$  mm “inside” the IPD. The corresponding data for the area from 2 to 6 mm were  $2.8 \pm 2.5$  mm and  $0.3 \pm 0.5$  mm (“inside”), respectively (Figure 3c).

### **Correlation between graft resorption ( $E_{res} + L_{res}$ ) and the amount of grafting outside the IPD**

Figure 4 shows the correlation between the initial amount of bone augmentation “beyond (outside)” the IPD (mirrored line) and the amount of bone resorption  $\geq 1.5$  years after GBR (representing the sum of  $E_{res} + L_{res}$ ) at different levels (2, 3, 4, 5, and 6 mm apical to the alveolar crest), based on the data of group B. The correlation coefficients of the respective regression lines ranged from 0.84 to 0.98 ( $p < .001$ ), and none of them (except the 3 mm registrations) was statistically different from the  $45^{\circ}$  line through the zero point.

### **Three-dimensional measurement of central part of the graft**

The 3D SPCA analysis (Figure 2b) of all cases presenting a follow-up CBCT ( $\geq 1.5$  years after GBR), comparing the final outline of the entire graft with the IPD, showed an excellent match between both of them, with a mean deviation of  $0.0 \pm 0.5$  mm (median:  $-0.02$  mm; minimum:  $-1.4$  mm; maximum:  $+1.3$  mm).



The correlation coefficients and P values for these regression lines are:

2 mm: 0.935, P = 0

3 mm: 0.933, P = 0

4 mm: 0.883, P = 0

5 mm: 0.969, P = 0

6 mm: 0.967, P = 0

**Figure 4.** Correlation between the amount of initial bone augmentation beyond the mirrored line and the amount of graft resorption  $\geq 1.5$  years after GBR (Eres + Lres together). Measurements were performed at different levels (2, 3, 4, 5, and 6 mm apical to the alveolar crest), represented by different colours.

## DISCUSSION

The aim of this study was to evaluate whether the individual phenotypic dimensions (represented by the contra-lateral healthy site) determined the degree of graft resorption after GBR as well as the overall outline of the graft. From a total of 17 patients (23 augmented sites), the results showed that after  $E_{res}$ , the outline of the augmentation was in general located  $\pm 1$  mm outside the IPD, but  $\geq 1.5$  years after GBR, it further moved towards the IPD (85% within 0.5 mm distance). To the best of our knowledge, this is the first study applying a 3D mirroring concept (from a contra-lateral site to the augmented site) to explore the impact of patient-specific phenotype as limiting boundaries for a GBR procedure.

The general drawbacks of GBR with particulate bone substitutes and barrier membranes are the poor mechanical properties and the low resistance to tissue collapse (Troeltzsch et al., 2016). Compressive forces on the grafted area may cause membrane collapse and displacement of parts of the grafting materials, thereby impairing space maintenance and new bone formation, thereby compromising the regeneration (Mellonig et al., 1998; Strietzel et al., 2006; Schwarz et al., 2007; Benic et al., 2016). This may already occur at time of flap-suturing (Mir-Mari et al., 2016, 2017) or during the healing phase (Thoma et al., 2012; Benic et al., 2016; Benic, Bernasconi, et al., 2017; Benic, Thoma, et al., 2017) and might explain why less contained buccal defects show less favorable outcomes after a GBR (Park et al., 2018; Garaicoa et al., 2015; Li et al., 2020). This should not be a surprise since Tonetti and co-workers already demonstrated in 1993 better outcomes for guided tissue regeneration in more contained defects, primarily because of a smaller risk of barrier membrane collapse.

It is currently unclear how important the above-mentioned compressive forces are, especially on the part of the augmentation that is located outside of the phenotypical bone boundaries, and whether they could be responsible for the continuous resorption after graft healing ( $L_{res}$ ). Jiang et al. (2018) compared the graft resorption (GBR combined with implant placement) towards the position

of a periodontal probe connecting the most labially prominent point of the adjacent alveolar ridge at the level of the bone zenith of the neighboring teeth (as reference of the boundary line of the individual phenotypic bone dimension). Even though the bone was augmented outside (beyond) the boundary line of the bony envelope, after 6 months of healing the graft shrank ( $E_{res}$ ) inside but close to this boundary line independent of the degree of buccal-coronal over-augmentation. These data are similar to ours, now using the dimensions of the contra-lateral ridge as reference for the “individual phenotypic boundaries”.

So far, one can only speculate on an explanation for the impact of IPDs of the graft resorption in time. Some papers mention compressive forces on the augmentation. In a clinical study on ridge preservation, Jiang et al. (2017) screwed a micro-titanium stent over the facial bone wall of the extraction socket to counteract the labial pressure. Compared to unassisted healing, the stent significantly reduced the alveolar ridge resorption (45% vs. 22%). Interestingly, some of these ridged stents even showed slight deformation, implying the strength of soft tissue pressure against the buccal bony wall. Li and co-workers (2022) compared the graft resorption (GBR, staged approach) between using either a resorbable membrane or a 0.2-mm-thick titanium mesh (covered by a resorbable membrane) during the healing phase (to counteract the compressive forces). The Ti mesh significantly reduced the  $E_{res}$  (volumetric evaluation: 23% vs. 38%), but after removal of the mesh, these sites showed more  $L_{res}$  (at 1-year follow-up, no significant difference was found between test and control). In one animal study using the rabbit calvaria (a region that is pressure- and movement-free), the authors observed that some typical behaviors and gestures of the animal (e.g., grooming) already caused an undesirable reduction of the grafted regions (Bae et al., 2014). Thus, small forces seem to be important.

Naenni et al. (2019) observed a significant inverse relationship between lateral bone gain and baseline bone width (-0.35 mm/mm width). The authors gave two explanations for this observation: the natural anatomy of the original

ridge, and/or the more the ridge width prior to augmentation, the less the bone graft material applied. Perhaps one could add that, in case of a small baseline bone width, more augmentation occurs within the individual bone boundaries.

The question whether one can counteract these compressive forces remains debatable. To reduce the resorption of an autogenous block graft for lateral augmentation, the application of a thin layer of inorganic bovine bone particles protected by a collagen membrane over the grafted area, immediately or at the time of implant insertion (augmentative re-lining), has been proposed (von Arx & Buser, 2006; Cordaro et al., 2011; De Stavola & Tunkel, 2013). The integration of the xenograft was found to work like a barrier for future bone volume remodeling, as this material is non- or slow-resorbable (Skoglund et al., 1997; Schlegel & Donath, 1998; Mordenfeld et al., 2010; Klein & Al-Nawas, 2011). As such, the significant block graft resorption (up to 60%, Cordaro et al., 2002; Widmark et al., 1997) could be reduced significantly in the short (von Arx & Buser, 2006; Cordaro et al., 2011; De Stavola & Tunkel, 2013) and long term (Chappuis et al., 2017). A similar result was obtained by Tunkel et al. (2021) by applying the shell technique and an augmentative re-lining at implant insertion. Whether such an augmentative re-lining at implant placement could be helpful to prevent “late” graft resorption after a staged GBR procedure remains unclear, however. Furthermore, Chappuis et al. (2018) clearly illustrated (10 years follow-up) that if one stays within the anatomical boundaries of the patients' alveolus, graft resorption can be reduced to a minimum.

If our observations are correct, this might have a serious impact on a small group of our patient population. Zhang et al. (2008) analyzed the morphological features of the alveolus from relatively healthy maxillary and mandibular incisors (318 patients) using CBCT. They observed that 1.7% of the upper incisors had a thin alveolar bone with double-plate concavities. The same morphology was found in 3.3% of the lower incisors, but 5.1% even presented with a vulnerably thin alveolar bone. Wilson and Johnson (2019)

measured the bucco-lingual alveolar width in the anterior region of 205 patients 3 mm away from the cemento-enamel junction of healthy teeth. They reported a mean width of  $9.1 \pm 1.1$  mm,  $7.2 \pm 0.9$  mm, and  $7.8 \pm 0.9$  mm for upper canines, lateral and central incisors, respectively. The corresponding data for the lower jaw were  $8.9 \pm 1.2$  mm,  $6.8 \pm 0.8$  mm, and  $6.3 \pm 0.7$  mm, respectively. If a guided bone augmentation cannot extend these phenotypic dimensions, a number of patients might/will suffer from severe bone graft resorption after GBR, in short and/or long term, with implant exposure as a consequence.

This study has some limitations. They are mainly the heterogeneity of graft materials as well as its retrospective design, and the limited number of patients. Even though for the largest portion of GBRs ( $n = 19$ ) a combination of Bio-Oss mixed with L-PRF (L-PRF bone block) was used, a number of GBRs ( $n = 4$ ) were treated using the “gold standard”, namely a composite bone block (50% Bio-Oss + 50% autogenous bone). A sub-analysis considering both treatment options (Table S1) could not identify any clear differences between them. When analyzing the results at the different measured depths (2–8 mm from coronal to apical direction) for the split-mouth cases, no statistically significant differences were observed in the pattern of bone resorption following GBR with regard to the IPD between L-PRF bone blocks and composite bone blocks ( $p$ -value  $>.05$ ) more than 1 year after implant loading ( $E_{res} + L_{res}$ ) (Figures S1–S3). Additionally, an analysis between the results obtained (following  $E_{res} + L_{res}$  together) for self-contained ( $n = 13$ ) versus non-self-contained defects ( $n = 2$ ) did not seem to show significant differences between the patterns of bone resorption following GBR when compared to the mirrored side (Table S2). A post-hoc analysis indicated that 227 GBRs would be needed to show any potential difference between L-PRF bone blocks and composite grafts.

The results deriving from a larger number of subjects enrolled in a prospective controlled study could therefore further confirm the results from the present study.

## **CONCLUSION**

Our results suggest that the individual phenotypic dimensions of the bony envelope may be a predictor of how much buccally one can regenerate bone when applying a GBR concept. Moreover, based on the above-mentioned studies and our results, one may need to reconsider whether over-augmentation benefits more hard tissue regeneration.

## REFERENCES

1. Arújo, P. M. (2016). Análise clínica de substituto 'osseo em bloco para aumento horizontal e influência no sucesso dos implantes osseointegrados estudo em humanos Odontologia do Centro de Ciências. Saúde da Universidade Federal de Santa Catarina.
2. Bae, S. Y., Park, J. C., Shin, H. S., Lee, Y. K., Choi, S. H., & Jung, U. W. (2014). Tomographic and histometric analysis of autogenous bone block and synthetic hydroxyapatite block grafts without rigid fixation on rabbit calvaria. *Journal of Periodontal & Implant Science*, 44(5), 251–258.
3. Barreto, M. S., da Silva Barbosa, I., Miranda Leite-Ribeiro, P., de Araújo, T. M., & Almeida Sarmiento, V. (2020). Accuracy of the measurements from multiplanar and sagittal reconstructions of CBCT. *Orthodontics & Craniofacial Research*, 23(2), 223–228.
4. Benic, G. I., Bernasconi, M., Jung, R. E., & Hammerle, C. H. (2017). Clinical and radiographic intra-subject comparison of implants placed with or without guided bone regeneration: 15-year results. *Journal of Clinical Periodontology*, 44, 315–325.
5. Benic, G. I., Eisner, B. M., Jung, R. E., Basler, T., Schneider, D., & Hämmerle, C. H. (2019). Hard tissue changes after guided bone regeneration of peri-implant defects comparing block versus particulate bone substitutes: 6-month results of a randomized controlled clinical trial. *Clinical Oral Implants Research*, 30(10), 1016–1026.
6. Benic, G. I., Thoma, D. S., Jung, R. E., Sanz-Martin, I., Unger, S., Cantalapiedra, A., & Hämmerle, C. H. F. (2017). Guided bone regeneration with particulate vs. block xenogenic bone substitutes: A pilot cone beam computed tomographic investigation. *Clinical Oral Implants Research*, 28(11), e262–e270.
7. Benic, G. I., Thoma, D. S., Munoz, F., Sanz Martin, I., Jung, R. E., & Hämmerle, C. H. F. (2016). Guided bone regeneration of peri-implant defects with particulated and block xenogenic bone substitutes. *Clinical Oral Implants Research*, 27(5), 567–576.
8. Blanco, J., Alonso, A., & Sanz, M. (2005). Long-term results and survival rate of implants treated with guided bone regeneration: A 5-year case series prospective study. *Clinical Oral Implants Research*, 16(3), 294–301.
9. Chappuis, V., Araújo, M. G., & Buser, D. (2017). Clinical relevance of dimensional bone and soft tissue alterations post-extraction in esthetic sites. *Periodontology 2000*, 73(1), 73–83.
10. Chappuis, V., Rahman, L., Buser, R., Janner, S. F. M., Belsler, U. C., &

- Buser, D. (2018). Effectiveness of contour augmentation with guided bone regeneration: 10-year results. *Journal of Dental Research*, 97(3), 266–274.
11. Chargo, N. J., Robison, C. I., Akaeze, H. O., Baker, S. L., Toscano, M. J., Makagon, M. M., & Karcher, D. M. (2019). Keel bone differences in laying hens housed in enriched colony cages. *Poultry Science*, 98(2), 1031–1036.
  - Chiapasco, M., Abati, S., Romeo, E., & Vogel, G. (1999). Clinical outcome of autogenous bone blocks or guided bone regeneration with e-PTFE membranes for the reconstruction of narrow edentulous ridges. *Clinical Oral Implants Research*, 10, 278–288.
  12. Cordaro, L., Amadè, D. S., & Cordaro, M. (2002). Clinical results of alveolar ridge augmentation with mandibular block bone grafts in partially edentulous patients prior to implant placement. *Clinical Oral Implants Research*, 13, 103–111.
  13. Cordaro, L., Torsello, F., Morcavallo, S., & di Torresanto, V. M. (2011). Effect of bovine bone and collagen membranes on healing of mandibular bone blocks: A prospective randomized controlled study. *Clinical Oral Implants Research*, 22, 1145–1150.
  14. Cortellini, S., Castro, A. B., Temmerman, A., Van Dessel, J., Pinto, N., Jacobs, R., & Quirynen, M. (2018). Leucocyte-and platelet-rich fibrin block for bone augmentation procedure: A proof-of-concept study. *Journal of Clinical Periodontology*, 45(5), 624–634.
  15. de Azambuja Carvalho, P. H., dos Santos Trento, G., Moura, L. B., Cunha, G., Gabrielli, M. A. C., & Pereira-Filho, V. A. (2019). Horizontal ridge augmentation using xenogenous bone graft—systematic review. *Oral and Maxillofacial Surgery*, 23(3), 271–279.
  16. De Stavola, L., & Tunkel, J. (2013). A new approach to maintenance of regenerated autogenous bone volume: Delayed relining with xenograft and resorbable membrane. *International Journal of Oral & Maxillofacial Implants*, 28(4), 1062–1067.
  17. Donos, N., Mardas, N., & Chadha, V. (2008). Clinical outcomes of implants following lateral bone augmentation: Systematic assessment of available options (barrier membranes, bone grafts, split osteotomy). *Journal of Clinical Periodontology*, 35, 173–202.
  18. Elgali, I., Omar, O., Dahlin, C., & Thomsen, P. (2017). Guided bone regeneration: Materials and biological mechanisms revisited. *European Journal of Oral Sciences*, 125, 315–337.
  19. Elnayef, B., Porta, C., Del Amo, F. S. L., Mordini, L., Gargallo-Albiol, J., & Hernández-Alfaro, F. (2018). The fate of lateral ridge augmentation: A systematic review and meta-analysis. *International Journal of Oral &*

- Maxillofacial Implants, 33(3), 622–635.
20. Eskan, M. A., Greenwell, H., Hill, M., Morton, D., Vidal, R., Shumway, B., & Girouard, M. E. (2014). Platelet-rich plasma-assisted guided bone re generation for ridge augmentation: A randomized, controlled clinical trial. *Journal of Periodontology*, 85, 661–668.
  21. Fernandes, T. M. F., Adamczyk, J., Poleti, M. L., Henriques, J. F. C., Friedland, B., & Garib, D. G. (2014). Comparison between 3D volumetric rendering and multiplanar slices on the reliability of linear measurements on CBCT images: An in vitro study. *Journal of Applied Oral Science*, 23, 56–63.
  22. Garaicoa, C., Suarez, F., Fu, J. H., Chan, H. L., Monje, A., Galindo-Moreno, P., & Wang, H. L. (2015). Using cone beam computed tomography angle for predicting the outcome of horizontal bone augmentation. *Clinical Implant Dentistry and Related Research*, 17, 717–723.
  23. Gultekin, B. A., Cansiz, E., & Borahan, M. O. (2017). Clinical and 3-dimensional radiographic evaluation of autogenous iliac block bone grafting and guided bone regeneration in patients with atrophic maxilla. *Journal of Oral and Maxillofacial Surgery*, 75(4), 709–722.
  24. Jensen, S. S., & Terheyden, H. (2009). Bone augmentation procedures in localized defects in the alveolar ridge: Clinical results with different bone grafts and bone-substitute materials. *International Journal of Oral and Maxillofacial Implants*, 24(Suppl), 218–236.
  25. Jiang, X., Zhang, Y., Chen, B., & Lin, Y. (2017). Pressure bearing device affects extraction socket remodeling of maxillary anterior tooth. A prospective clinical trial. *Clinical Implant Dentistry and Related Research*, 19(2), 296–305.
  26. Jiang, L., Zhang, W., Wei, L., Zhou, Q., Yang, G., Qian, N., Tang, Y., Gao, Y., & Jiang, X. (2018). Early effects of parathyroid hormone on vascularized bone regeneration and implant osseointegration in aged rats. *Bio- materials*, 179, 15–28.
  27. Jung, R. E., Fenner, N., Hammerle, C. H., & Zitzmann, N. U. (2013). Long- term outcome of implants placed with guided bone regeneration (GBR) using resorbable and non-resorbable membranes after 12–14 years. *Clinical Oral Implants Research*, 24, 1065–1073.
  28. Klein, M. O., & Al-Nawas, B. (2011). For which clinical indications in dental implantology is the use of bone substitute materials scientifically substantiated. *European Journal of Oral Implantology*, 4((Supplement)), S11–S29.
  29. Li, B., Chen, Y., He, J., Zhang, J., Wang, S., Xiao, W., Liu, Z., & Liao,

- X. (2020). Biomimetic membranes of methacrylated gelatin/nanohydroxyapatite/poly (l-lactic acid) for enhanced bone regeneration. *ACS Bio- materials Science & Engineering*, 6(12), 6737–6747.
30. Li, L., Gao, H., Wang, C., Ji, P., Huang, Y., & Wang, C. (2022). Assessment of customized alveolar bone augmentation using titanium scaffolds vs polyetheretherketone (PEEK) scaffolds: A comparative study based on 3D printing technology. *ACS Biomaterials Science & Engineering*, 8(5), 2028–2039.
31. Li, Y., Qiao, S. C., Gu, Y. X., Zhang, X. M., Shi, J. Y., & Lai, H. C. (2019). A novel semiautomatic segmentation protocol to evaluate guided bone regeneration outcomes: A pilot randomized, controlled clinical trial. *Clinical Oral Implants Research*, 30(4), 344–352.
32. Maiorana, C., Beretta, M., Salina, S., & Santoro, F. (2005). Reduction of autogenous bone graft resorption by means of bio-oss coverage: A prospective study. *International Journal of Periodontics and Restorative Dentistry*, 25, 19–25.
33. Mellonig, J. T., Nevins, M., & Sanchez, R. (1998). Evaluation of a bioabsorbable physical barrier for guided bone regeneration. Part I. Material alone. *The International Journal of Periodontics & Restorative Dentistry*, 18, 139–149.
34. Mir-Mari, J., Wui, H., Jung, R. E., Hammerle, C. H., & Benic, G. I. (2016). Influence of blinded wound closure on the volume stability of different GBR materials: An in vitro cone-beam computed tomographic examination. *Clinical Oral Implants Research*, 27(2), 258–265.
35. Mir-Mari, J., Benic, G. I., Valmaseda-Castellón, E., Hämmerle, C. H., & Jung, R. E. (2017). Influence of wound closure on the volume stability of particulate and non-particulate GBR materials: An in vitro cone-beam computed tomographic examination. Part II. *Clinical Oral Implants Research*, 28(6), 631–639.
36. Mordenfeld, A., Hallman, M., Johansson, C. B., & Albrektsson, T. (2010). Histological and histomorphometrical analyses of biopsies harvested 11 years after maxillary sinus floor augmentation with deproteinized bovine and autogenous bone. *Clinical Oral Implants Research*, 21(9), 961–970.
37. Mordenfeld, A., Johansson, C. B., Albrektsson, T., & Hallman, M. (2014). A randomized and controlled clinical trial of two different compositions of deproteinized bovine bone and autogenous bone used for lateral ridge augmentation. *Clinical Oral Implants Research*, 25, 310–320. <https://doi.org/10.1111/clr.12143>

38. Mordini, L., Hur, Y., Ogata, Y., Finkelman, M., Cavani, F., & Steffensen, B. (2020). Volumetric changes following lateral guided bone regeneration. *International Journal of Oral & Maxillofacial Implants*, 35(5), e77–e85.
39. Naenni, N., Lim, H. C., Papageorgiou, S. N., & Hämmerle, C. H. (2019). Efficacy of lateral bone augmentation prior to implant placement: A systematic review and meta-analysis. *Journal of Clinical Periodontology*, 46, 287–306.
40. Park, S. A., Lee, H. J., Kim, K. S., Lee, S. J., Lee, J. T., Kim, S. Y., Chang, N. H., Park, S. Y. (2018). In vivo evaluation of 3D-printed polycaprolactone scaffold implantation combined with  $\beta$ -TCP powder for alveolar bone augmentation in a beagle defect model. *Materials*, 11(2), 238.
41. Sanz-Sánchez, I., Ortiz-Vigón, A., Sanz-Martín, I., Figuero, E., & Sanz, M. (2015). Effectiveness of lateral bone augmentation on the alveolar crest dimension: A systematic review and meta-analysis. *Journal of Dental Research*, 94(9\_suppl), 128S–142S.
42. Schlegel, A. K., & Donath, K. (1998). BIO-OSS--a resorbable bone substitute? *Journal of Long-Term Effects of Medical Implants*, 8(3–4), 201–209.
43. Schwarz, F., Herten, M., Ferrari, D., Wieland, M., Schmitz, L., Engelhardt, E., & Becker, J. (2007). Guided bone regeneration at dehiscence-type defects using biphasic hydroxyapatite + beta tricalcium phosphate (bone ceramic) or a collagen-coated natural bone mineral (BioOss collagen): An immunohistochemical study in dogs. *International Journal of Oral and Maxillofacial Surgery*, 36, 1198–1206.
44. Skoglund, A., Hising, P., & Young, C. (1997). A clinical and histologic examination in humans of the osseous response to implanted natural bone mineral. *International Journal of Oral & Maxillofacial Implants*, 12(2), 194–199.
45. Strietzel, F. P., Khongkhunthian, P., Khattiya, R., Patchanee, P., & Reichart, P. A. (2006). Healing pattern of bone defects covered by different membrane types—a histologic study in the porcine mandible. *Journal of Biomedical Materials Research. Part B, Applied Biomaterials*, 78B(1), 35–46.
46. Thoma, D. S., Bienz, S. P., Figuero, E., Jung, R. E., & Sanz-Martín, I. (2019). Efficacy of lateral bone augmentation performed simultaneously with dental implant placement: A systematic review and meta-analysis. *Journal of Clinical Periodontology*, 46, 257–276.
47. Thoma, D. S., Dard, M. M., Hälg, G.-A., Ramel, C. F., Hämmerle, C. H.

- F., & Jung, R. E. (2012). Evaluation of a biodegradable synthetic hydrogel used as a guided bone regeneration membrane: An experimental study in dogs. *Clinical Oral Implants Research*, 23(2), 160–168.
48. Thoma, D. S., Payer, M., Jakse, N., Bienz, S. P., Husler, J., Schmidlin, P. R., Jung, U.-W., Hämmerle, C. H. F., & Jung, R. E. (2018). Randomized, controlled clinical two-Centre study using xenogeneic block grafts loaded with recombinant human bone morphogenetic protein-2 or autogenous bone blocks for lateral ridge augmentation. *Journal of Clinical Periodontology*, 45, 265–276.
49. Troeltzsch, M., Troeltzsch, M., Kauffmann, P., Gruber, R., Brockmeyer, P., Moser, N., Rau, A., Schliephake, H., & Schliephake, H. (2016). Clinical efficacy of grafting materials in alveolar ridge augmentation: A systematic review. *Journal of Cranio-Maxillofacial Surgery*, 44(10), 1618–1629.
50. Tunkel, J., de Stavola, L., & Kloss-Brandstätter, A. (2021). Alveolar ridge augmentation using the shell technique with allogeneic and autogenous bone plates in a split-mouth design—A retrospective case report from five patients. *Clinical Case Reports*, 9(2), 947–959.
51. Urban, I. A., & Monje, A. (2019). Guided bone regeneration in alveolar bone reconstruction. *Oral and Maxillofacial Surgery Clinics of North America*, 31, 331–338.
52. Verhelst, P. J., Smolders, A., Beznik, T., Meewis, J., Vandemeulebroucke, A., Shaheen, E., Van Gerven, A., Willems, H., Politis, C., & Jacobs, R. (2021). Layered deep learning for automatic mandibular segmentation in cone- beam computed tomography. *Journal of Dentistry*, 114, 103786.
53. von Arx, T., & Buser, D. (2006). Horizontal ridge augmentation using autogenous block grafts and the guided bone regeneration technique with collagen membranes: A clinical study with 42 patients. *Clinical Oral Implants Research*, 17(4), 359–366.
54. Wang, H. L., & Boyapati, L. (2006). “PASS” principles for predictable bone regeneration. *Implant Dentistry*, 15, 8–17.
55. Widmark, G., Andersson, B., & Ivanoff, C.-J. (1997). Mandibular bone graft in the anterior maxilla for single-tooth implants. Presentation of a surgical method. *International Journal of Oral and Maxillofacial Surgery*, 26, 106–109.
56. Wilson, J. P., & Johnson, T. M. (2019). Frequency of adequate mesiodistal space and faciolingual alveolar width for implant placement at anterior tooth positions. *The Journal of the American Dental Association*, 150(9), 779–787.

57. Zhang, X., Awad, H. A., O'Keefe, R. J., Guldberg, R. E., & Schwarz, E. M. (2008). A perspective: Engineering periosteum for structural bone graft healing. *Clinical Orthopaedics and Related Research*, 466(8), 1777–1787.





GENERAL DISCUSSION



## GENERAL DISCUSSION

### Overview of Findings

The research presented in this thesis explored the **development** and **validation** of AI-driven planning tools for **patient-specific** oral surgical procedures, particularly focusing on **tooth autotransplantation** (TAT) and **implant placement**. The work combined advanced techniques in artificial intelligence (AI) and **biomechanical modeling** to enhance the **precision**, **predictability**, and **efficiency** of these complex surgical interventions. The findings demonstrate significant potential for AI to revolutionize surgical planning in oral and maxillofacial surgery by addressing existing challenges such as the **complexity** of workflows, **time** constraints, and **cost** implications.

### The Impact of AI on Oral and Maxillofacial Surgery

AI has rapidly advanced across various medical domains, yet its application in oral and maxillofacial surgery remains **underexplored**. This research contributes to filling this gap by demonstrating how AI can be harnessed to **support decision-making** and **surgical planning** in **oral surgical procedures**. The **success** of AI in other fields, such as **medical imaging** and **diagnostics**, is largely attributed to its ability to process vast amounts of **data** and **identify patterns** that may not be immediately apparent to human practitioners. This thesis extends these capabilities to oral surgery, where **patient-specific anatomical** and **biomechanical considerations** are paramount.

The **integration** of AI into the planning stages of oral surgery offers several key **benefits**. First, AI-driven tools can **analyze** complex datasets from 3D imaging and other diagnostic modalities to **generate** optimized treatment plans **tailored** to the **individual** patient. This level of **customization** is particularly crucial in procedures like TAT and implant placement, where the anatomical differences between patients can **significantly** influence

**outcomes.** The research demonstrated that AI could reduce the **time** required to **develop** these plans, potentially lowering the overall **costs** associated with digital planning procedures. Moreover, AI's ability to continually **learn** and **improve** from new data suggests that its **effectiveness** will only increase over time, offering **long-term benefits** to practitioners and patients alike.

However, the **adoption** of AI in oral surgery is not without its **challenges**. The current **digitalization** of dentistry has been **slow**, partly due to the **complexity** of integrating new technologies into existing workflows. The findings of this thesis highlight that while AI has the potential to **simplify** these workflows, the **transition** will require significant changes in how dental professionals are **trained** and how they approach treatment planning. There is also a need for further **validation** of AI models in clinical settings to ensure their **reliability** and **generalizability** across different patient populations and surgical contexts.

### **Biomechanical Modeling and its Role in Surgical Planning**

**Biomechanical modeling** plays a critical role in understanding the **interactions** between biological tissues and surgical interventions. In the context of oral surgery, accurate biomechanical models can **simulate** the physical forces at play during and after procedures like TAT and implant placement. This research **integrated** biomechanical modeling with AI to create **simulations** that **studies** the outcomes of various surgical scenarios, offering surgeons and researchers valuable **insights** into potential **complications** and the long-term success and survivals of various **treatment** options.

One of the significant contributions of this thesis is the **development** of **patient-specific** biomechanical models that account for **individual variations** in bone density, periodontal ligament integrity, and occlusal forces. These models provide a more nuanced understanding of how transplanted

teeth **interact** with the surrounding oral structures, helping to **optimize** surgical techniques and **improve** patient outcomes. The **integration** of AI allows for the rapid **generation** and **analysis** of these models, making it **feasible** to include **biomechanical considerations** in **routine** clinical practice.

Despite the **advantages**, there are **limitations** to the current state of **biomechanical modeling**. The **accuracy** of these models depends heavily on the **quality** and **resolution** of the **input data**, which can vary depending on the **imaging technology** used. Additionally, while the models can **simulate** many aspects of **oral biomechanics**, they cannot yet fully **replicate** the **complexity** of **biological systems**, particularly in **predicting** long-term tissue **remodeling**. As such, there is a need for **continued research** to **refine** these models and enhance their **predictive capabilities**.

### **Challenges and Limitations**

While this research has **demonstrated** the potential of AI and **biomechanical modeling** to **improve** patient-specific surgical planning, several **challenges** and **limitations** must be acknowledged. One of the primary challenges is the **integration** of these **advanced technologies** into clinical workflows. The **complexity** of **AI algorithms** and **biomechanical models** requires a high level of **expertise**, which may not be readily available in all dental practices. Moreover, the **adoption** of such **technologies** may be hindered by **financial constraints**, particularly in smaller clinics that may not have the **resources** to invest in the necessary **hardware** and **software**.

Another limitation is the current lack of **large, high-quality datasets** specific to oral and maxillofacial surgery, which are essential for **training** and **validating** AI models. While the use of AI in other medical fields has benefited from extensive datasets, the same is not true for dentistry, where **data collection** is often **fragmented** and **inconsistent**. This limitation

underscores the need for more **collaborative efforts** to create **comprehensive databases** that can support the **development** of robust AI-driven tools.

Furthermore, while AI offers the potential for more **efficient** and **accurate** surgical planning, there is still a need for **human oversight** or ‘**human intelligence**’. AI models, no matter how **advanced**, can make errors or **generate** recommendations that may not be **appropriate** in certain clinical contexts. Therefore, it is crucial that these tools are used as **aids** to, rather than **replacements** for, skilled surgeons. The role of the clinician in **interpreting** and **validating** AI-generated plans **cannot be overstated**, as their **expertise** and **judgment** remain **critical** to the **success** of surgical outcomes.

When using AI models for oral and maxillofacial surgical planning, several **ethical limitations** must be addressed. First, **patient privacy** and **data security** are paramount, as **AI** relies on **large datasets**, often including **sensitive medical information**. Ensuring **data anonymization** and **compliance** with regulations like **GDPR** and the **EU AI-Act** is crucial. Additionally, **biases** in **training data** can lead to unequal outcomes, potentially **disadvantaging** certain **patient groups**. It is also important to maintain **transparency**, allowing surgeons to understand AI decision-making processes, as **over-reliance** on AI without human oversight can lead to errors. Finally, **informed consent** from patients must be obtained, ensuring they are aware of the role **AI** plays in their treatment planning.

### **Implications for Clinical Practice**

The **findings** of this research have significant **implications** for clinical practice in oral and maxillofacial surgery. The **development** of AI-driven planning tools has the potential to **streamline** the surgical planning process, making it more **efficient** and **accessible**. By **reducing** the **time** and **effort** required to create **detailed** surgical plans, these tools can help to **lower** the

costs associated with **digital planning** and make **advanced surgical techniques** more **widely available**.

Moreover, the use of **AI** and **biomechanical modeling** can lead to more **predictable** surgical outcomes, **improving** patient **satisfaction** and **reducing** the **risk of complications**. The ability to **simulate** various surgical **scenarios** and assess their potential **outcomes** allows surgeons to make more **informed decisions**, ultimately leading to better **patient care**.

However, for these **benefits** to be realized, it is essential that dental professionals receive appropriate **training** in the use of **AI** and **biomechanical modeling** tools. This may require changes to **dental education** curricula, as well as ongoing **professional development** opportunities to ensure that practitioners are **equipped** with the **skills** and **knowledge** needed to **effectively use** these **technologies**.

### **Future Research Directions**

The research presented in this thesis opens up several avenues for **future investigation**. One important direction is the **continued development** and **refinement** of **AI algorithms** and **biomechanical models**, with a focus on **improving** their **accuracy** and **reliability**. This will likely involve the collection of **larger** and **more diverse datasets**, as well as the **incorporation** of **new types of data**, such as **genetic** or **molecular information**, that could further **enhance** the **precision** of **surgical planning** towards more inclusive **in-silico models**.

Another area for future research is the **exploration** of **AI's** potential to support **intraoperative decision-making**. While this thesis focused on **preoperative planning**, there is considerable **potential** for **AI** to **assist** surgeons during the actual **procedure**, providing **real-time guidance** and **adapting** to **unforeseen challenges**. This could lead to the **development of fully integrated AI**

**systems** that **support** all stages of the **surgical process**, from **planning** to **execution** and **post-operative care**.

Finally, there is a need for more **clinical trials** to **validate** the **effectiveness** of **AI-driven** planning tools in **diverse patient populations** and **clinical settings**. Such **trials** will be **crucial** for demonstrating the **practical value** of these **technologies** and ensuring that they can be **safely** and **effectively** implemented in **routine practice**.

## **CONCLUSION**

The **integration** of **AI** and **biomechanical modeling** into **oral and maxillofacial surgery** represents a significant step forward in the field of **digital dentistry**. This research has demonstrated the potential of these technologies to enhance **patient-specific surgical planning**, leading to more **predictable** outcomes and improved **patient care**. However, realizing this potential will require overcoming several **challenges**, including the need for greater **expertise**, better **data**, and more streamlined **workflows**.

As **AI** and **biomechanical modeling** continue to evolve, they are likely to play an increasingly important role in oral surgery, offering new **opportunities** to improve the **precision** and **effectiveness** of **treatment**. By continuing to **explore** and **develop** these **technologies**, the field of dentistry can move closer to achieving the vision of truly **personalized medicine**, where every patient receives the most **appropriate** and **effective** care based on their unique **specific characteristics**.

## SUMMARY

The main objective of this doctoral thesis was to use Artificial Intelligence and biomechanical analysis for the planning of oral surgical procedures. It was hypothesized that Artificial Intelligence could help clinicians and researcher improve their digital workflow through (1) rendering the use of complex planning tools user-friendly and accessible to a wider audience, while (2) being at the same time as accurate as expert users, and by (3) providing a solid foundation for promoting in-silico studies and patient-specific modeling.

**Part I** focused on reviewing the literature regarding the current knowledge pertaining to personalized dentistry (**chapter 1**) and finite element modeling in dentistry (**chapter 2**).

The main results of these investigations revealed that Patient-Specific Modeling may allow optimized surgical treatment planning, increase predictability, and potentially lower risks of pre- and post- operative complications. Recent advancements in the fields of AI may allow for the automation of several parts of these laborious modeling technologies, bringing user-assisted decision-support tools closer than ever to both clinicians and researchers.

Additionally, FEA is becoming increasingly important in the medical field in general and dental research in particular. Thanks to the recent proliferation of high-quality imaging modalities and fast computing resources, FEA currently holds the potential to be employed in junction with in-silico modeling tool to study patient-specific scenarios and therefore offer tailored treatments to patients. However, more research is still needed to develop in-vivo protocols to enable implementation and clinical validation of PSM and FEA in dental practice. At the same time, ethical and legal constraints should be carefully considered when applying data-driven models in current clinical practice.

**Part II** related to the development of AI-driven tools for aiding automation of oral surgical planning. A focus was laid on the development and validation of

AI-driven modules for tooth (**chapter 3**) and mandibular canal (**chapter 4**) segmentation on CBCT.

Results from these two studies show that AI holds great potential in delivering fast and accurate segmentations of oral and maxillofacial structures on CBCT. Patient-specific anatomical segmentations of oral and maxillofacial structures allowed for the development of biomechanically focused in-silico models for the study of tooth auto-transplantation outcomes, where we aimed to develop and use accurate patient-specific in-silico modeling to investigate the influence of oral biomechanics on tooth autotransplantation outcomes (**chapter 5**). Results from this study showed that in-silico modeling offers a promising approach for studying complex biological phenomena, including TAT and its associated biomechanical factors and confirms that in the case of TAT, patient-specific variations, including anatomy, masticatory forces and specific tissues involved, might influence the overall biomechanical tissue reaction.

**Part III** focused on the application of developed AI-driven tools, for planning and studying oral surgical procedures.

In **chapter 6**, Model Order Reduction techniques were developed and applied to the established in-silico based biomechanical models of TAT described in **chapter 5**.

This resulted in accurate real-time simulation of TAT biomechanics while drastically reducing the time for delivering the root stresses.

Finally in **chapter 7**, we explored the hypothesis that the “individual phenotypic dimensions” may partially explain the degree of such resorptions. While relying on CBCT-based patient-specific models based on accurate anatomical segmentations, results indicate that the dimensions of a lateral bone augmentation are to some extent defined by the “individual phenotypic bone boundaries” of the patient. This finding could help clinicians anticipate the degree of resorption following guided bone augmentation and plan implant placement accordingly.

In summary, this doctoral thesis focused on the development, validation, and application of Artificial Intelligence for planning oral surgical procedures. The performed research demonstrates the potential of AI and biomechanical modeling to revolutionize personalized dentistry by improving the accuracy and efficiency of surgical planning and in-silico modeling in the pursue of studying and understanding complex biological phenomena.

## SAMENVATTING

Het hoofddoel van dit doctoraatsonderzoek was om Artificiële Intelligentie en biomechanische analyse te gebruiken voor de planning van orale chirurgische procedures. De hypothese was dat Artificiële Intelligentie klinici en onderzoekers zou kunnen helpen hun digitale workflow te verbeteren door **(1)** het gebruik van complexe planningstools gebruiksvriendelijk en toegankelijk te maken voor een breder publiek, terwijl **(2)** het tegelijkertijd even nauwkeurig is als expertgebruikers, en door **(3)** een solide basis te bieden voor het bevorderen van in-silicostudies en patiëntspecifieke modellering.

**Deel I** richtte zich op een overzicht van de literatuur over de huidige kennis met betrekking tot gepersonaliseerde tandheelkunde (**hoofdstuk 1**) en Finite Element Modeling in de tandheelkunde (**hoofdstuk 2**).

De belangrijkste resultaten van deze studies toonden aan dat patiëntspecifieke modellering een geoptimaliseerde planning van chirurgische behandelingen mogelijk maakt, de voorspelbaarheid verhoogt en mogelijk de risico's van pre- en postoperatieve complicaties verlaagt. Recente ontwikkelingen op het gebied van AI kunnen de automatisering van verschillende onderdelen van deze bewerkelijke modelleringstechnologieën mogelijk maken, waardoor gebruikersondersteunde hulpmiddelen voor besluitvorming dichter dan ooit bij klinici en onderzoekers komen.

Daarnaast wordt FEA steeds belangrijker op medisch gebied in het algemeen en tandheelkundig onderzoek in het bijzonder. Dankzij de recente proliferatie van hoogwaardige beeldvormingsmodaliteiten en snelle computermiddelen heeft FEA momenteel het potentieel om gebruikt te worden in combinatie met in-silico modelleringstools om patiëntspecifieke scenario's te bestuderen en zo patiënten behandelingen op maat aan te bieden. Er is echter nog meer onderzoek nodig om in-vivo protocollen te ontwikkelen om de implementatie en klinische validatie van PSM en FEA in de tandheelkundige praktijk mogelijk te maken. Tegelijkertijd moet er zorgvuldig rekening worden

gehouden met ethische en wettelijke beperkingen bij het toepassen van datagestuurde modellen in de huidige klinische praktijk.

**Deel II** had betrekking op de ontwikkeling van AI-gebaseerde tools voor het automatiseren van orale chirurgische planning. De nadruk lag op de ontwikkeling en validatie van AI-gebaseerde modules voor segmentatie van tanden (**hoofdstuk 3**) en mandibulaire kanalen (**hoofdstuk 4**) op CBCT.

De resultaten van deze twee onderzoeken lieten zien dat AI een groot potentieel heeft in het leveren van snelle en nauwkeurige segmentaties van orale en maxillofaciale structuren op CBCT.

Patiëntspecifieke anatomische segmentaties van orale en maxillofaciale structuren maakten de ontwikkeling mogelijk van biomechanisch gerichte in-silicomodellen voor het onderzoek naar uitkomsten van autotransplantatie van tanden, waarbij we ernaar streefden nauwkeurige patiëntspecifieke in-silicomodellen te ontwikkelen en te gebruiken om de invloed van orale biomechanica op uitkomsten van autotransplantatie van tanden te onderzoeken (**hoofdstuk 5**). De resultaten van dit onderzoek toonden aan dat in-silicomodellering een veelbelovende aanpak biedt voor het bestuderen van complexe biologische processen, waaronder TAT en de bijbehorende biomechanische factoren, en bevestigt dat in het geval van TAT patiëntspecifieke variaties, waaronder anatomie, kauwkrachten en specifieke betrokken weefsels, van invloed kunnen zijn op de algehele biomechanische weefselreactie.

**Deel III** richtte zich op de toepassing van ontwikkelde AI-gebaseerde tools voor het plannen en bestuderen van orale chirurgische behandelingen.

In **hoofdstuk 6** werden Model Order Reduction-technieken ontwikkeld en toegepast op de in-silico gebaseerde biomechanische modellen van TAT die in hoofdstuk 5 zijn beschreven.

Dit resulteerde in nauwkeurige real-time simulatie van de biomechanica van de TAT, terwijl de tijd voor het leveren van de wortelspanningen drastisch werd verkort.

Tot slot onderzochten we in **hoofdstuk 7** de hypothese dat de “individuele fenotypische dimensies” de mate van dergelijke resorpties gedeeltelijk kunnen verklaren. Door gebruik te maken van CBCT-gebaseerde patiëntspecifieke modellen op basis van nauwkeurige anatomische segmentaties, geven de resultaten aan dat de afmetingen van een laterale botaugmentatie tot op zekere hoogte worden bepaald door de “individuele fenotypische botgrenzen” van de patiënt. Deze bevinding zou klinici kunnen helpen te anticiperen op de mate van resorptie na een geleide botaugmentatie en de plaatsing van implantaten dienovereenkomstig te plannen.

Samengevat richtte dit doctoraatsonderzoek zich op de ontwikkeling, validatie en toepassing van Artificiële Intelligentie voor het plannen van orale chirurgische behandelingen. Het uitgevoerde onderzoek toont het potentieel aan van AI en biomechanische modellering om een revolutie teweeg te brengen in de gepersonaliseerde tandheelkunde door de nauwkeurigheid en efficiëntie van chirurgische planning en in-silicomodellering te verbeteren bij het bestuderen en begrijpen van complexe biologische processen.

## **SCIENTIFIC ACKNOWLEDGMENTS**

This PhD thesis is written by the doctoral candidate Pierre Lahoud and properly revised by the promotor Prof. Dr. Reinhilde Jacobs and the co-promotors Prof. Dr. Marc Quiryne, Prof. Dr. Michael Bornstein and Dr. Mostafa EzEldeen.

All experiments were performed by or under the supervision of the PhD candidate with the collaboration and technical support from other researchers and colleagues.

All manuscripts from this thesis were written by the PhD candidate and revised by all co-authors.

## PERSONAL ACKNOWLEDGMENTS

First and foremost, I wish to extend my deepest gratitude to my promoter, **Prof. Dr. Reinhilde Jacobs**, for her unwavering guidance, support, and encouragement throughout my PhD journey. From our very first meeting in Leuven during Easter Break of 2018, when I came for my interview, your belief in my potential has been a constant source of motivation and confidence. Your mentorship has not only enriched my research experience but has also profoundly shaped my personal and professional growth. I feel privileged to have had the opportunity to learn from your extensive knowledge, critical insights, and unparalleled expertise. Thank you for your dedication, patience, and for setting an inspiring example in both academia and leadership. I am forever grateful for your support and for the invaluable experiences gained under your supervision.

I would also like to extend my heartfelt thanks to **Prof. Dr. Marc Quiryne**. Throughout my clinical journey into periodontology and implant surgery, you have been a pillar of support and mentorship. Your expertise and wisdom have not only shaped my clinical skills but also inspired my academic and research pursuits. Your dedication and passion for the field have left a lasting impact on me, and I am truly honored to have learned from you.

**Prof. Dr. Michael Bornstein**, thank you for your continuous support and mentorship. Your expertise and thoughtful guidance have been instrumental in refining this research. I am particularly grateful for your valuable suggestions, which enriched the quality of this work.

My deepest gratitude also goes to **Dr. Mostafa EzEldeen**, who has been there since day one of this journey. From the very beginning, he believed in me, offering his constant support, guidance, and motivation when it was most needed. His patience and dedication have been a cornerstone of my progress, and I am incredibly fortunate to have had him by my side throughout this entire process. I still vividly remember the countless long days we spent

brainstorming together, tackling challenges and solving complex problems in MeVisLab. Those moments not only shaped the direction of my research but also deepened my understanding of problem-solving and perseverance. Mostafa, finishing this PhD with you as my co-promotor is truly a great honor, and I am proud and grateful to call you both a mentor and a friend and to be your first-ever PhD student on what I am sure will be a great academic career of yours. Thank you, dear Mostafa, for your invaluable contributions, for believing in me and for always pushing me to be my best.

I would like to sincerely thank my internal jury members, **Prof. Dr. Peter Claes** and **Prof. Dr. Andy Temmerman**, for their constant support and their critical eye throughout this PhD journey. Their insightful feedback and thoughtful suggestions have been invaluable in improving the quality of this work, and I am truly grateful for their dedication and guidance over the years.

Additionally, a heartfelt thanks to **Prof. Dr. Selena Toma** and **Prof. Dr. Georgios N. Belibasakis** for graciously agreeing to serve as external jury members for my public doctoral defense. Your time, expertise, and commitment are deeply appreciated. I am also sincerely grateful to **Prof. Dr. Koen Van Laere** for kindly agreeing to chair the defense and for overseeing this important milestone in my academic journey.

I would like to extend my sincere gratitude to **Prof. Dr. Tatiana Kuznetsova** for chairing the examining committee during the thesis revision process. Thank you for ensuring everything proceeded smoothly and for your invaluable support and oversight.

Combining my PhD with a clinical specialization has been an intense and challenging journey. Yet, I was fortunate to be surrounded by an incredible group of people who supported and guided me every step of the way. This journey would not have been possible without **Mevr. Christel Dekeyser**: thank you for your unwavering daily support in the clinic. Your attention to details and compassion, both for us and for the patients, are truly admirable,

and I am deeply grateful for everything I have learned from you and for your continuous support.

I would also like to extend my heartfelt thanks to **Prof. Dr. Ana Castro**, under whose supervision I had the privilege to begin my clinical and surgical specialization. Thank you for believing in me and for offering your constant support, both in the clinic and in research. I have learned so much from you, particularly from your meticulous approach and refined surgical skills. You have also helped me integrate my clinical expertise with my research goals and ideas, and for that, I am truly grateful.

**Prof. Dr. Wim Teughels** thank you for your consistent support and assistance within the department. Your guidance has been invaluable to me throughout this journey both as a researcher as well as a clinician.

**Prof. Dr. Constantinus Politis**, thank you for your constant support within the department of oral and maxillofacial surgery, and for your trust and support in helping with the planning of tooth autotransplantation procedures. You have always been there for support, and for that I am extremely grateful.

Additionally, I would like to sincerely thank **Prof. Dr. Raphaël Richert** for his invaluable support and expertise over the past few years. Since we first met in the summer of 2021, I have truly enjoyed every single collaboration we embarked on, and together, we have achieved so much in such a short time. I am grateful for not only his professional guidance but also for his friendship throughout this journey. Raphaël, I am truly grateful to having you not only as a colleague, but also as a friend. I look forward to the exciting journey and discoveries ahead of us.

A special thank you to **Cato Verstappen**. Your unwavering support, understanding, and patience have been my constant source of strength throughout this challenging phase. You have stood by me during late nights and stressful moments, always offering comfort and encouragement. Words cannot fully express how much your love and positivity have meant to me.

You have been my greatest cheerleader, and for that, I will be forever grateful. **Liesbeth Voordeckers** and **Herman Verstappen**, thank you for your warm welcome in the family.

My heartfelt thanks also go to **Dr. Bruno Collaert**, with whom I have the pleasure of conducting my external internship. I have learned so much under his guidance, and I am deeply grateful for the knowledge and insights he has shared with me. I would also like to thank both him and **Lieve Wijnen** for their continuous support and encouragement throughout this experience, which has greatly enriched my personal and professional growth.

I would also like to express my deepest gratitude to **Prof. Dr. Maria Cadenas de Llano Perula** for her unwavering support and friendship since day one. Her dedication to her work, her unwavering support and assistance to everyone, and her constant pursuit of excellence have been a source of inspiration throughout this journey. Maria, thank you for being an incredible mentor and an amazing friend.

**Dr. Andrés Torres**, we have shared together with Mostafa our office in the past few years, and you will too, soon be moving taking on new adventures. From the countless hours spent working together in the office and nerding out about coffee, to biking for dozens of kilometers in the cold without handgloves, I have cherished every moment. Thank you for your friendship, support, and for making this journey all the more enjoyable. I am truly grateful for the wonderful memories we've created, both professionally and personally.

**Nele Vanloocke**, thank you for all your help and assistance during this doctoral trajectory. You have always been there for me and for everyone in our group who needed you and helped making sure everything went smoothly in our journey.

I would also like to extend my gratitude to my colleagues from **UZ Leuven**, who have made this journey a collaborative and fulfilling experience. In particular, I would like to thank **Hannelore Jehoul**, **Jill Hadisurya**, and all

of the other colleagues **Moaad Alami, Lina Bakali, Sophie Caufriez, Caroline Dequae, Sofie Depuydt, Lieve Desmet, Britt Dupont, Nick Ntovas, Pieter-Jan Germonpré, Massih Naimi, Jits Robben, Thijs Schumans, Manoetjer Siawasch, Maria Tsihlaki, Kato Van Caesbroeck.** I had the pleasure of working with during these years. Your friendship, insightful discussions, and invaluable support made this journey far more enjoyable. I am thankful for the many shared moments in the clinic and outside and for the support you have given me.

I am also grateful to all the researchers and clinicians I had the pleasure of meeting and collaborating with throughout these years, including **Prof. Dr. Mariano N. Simón Pedano De Piero, Prof. Dr. Falk Schwendicke, Prof. Prof. Dr. Najla Chebib, Dr. Maxime Ducret, Prof. Dr. Marcio Vivan Cardoso, Prof. Dr. Joseph Sabbagh, Prof. Dr. André Ferreira Leite, Prof. Dr. Victor Aquino Wanderley, Prof. Dr. Hugo Gaêta-Araujo, Prof. Dr. Khalid Alqattani, Prof. Dr. Mihai Tarce, Dr. Nastaran Meschi, Dr. Karla de Faria Vasconcelos, Dr. Eman Shaheen, Dr. Jan Meeus, Dr. Elias Walter, Dr. Isabelle Laleman, Dr. Heidi Opdebeeck, Dr. Amit Rajbhaj, Dr. Wim Coucke, Dr. Jesica Dadamio, Zuodong Zhao, Wouter Reybrouck, Isabelle Savoye, Jan Wyatt, Wout Jacobs, Rayann Sellami, Marie-Louise Slim, Bahaa Elgarba, Thanatchaporn Jindanil, Una Ivković, Rellyca Sola Gracea, Flavia Preda, Ilya Tsiklin, Jeroen Van Dessel, Wannes Van Holm, Tamara Alzoubi, Natália Siqueira Lobo, Alexander De Greef, Rutger Dhondt, Simone Cortellini, Elena Borsci, Sandipan Roy, Thomas Beznik, Holger Willems, Siebe Diels.** Each of you has contributed in some way to the evolution of my research, and I am thankful for the conversations, exchanges of ideas, and moments of shared learning. The community of scholars and practitioners has been an essential part of my development, and I value the friendships and professional relationships we have shared over the years.

A big thanks goes to my second family, my friends, **Dr. Charbel Aoun, Joe Abi Nader, Christian Atallah, Fares Boulos, Jeroen Christiaens, Danie Daaboul, Dr. Brigitte Doueihy, Dr. Lukas Driesen, Dr. Antoine El Asmar, Dr. Samy El Bachaoui, Dr. Gebrael El Hachem, Dr. May El Hajj, Chris Feghali, Leya Hage, Isabelle Janssens, Labib Kachkouch, Julien Kaikati, Joe Keirouz, Karim Houry, Yara Houry, Katalina Lauwens, Wout Lauwers, Jörg Lüdemann, Christelle Macari, Karen Macari, Louise Mathijs, Marc Mouallem, Eva Mulckhuysse, Dr. Denise Murgia, Dr. Paul Najem, Dr. Paméla Nakad, Liselot Niclaes, Alana Lutz, Sonya Radi, Sonia Romano, Dr. Joseph Sabbagh, Charbel Safi, Joanne Sayegh, Marlène Simonini, Stijn Van Aelst, David Van der Haute, Seppe Verstraeten, Ellen Wouters, Dr. Christophe Zougheib.** A heartfelt thank you to all of you, both near and far. You have been a source of comfort and joy, even when home seemed away from home. Whether through words of encouragement, a shared laugh, or simply offering a listening ear, you have made this journey much more enjoyable. Your support, in both big and small ways, has meant more than you know.

Finally, I owe the greatest debt of gratitude to my family. To my parents **Gisèle** and **Zahi**, sisters **Rachelle** and **Christelle**, and extended family. Your unconditional love and belief in me have been my foundation. You have supported me in countless ways—emotionally, morally, and practically—throughout every stage of this process. I would not be where I am today without your encouragement and love. Thank you for always being there for me, through the highs and the lows, and for inspiring me to persevere.

This thesis is as much a reflection of your support as it is of my work. Thank you all.

## **CONFLICT OF INTEREST**

The authors declare no potential conflicts of interest with respect to the authorship and/or publication of this work.



CURRICULUM VITAE



## PIERRE LAHOUD

Born on June 7<sup>th</sup>, 1996, in Amchit, Lebanon

### EDUCATION

**Master-after-Master in Periodontology (MSc. Clin.) - EFP accredited** | *KU Leuven*, Faculty of Medicine - Leuven, Belgium, 10.2021 - Present

**Doctoral Studies in Biomedical Sciences (Ph.D)** | *KU Leuven*, Faculty of Medicine - Leuven, Belgium, 09.2020 - 12.2024

**Postgraduate Studies in Advanced Medical Imaging (PGD - *Magna Cum Laude*)** | *KU Leuven*, Faculty of Medicine - Leuven, Belgium, 09.2019 - 09.2020

**Erasmus+ Exchange Studies** | *UC Louvain*, Faculty of Medicine and Dental Medicine, *Cliniques Universitaires Saint-Luc* - Brussels, Belgium, 2018

**Diploma of Dental Surgery (DDS - *Summa Cum Laude*)** | *Université Libanaise*, Faculty of Dental Medicine - Beirut, Lebanon, 2014 - 2019

**French Baccalaureate (with *Distinction*), Scientific Section** | *Collège Notre-Dame de Lourdes* - Byblos, Lebanon, 2014

### EXPERIENCE

**Guest Professor**, Department of Conservative Dentistry and Periodontology, LMU Klinikum, Ludwig Maximilian University of Munich, Germany | 10.2024 - Present

**Clinical Internship** – Centrum Parodontologie en Implantologie Leuven ; Heverlee, Belgium | 08.2024 - Present

**Principal Investigator - Benchmarking Group** – World Health Organisation, International Telecommunication Union & World Intellectual Property Organisation (WHO-ITU-WIPO) Global Initiative on AI for Health (GI-AI4H) Topic Group Dental ; Geneva, Switzerland | 02.2024 - Present

**Scientific Collaborator** – World Health Organisation, International Telecommunication Union & World Intellectual Property Organisation

(WHO-ITU-WIPO) Global Initiative on AI for Health (GI-AI4H) ; Geneva, Switzerland | 10.2023 - Present

**Research Collaborator** – European Federation of Organisations for Medical Physics (EFOMP) - Special Interest Group (SIG) in Dental Imaging ; Utrecht, Netherlands | 05.2023 - Present

**Member** – KU Leuven Institute of Physics-based Modelling for in-Silico Health (iSi Health) ; Leuven, Belgium | 11.2022 - Present

**Board Member** - Junior Committee of *Digital Dentistry Belgium* ; Brussels, Belgium | 10.2022 - Present

**Clinical Resident in Periodontology & Implant Surgery** – Department of Periodontology & Oral Microbiology, Department of Oral Health Sciences, KU Leuven & University Hospitals Leuven ; Leuven, Belgium | 10.2021 – Present

**Consultant for Trans-Alveolar Dental Transplantations** – Department of Oral and Maxillofacial Surgery, University Hospitals Leuven ; Leuven, Belgium | 11.2020 - 06-2023

**Doctoral Researcher** - OMFS-IMPACT Research Group, KU Leuven ; Leuven, Belgium | 09.2020 - Present

**Orthodontic Assistant** - Opdebeeck & Partners Orthodontie ; Halle, Belgium | 11.2019 - 06.2021

**Pre-Doctoral Researcher** - OMFS-IMPACT Research Group, KU Leuven ; Leuven, Belgium | 08.2019 - 09.2020

**President** - AIESEC ; Beirut, Lebanon | 06.2017 -09.2018

**Paramedic (Emergency Medical Technician)** - Red Cross, Emergency Medical Department ; Byblos, Lebanon | 06.2016 - 08.2018

**Delegate** - Model United Nations ; Beirut, Lebanon | 09.2012 - 05.2013

## ACADEMIC FUNCTIONS | ROLES

**Guest Professor**, Department of Conservative Dentistry and Periodontology, LMU Klinikum, Ludwig Maximilian University of Munich, Germany | 10.2024 - Present

**Departmental Board Representative** for the Residents in Clinical Specialisation Training (Dentistry - TSO/TIO) – Department of Oral Health Sciences, KU Leuven & University Hospitals Leuven ; Leuven, Belgium | 08.2024 - Present

**Guest Lecturer** Department of Oral and Maxillofacial Surgery, Faculty of Medicine - Course E07M2A: Topics uit de maxillo-faciale heelkunde (3 STP) KU Leuven (Leuven, Belgium) | 2023-2024

**Topic Coordinator** in Frontiers in Bioengineering and Biotechnology (JIF 5.7, CiteScore 6.7) with Prof. Markus O'Heller. Section: Biomechanics (Lausanne Switzerland).

**Scientific Committee Member** of the Oral Health Research Congress - Central European & Scandinavian Divisions of the International Association of Dental Research (September 2023), Rhodes, Greece

**Session Chair** during the Oral Health Research Congress - Central European & Scandinavian Divisions of the International Association of Dental Research (September 2023), Rhodes, Greece

**Organising Committee Member** in the IADMFR World Tour Congress 2023, of the International Association of DentoMaxilloFacial Radiology (July 2023), Brussels, Belgium

**Organising Committee Board Member** in the AI for Good Global Summit (Workshop and Meeting “R”) - World Health Organisation & International Telecommunication Union Headquarters (July 2023), Geneva, Switzerland

**Organising Committee Board Member** in the ITU-WHO AI for Health (Workshop and Meeting “S” MIT Media Lab & Harvard Kennedy School, Cambridge, US) World Health Organisation & International Telecommunication Union (March 2023), MIT-Harvard University, Cambridge, Massachusetts, USA

**Session Chair** during the Oral Health Research Congress - Pan-European Divisions of the International Association of Dental Research (September 2022), Marseille, France.

### **ADDITIONAL CERTIFICATIONS**

**Advanced Training Workshop on Periodontal Regeneration**, Certificate | *Cortellini Perio Academy* - Firenze, Italy, 2024

**Supervising a Master's Thesis**, Certificate | *KU Leuven* - Leuven, Belgium, 2024

**ICH-GCP E6 (R2) - Good Clinical Practice**, Certificate | *Good Clinical Practice Alliance - Europe (GCPA)* - 2022

**Segmentation and Design**, Certificate | *Materialise* - Leuven, Belgium, 2022

**Diagnostic Reference Levels (DRLs) in Medical Imaging**, Certificate | *International Atomic Energy Agency (IAEA)* - Vienna, Austria, 2021

**Radiation Protection in Dental Radiology**, Certificate | *International Atomic Energy Agency (IAEA)* - Vienna, Austria, 2021

**Implant Dentistry**, Course Certificate | *Hong Kong University* - Hong Kong, 2021

**Qualification Certification for Cone Beam CT Usage in Dental Practice** | Federal Agency for Nuclear Control (FANC) & *KU Leuven* - Belgium, 2020

**Qualification Certification for Radiation Protection in Dental Practice** | Federal Agency for Nuclear Control (FANC) & *KU Leuven* - Belgium, 2019

**Emergency Medical Technician (EMT) Certificate** | *Red Cross* - Lebanon, 2017

## AWARDS & HONOURS

**Aria Digital Award, 1st Prize Clinical Category (2024)** - 9èmes Rencontres Internationales Aria Digital — Lyon, France

**Most Cited Article(s) in Journal of Dentistry (2024 - since 2022)** — Lahoud et al. (2022) Development and validation of a novel artificial intelligence driven tool for accurate mandibular canal segmentation on CBCT — Elsevier

**Most Cited Article(s) in Journal of Endodontics (2023 - since 2020)** — Lahoud et al. (2021) Artificial intelligence for fast and accurate 3D tooth segmentation on CBCT — Chicago, IL, USA

**Finalist, Robert Frank Senior Clinical Research Award (2023)** — Central European Division of the International Association of Dental Research (CED-IADR) — Rhodes, Greece

**Albert J. Stichting Travel Award (2023)** - In Recognition for Multidisciplinary and Inter-University Project in the Research Field of Odontostomatology | Fondation Albert Joachim Stichting — Brussels, Belgium

**Most Cited Article(s) in Clinical Oral Investigations (2023/2022/2021 - since 2020)** — Leite et al. (2020) Artificial intelligence-driven novel tool for tooth detection and segmentation on panoramic radiographs — Springer Nature Switzerland.

**ABRO Research Award (2022)** - 13th Congress of the Brazilian Association of Oral Radiology and Diagnostic Imaging | Brazilian Association of Oral Radiology and Diagnostic Imaging — Goiânia, Brazil

**Journal of Endodontics - Best Article Award (2022)** - Best Article in the Category of Regenerative Endodontics — Chicago, IL, USA

**IADMR MaxilloFacial Research Award - 1st Prize (2021)** | 23rd International Congress of DentoMaxilloFacial Radiology | International Association of DentoMaxilloFacial Radiology - Gwangju, South Korea, April 2021

**Magna Cum Laude (2020)**, Postgraduate Studies in Advanced Medical Imaging, KU Leuven, July 2020

**Summa Cum Laude (2019)**, Diploma of Dental Surgery, Université Libanaise, July 2019

**Erasmus+ Scholarship (2018)**, Université Catholique de Louvain (UCLouvain) | Brussels, Belgium - 2018

**Position Paper Award (2012)**, VI's Committee of the General Assembly | Model United Nations (GC LAU MUN) - Beirut, Lebanon, April 2012

**Distinction**, French Baccalaureate (2014) | Académie de Paris - Paris, France, September 2014

### **SCIENTIFIC REVIEWER**

Journal of Dental Research | Journal of Dentistry | Clinical Implant Dentistry and Related Research | Clinical Oral Investigations | Scientific Reports | Journal of Oral and Maxillofacial Surgery | International Journal of Paediatric Dentistry | BMC Oral Health | BMC Medical Imaging | IEEE Journal of Biomedical and Health Informatics | IEEE Access | Frontiers in Bioengineering and Biotechnology | Head & Face Medicine | SN Applied Sciences | PLOS ONE | Journal of Clinical Medicine | Quantitative Imaging in Medicine and Surgery | Heliyon | International Journal of Environmental Research and Public Health | International Journal of Clinical Research | Polish Journal of Radiology | Image Analysis & Stereology.

### **LANGUAGES**

**Dutch** (C1): Communication: Excellent | Written: Excellent (ITNA Cert.)

**English** (C1): Communication: Excellent | Written: Excellent (TOEFL Cert. - 104)

**Arabic** (C2): Communication: Excellent | Written: Excellent (Leb. Bac.)

**French** (C2): Communication: Excellent | Written: Excellent (Fr. Bac.)

**German** (A1): Communication: Beginner | Written: Beginner



SCIENTIFIC OUTPUT



## PIERRE LAHOUD

Researcher Metrics (*Scopus*)

**FWCI: 7.843 | h-index: 10**

**Documents in top 25% Journals: 92.3%**

**International Collaborations: 84.6%**

### INTERNATIONAL PEER-REVIEWED PUBLICATIONS

Binvignat P, Valette S, Hara A, **Lahoud P**, Jacobs R, Chaurasia A, Ducret M, Richert R. A Comparative Analysis of AI Approaches in Learning Anatomy and Virtually Restoring Central Incisors. *Journal of Dental Research* (submitted)

**Lahoud P**, Castro AB, Jacobs W, De Greef A, Jacobs R. SEALPRINT: A Novel Fast and Precise Sealing Socket Abutment Technique for Immediate Implant Placement. A proof of concept (2024). (*In Preparation*).

Dhondt RAL, Quirynen M, **Lahoud P**, Cortellini S, Temmerman A. Horizontal guided bone regeneration: L-PRF bone-block vs a mixture of autogenous bone with deproteinized bovine bone mineral. A split-mouth RCT study with 25 months follow-up. *International Journal of Oral & Maxillofacial Implants* (Submitted).

Dhondt RAL, Quirynen M, Cortellini S, **Lahoud P**, Temmerman A. Vertical guided bone regeneration: leukocyte and platelet rich fibrin bone-block vs a mixture of autogenous bone with deproteinized bovine bone mineral. A split-mouth randomized controlled trial study with 25 months follow-up. *Int J Periodontics Restorative Dent* (Submitted).

Jindanil P, Fontenele RC, de-Azevedo-Vaz SL, **Lahoud P**, Neves FS, Jacobs R. AI-based incisive canal visualization for preventing and detecting post-

implant mandibular nerve injuries using cone beam computed tomography (2024). (*Submitted*).

**Lahoud P**, Faghiehian H, Richert R, Jacobs R, EzEldeen M. Finite Element Models: A Road to In-Silico Modeling in The Age of Personalized Dentistry (2024). *Journal of Dentistry*.

Binvignat P, Chaurasia A, **Lahoud P**, Jacobs R, Pokhojaev A, Sarig R, Ducret M, Richert R. Isotopological Remeshing and Statistical Shape Analysis: Enhancing Premolar Tooth Wear Classification and Simulation with Machine Learning Learning. *J Dent*. 2024 Jul 31:105280.

Jacobs R, Fontenele RC, **Lahoud P**, Shujaat S, Bornstein MM. Radiographic diagnosis of periodontal diseases – Current evidence versus innovations. *Periodontology 2000*. 2024; 00: 1-19.

Dhondt RAL, **Lahoud P**, Siawasch M, Castro AB, Quirynen M, Temmerman A. The Socket Shield Technique: Stability of the Buccal Peri-implant Bone after Partial Root Removal - A Prospective Case Series of 20 patients, with 18 Months Follow-up. *Int J Periodontics Restorative Dent*. 2024 May 3;0(0):1-22.

**Lahoud P**, Jacobs R, Elahi SA, Ducret M, Lauwers W, van Lenthe GH, Richert R, EzEldeen M. Developing Advanced Patient-Specific In-Silico Models: A New Era in Biomechanical Analysis of Tooth Autotransplantation. *Journal of Endodontics*. 2024 Mar 5.

Tarce M, Becker K, **Lahoud P**, Shujaat S, Jacobs R, Quirynen M. Non-invasive oral implant position assessment: An ex vivo study using a 3D industrial scan as the reference model to mimic the clinical situation. *Clinical Oral Implants Research*. 2023 Nov 5.

Oliveira-Santos N, Jacobs R, Picoli F-F, **Lahoud P**, Niclaes L, Groppo F.C. Automated segmentation of the mandibular canal and its anterior loop by deep learning. *Sci Rep* 13, 10819 (2023).

**Lahoud P**, Badrou A, Ducret M, Farges J-C, Jacobs R, Bel-Brunon A, EzEldeen M, Blal N and Richert R. Real-time simulation of the transplanted tooth using model order reduction (2023). *Front. Bioeng. Biotechnol* 11:1201177.

Rokhshad R, Ducret M, Chaurasia A, Karteva T, Radenkovic M, Roganovic J, Hamdan M, Mohammad-Rahimi H, Krois J, **Lahoud P**, Schwendicke F.

Ethical Considerations on Artificial Intelligence in Dentistry: A Framework and Checklist. *Journal of Dentistry*. 2023 Jun 22;104593.

Quirynten M, Van der Veken D, **Lahoud P**, Neven J, Politis C, Jacobs R. Diffuse Sclerosing Osteomyelitis: A Potential Risk Indicator for Peri-implantitis? A Case Series. *International Journal of Oral & Maxillofacial Implants*. 2023 May 1;38(3).

Richert R, Farges J-C, EzEldeen M, **Lahoud P**, Jacobs R, Ducret M. Les techniques de revascularisation endodontique peuvent-elles réellement renforcer les dents? (2023) *BioMatériaux Dentaires Cliniques* 8(1) <http://bit.ly/2TzWMFi>.

Wang X, Shaheen E, Shujaat S, Meeus J, Legrand P, **Lahoud P**, do Nascimento Gerhardt M, Politis C, Jacobs R. Performance of novice versus experienced surgeons for dental implant placement with freehand, static guided and dynamic navigation approaches (2023). *Sci Rep* **13**, 2598.

Quirynten M\*, Lahoud P\* (co-first authors), Teughels W, Cortellini S, Dhondt R, Jacobs R, Temmerman A. Individual “alveolar phenotype” limits dimensions of lateral bone augmentation (2023). *Journal of Clinical Periodontology*

Tarce M\*, de Greef A\*, **Lahoud P**, de Faria Vasconcelos K, Jacobs R, Quirynten M. The impact of implant-related characteristics on dental implant blooming: An in vitro study (2022). *Clinical Oral Implants Research*.

Wang X, Shaheen E, Shujaat S, Meeus J, Legrand P, **Lahoud P**, do Nascimento Gerhardt M, Politis C, Jacobs R. Influence of experience on dental implant placement: an in vitro comparison of freehand, static guided and dynamic navigation approaches (2022). *International journal of implant dentistry*. 8(1):1-9.

**Lahoud P**, Jacobs R, Boisse P, EzEldeen M, Ducret M, Richert R. Precision medicine using patient-specific modelling: State of the art and perspectives in dental practice. *Clinical Oral Investigations*. 2022 Aug;26(8):5117-28.

do Nascimento Gerhardt M, Fontenele RC, Leite AF, **Lahoud P**, Van Gerven A, Willems H, Smolders A, Beznik T, Jacobs R. Automated detection and labelling of teeth and small edentulous regions on cone-beam computed tomography using convolutional neural networks (2022). *Journal of Dentistry* 1;122:104139.

**Lahoud P**, Diels S, Niclaes L, Van Aelst S, Willems H, Van Gerven A, Quirynen M, Jacobs R. Development and validation of a novel artificial intelligence driven tool for accurate mandibular canal segmentation on CBCT. *Journal of Dentistry* (2022). 116:103891.

Meschi N, EzEldeen M, Torres Garcia AE, **Lahoud P**, Van Gorp G, Coucke W, Jacobs R, Vandamme K, Teughels W, Lambrechts P. Regenerative endodontic procedure of immature permanent teeth with leukocyte and platelet rich fibrin: a multi-center controlled clinical trial (2021). *Journal of Endodontics*

**Lahoud P**, EzEldeen M, Beznik T, Willems H, Leite A, Van Gerven A, Jacobs R, Artificial intelligence for fast and accurate 3D tooth segmentation on CBCT (2021). *Journal of Endodontics*.

Leite AF, Van Gerven A, Willems H, Beznik T, **Lahoud P**, Gaêta-Araujo H, Vranckx M, Jacobs R. Artificial intelligence-driven novel tool for tooth detection and segmentation on panoramic radiographs (2020). *Clinical Oral Investigations*

## CONFERENCE PROCEEDINGS

Binvignat P, Valette S, Hara A, **Lahoud P**, Jacobs R, Chaurasia A, Ducret M, Richert R. Machine Learning vs Deep Learning Techniques for Tooth Wear Analysis (2024). Presented at CED-IADR 2024, Geneva, Switzerland.

Binvignat P, Chaurasia A, **Lahoud P**, Jacobs R, Pokhojaev A, Sarig R, Ducret M, Richert R. Accuracy to Diagnose and Simulate Premolar Alterations Using Statistical Shape Analysis (2024). Presented at IADR General Session in New Orleans, LA, USA.

**Lahoud P**, Castro A, Jacobs R. A Novel AI-driven 3D-Printed Sealing Socket Abutment for Immediate Implantology (2023). Digital Dentistry Society Global Congress, Casablanca, Morocco.

**Lahoud P**, Faghihian H, Ducret M, Jacobs R, Richert R, Ezeldeen M. Advancing Tooth Autotransplantation: In-Silico Modelling and Finite Element Analysis Insights (2023). Oral Health Research Congress (CED/NOF-IADR), Rhodes, Greece.

**Lahoud P**, Badrou A, Ducret M, Farges J-C, Jacobs R, Bel-Brunon A, EzEldeen M, Blal N, Richert R. Model order reduction for real-time simulation of tooth autotransplantation (2023). Oral Health Research Congress (CED/NOF-IADR), Rhodes, Greece.

**Lahoud P**, Lauwers W, Wyatt J, Ducret M, Valette S, Quiryne M, Van Lenthe H, Jacobs R, Richert R, Ezeldeen M. CBCT-based biomechanical models for the study of tooth auto-transplantation outcomes (2022). Oral Health Research Congress (PER-IADR), Marseille, France.

Oliveira-Santos N, Picoli FF, Niclaes L, Gerven A, **Lahoud P**, Jacobs R, Groppo FC (2022). Detecção automática do canal mandibular e seu loop anterior por inteligência artificial. 39th Annual Meeting of the SBPQO 2022, Campinas, Brazil

**Lahoud P**, EzEldeen M, Lauwers W, Ducret M, Quiryne M, Jacobs R, Richert, R (2022). Development of a biomechanical model for the study of tooth auto-transplantation outcomes: towards in-silico modelling. EuroPerio 10, Copenhagen, Denmark

**Lahoud, P.**, Diels, S., Niclaes, L., Van Aelst, S., Willems, H., Van Gerven, A., Jacobs, R. (2021). Development and validation of a novel artificial

intelligence driven tool for accurate mandibular canal segmentation on CBCT. Presented at the 23<sup>rd</sup> International Congress of DentoMaxilloFacial Radiology. Gwangju, South Korea.

**Lahoud P**, EzEldeen M, Jacobs R (2020). Artificial Intelligence based segmentation for tooth autotransplantation. Presented at the Junior Meeting of the European Academy of Dento-Maxillo-Facial Radiology. ACTA, Amsterdam, Netherlands.

## INTERNATIONAL PRESENTATIONS

**Revolutionizing Dentistry: The Journey of Artificial Intelligence from Research to Clinical Practice**, Invited Speaker - Organizer: 2nd International Conference of the Egyptian Maxillofacial Radiology Alliance (EMRA), Location: Triumph Luxury Hotel - Cairo, Egypt - Date: January 28<sup>th</sup> 2025

**Tandheelkunde 4.0: De evolutie van artificiële intelligentie van abstracte concepten naar klinische praktijk**, Invited Speaker - Organizer: Vlaamse Beroepsvereniging Tandartsen (VBT), Location: Hotel Hilton Antwerp Old Town - Antwerp, Belgium - Date: January 23<sup>rd</sup> 2025

**Artificiële intelligentie bij chirurgische planning**, Invited Speaker - Organizer: OMFS-IMPACT, KU Leuven, Location: Webinar - Date: December 10<sup>th</sup> 2024

**Artificial Intelligence and Dental Research: from Bench to Chair-side**, Invited Speaker - Organizer: Central European Division of the International Association of Dental Research (CED-IADR), Location: International Conference Centre Geneva - Geneva, Switzerland - Date: September 12<sup>th</sup> 2024

**Digitalisation et Autotransplantation Dentaire : Innovations, Perspectives et Impact**, Invited Speaker - Organizer: ARIA Digital (Prof. Dr. Maxime Ducret), Location: Webinar - Date: June 18<sup>th</sup> 2024

**Automation in the Diagnosis, Treatment Planning and Follow-up of Tooth Auto-Transplantation**, Speaker - Clinical Research Presentation - Organizer: International Team of Implantology - ITI 's 4rd ITI Inter-University Meeting, Location: Van der Valk Hotel Ghent, Belgium - Date: January 12<sup>th</sup> 2024

**CBCT Beeldvorming: Automatisering voor Diagnose en Therapie**, Invited Speaker - Organizer: Digital Dentistry Belgium (2de Congres Digital Dentistry Belgium), Location: Vestar, Antwerp, Belgium - Date: December 14<sup>th</sup> 2023

**Artificial Intelligence-Driven Planning For Oral Surgical Procedures: How Far Have We Come?** Invited Speaker (Symposium: Bridging the Gap between Clinical Implant Dentistry and Tissue Engineering, sponsored by NOF-IADR) - Organizer: International Association of Dental Research (CED/NOF-IADR), Location: Rodos Palace Hotel, Rhodes, Greece - Date: September 22<sup>nd</sup> 2023

**Artificial Intelligence Applications For Oral Health: A Hype or a Hope?**

Invited Speaker (Young CED-IADR Workshop, sponsored by Kulzer) - Organizer: International Association of Dental Research (CED/NOF-IADR Oral Health Research Congress), Location: Rodos Palace Hotel, Rhodes, Greece - Date: September 21st 2023

**Advancing Tooth Autotransplantation: In-Silico Modelling and Finite Element Analysis Insights**, Speaker, Oral Presentation - Organizer:

International Association of Dental Research (CED/NOF-IADR), Location: Rodos Palace Hotel, Rhodes, Greece - Date: September 22nd 2023

**The Art of Artificial Intelligence**, Invited Speaker - Organizer: International Association of DentoMaxilloFacial Radiology - World Tour 2023, Location: Royal Library of Belgium, Brussels, Belgium - Date: July 7th 2023

**Artificial Intelligence Based In-Silico Modelling for Oral Surgical Procedures: A Fantasy or a Reality?** Invited Webinar Speaker - Organizer:

International Association of DentoMaxilloFacial Radiology - World Tour 2023, Location: Brussels, Belgium - Date: June 3rd 2023

**Individual “alveolar phenotype” limits dimensions of lateral bone augmentation**, Oral Presentation - Organizer: International Team of Implantology - ITI 's 3rd ITI Inter-University Meeting, Location: Van der Valk Hotel Liège, Belgium - Date: March 7<sup>th</sup> 2023

**In-Silico Modelling for Oral Surgical Procedures**, Speaker, Oral Presentation - Organizer: iSi Health - PhD & Postdoc Networking Event, KU Leuven, Location: KU Leuven Campus GHB, Leuven, Belgium - Date: December 15<sup>th</sup> 2022

**Digital workflows for dental applications: Automation & Validation**, Speaker, Oral Presentation - Organizer: KU Leuven, OHS Department Day, Location: GC Europe, Heverlee, Belgium - Date: November 22<sup>nd</sup> 2022

**CBCT-based biomechanical models for the study of tooth auto-transplantation outcomes**, Speaker, Oral Presentation - Organizer: International Association of Dental Research - Pan-European Oral Health Research Congress (PER-IADR), Location: Marseille, France - Date: September 15<sup>th</sup> - 17<sup>th</sup> 2022

**Development of a biomechanical model for the study of tooth auto-transplantation outcomes: towards in-silico modelling**, Oral Presentation -

Organizer: European Federation of Periodontology (EFP) - EuroPerio10,  
Location: Copenhagen, Denmark - Date: June 18<sup>th</sup> 2022

**Applicability of AI in Dental Research and Clinical Practice**, Invited Guest  
Speaker - Organizer: Universidad Federal de Goiás, Brazil - International  
Meeting on Dental Research, Location: Goiás, Brazil - Date: November 3<sup>rd</sup> -  
4<sup>th</sup> 2021

**A novel artificial intelligence driven tool for accurate mandibular canal  
segmentation on CBCT**, Research Award Nominee Speaker - Organizer:  
International Association of Dentomaxillofacial Radiology – 23<sup>rd</sup>  
International Congress of Dentomaxillofacial Radiology, Location: Gwangju,  
South Korea - Date: April 28<sup>th</sup> – May 1<sup>st</sup> 2021

**Artificial Intelligence Based Segmentation for Tooth Auto-  
Transplantation**, Speaker - Organizer: European Academy of  
Dentomaxillofacial Radiology – EADMFR Junior Meeting 2020, Location:  
ACTA (Academisch Centrum Tandheelkunde Amsterdam – Academic Center  
for Dentistry Amsterdam) - Gustav Mahlerlaan 3004, 1081 LA Amsterdam,  
Netherlands - Date: February 2<sup>nd</sup> – 5<sup>th</sup> 2020